University of São Paulo
"Luiz de Queiroz" College of Agriculture

Maize responsiveness to *Azospirillum brasilense*: insights into genetic control and genomic prediction

Miriam Suzane Vidotti

Thesis presented to obtain the degree of Doctor in Science. Area: Genetics and Plant Breeding

Piracicaba
2018

Miriam Suzane Vidotti
Agronomist

Maize responsiveness to *Azospirillum brasilense*: insights into genetic control and genomic prediction

Advisor:
Prof. Dr. **ROBERTO FRITSCHE NETO**

Thesis presented to obtain the degree of Doctor in Science. Area: Genetics and Plant Breeding

Piracicaba
2018

Dados Internacionais de Catalogação na Publicação
DIVISÃO DE BIBLIOTECA – DIBD/ESALQ/USP

Vidotti, Miriam Suzane

Maize responsiveness to *Azospirillum brasilense*: insights into genetic control and genomic prediction / Miriam Suzane Vidotti. - - Piracicaba, 2018.

91 p.

Tese (Doutorado) - - USP / Escola Superior de Agricultura “Luiz de Queiroz”.

1. Bactérias promotoras de crescimento de plantas 2. Estresse de nitrogênio 3. Análise dialélica 4. Predição genômica 5. Mapeamento associativo 6. *Zea mays* I. Título

AGRADECIMENTOS

A **Deus**, por conduzir o tempo e o acontecimento de todas as coisas, pela fortaleza nos momentos de dificuldades e pelos dons concedidos para realizar essa jornada, bem como a intercessão constante de **Nossa Senhora**;

Aos meus **pais** e meu **irmão**, bem como aos meus familiares, que compreenderam minha ausência em muitos momentos, que sempre me desejaram o melhor e contribuiram com inúmeros sacrifícios para que eu chegasse até aqui;

Ao meu namorado, **Renato Ornelas**, que mesmo estando longe, foi com quem pude partilhar diariamente os meus desafios e contar com sábias palavras e o companherismo no transcorrer do doutorado;

Ao meu orientador Prof. Dr. **Roberto Fritsche Neto**, pela oportunidade concedida, pelos ensinamentos compartilhados, pela confiança e liberdade depositadas para o desenvolvimento do trabalho;

Aos **colegas** do **"Laboratório de Melhoramento de Plantas Alógamas"**, pelo imprescindível auxílio na execução deste trabalho, pela troca de conhecimentos, pelo companheirismo e por todos os bons momentos que me proporcionaram;

Ao Dr. **José Crossa** e toda a **equipe** do Biometrics and Statistics Unit pertencente ao **International Maize and Wheat Improvement Center** (Texcoco, México), pela valiosa oportunidade de intercâmbio e por todas nossas discussões científicas;

Aos **membros** do **Laboratório de Genética de Microrganismos "Prof. João Lúcio de Azevedo"**, pelo suporte na produção do inoculante e pela troca de conhecimentos, em especial à Profª. Dra. Maria Carolina Quecine Verdi;

A todos os **docentes** da ESALQ/USP que contribuiram para a minha formação, em especial ao Prof. Dr. Luiz Eduardo Aranha Camargo;

A Dra. **Mariângela Hungria**, da Embrapa Soja, por disponibilizar a estirpe Ab-V5 de *Azospirillum brasilense* para esse estudo;

Ao **Conselho Nacional de Desenvolvimento Científico e Tecnológico** – CNPq pela bolsa de estudos, a **Fundação de Amparo à Pesquisa do Estado de São Paulo** (FAPESP) pelo financiamento do projeto (Processo 2015/01188-9). O presente trabalho foi realizado com apoio da **Coordenação de Aperfeiçoamento de Pessoal de Nível Superior** – Brasil (CAPES) – Código de Financiamento 001.

Finalmente, e não menos importante, a todos os meus **amigos** de **Piracicaba** e **Texcoco**, com os quais pude contar sempre com o auxílio e a amizade, por serem a minha segunda família e por tornar minha jornada mais leve mediante a tantos inesquecíveis e bons momentos.

CONTENTS

RESUMO

Responsividade do milho para *Azospirillum brasilense*: conhecimentos sobre controle genético e predição genômica

A inoculação com *Azospirillum brasilense* é uma das principais estratégias para suplementar os insumos inorgânicos de nitrogênio (N) e aumentar o desenvolvimento radicular do milho. No entanto, os efeitos benéficos da inoculação nem sempre são alcançados, o que, em parte, é devido à variação genotípica da planta hospedeira, que ocasiona diferentes graus de resultados. Neste contexto, nosso objetivo foi estudar o controle genético e a predição genômica de caracteres de milho relacionados à responsividade para a inoculação com *A brasilense*. Para isso, 118 híbridos de milho foram conduzidos sob estresse de N e estresse de N mais *A brasilense* em condições controladas nos anos de 2016 e 2017. Nós avaliamos características de raiz e parte aérea e realizamos análises dialélicas, mapeamento associativo e métodos de predição genômica considerando 59.215 marcadores *Single-Nucleotide Polymorphism* (SNP). Nossos resultados revelaram uma herança quantitativa das características do milho relacionadas à essa parceria, com efeitos genéticos aditivos e não-aditivos envolvidos no controle genético. Além disso, vários genes candidatos foram encontrados para a associação milho-*A brasilense*, especialmente com efeitos de (des)vantagens de heterozigotos. Em geral, as acurácias de predição foram mais maiores principalmente para o tratamento inoculado em comparação ao não inoculado. Finalmente, nossos resultados possibilitam uma compreensão mais aprofundada das bases genéticas da responsividade do milho à *A. brasilense* e podem auxiliar os melhoristas de plantas a estabelecerem estratégias de seleção visando o desenvolvimento de genótipos superiores para essa associação.

Palavras-chave: Bactérias Promotoras de Crescimento de Plantas (BPCP); Estresse de nitrogênio; Análise dialélica; Predição genômica; Mapeamento associativo; *Zea mays*

ABSTRACT

Maize responsiveness to *Azospirillum brasilense*: insights into genetic control and genomic prediction

The inoculation with *Azospirillum brasilense* is one of the main strategies to supplement the inorganic inputs of nitrogen (N) and to increase the root development in maize. However, the beneficial inoculation effects are not always reached, which, in part, is due to genotypic variation in the plant host, resulting in different degrees of outcome. In this context, we aimed to study the genetic control and genomic prediction of maize traits related to the responsiveness to *A. brasilense* inoculation. For this, 118 maize hybrids were conducted under N stress and N stress plus *A. brasilense* treatments in controlled conditions over 2016 and 2017 seasons. We evaluated root and shoot traits and performed diallel analyses, association mapping, and genomic prediction methods considering 59,215 Single-Nucleotide Polymorphism (SNP) markers. Our results revealed a quantitative inheritance of the partnership-related maize traits, with both additive and non-additive genetic effects involved in the genetic control. Furthermore, several candidate genes were identified for the maize-*A. brasilense* association, especially with heterozygous (dis)advantage effects. In general, the prediction accuracies were higher mostly for the inoculated treatment compared to the non-inoculated. Finally, our findings enable a deeper understanding towards the genetic basis of the maize responsiveness to *A. brasilense* and may support plant breeders to establish selection strategies aiming the development of superior genotypes for this association.

Keywords: Plant Growth-Promoting Bacteria (PGPB); Nitrogen stress; Diallel analysis; Genomic prediction; Association mapping; *Zea mays*

1. INTRODUCTION

One of the main strategies emerging in view of chemical fertilizers usage and biotic and abiotic stresses is the inoculation with Plant Growth-Promoting Bacteria (PGPB). Among them, *Azospirillum brasilense* have been broadly studied and proven to have benefits as the capacity of fixing N_2, biological control of plant pathogens, and phytohormones biosynthesis, including auxins, abscisic acid, and ethylene (Fukami *et al.*, 2018). The inoculation with this PGPB is used in ~3.5 million ha in South America, based on approximately 104 biological formulated products from more than fifty companies (Cassán and Diaz-Zorita, 2016). However, the adoption of this technology in agricultural systems of cereal crops as maize is still incipient, and a major obstacle for its widespread usage is the inconsistency of plant response to the inoculation.

The variation in results may be partially attributed to the genotypic variation among cultivars used by farmers. In turn, for the development of maize genotypes with better responsiveness to *A. brasilense*, it is important to understand the genetic control and heritability of the partnership-related traits (Kroll *et al.*, 2017). In addition, studies with genomic prediction of non-phenotyped genotypes could be useful since some of these traits are laborious and time-consuming to evaluate. Finally, the detection of genetic markers associated with maize-*A. brasilense* could allow the identification of candidate genes and, consequently, the performance of marker-assisted selection for desirable genotypes.

In the next sections, we report the results of two studies concerning this scenario. In the first study, we focused on unraveling the genetic control and the prediction accuracy of shoot and root traits related to the maize responsiveness to *A. brasilense* trough diallel analyses and genomic prediction methods, respectively. In the second, we aimed to dissect the genetic control and the genetic architecture by additive and heterozygous (dis)advantage Genome-Wide Association Study (GWAS) models and find candidate genes involved in maize-*A. brasilense* association.

REFERENCES

Cassán F, and Diaz-Zorita M. 2016. Azospirillum sp. in current agriculture: From the laboratory to the field. Soil Biology and Biochemisty 103: 117–130.

Fukami J, Cerezini P, and Hungria M. 2018. Azospirillum: benefits that go far beyond biological nitrogen fixation. AMB Express 8: 1–12.

Kroll S, Agler MT, and Kemen E. 2017. Genomic dissection of host–microbe and microbe–microbe interactions for advanced plant breeding. Current Opinon in Plant Biology 36: 71–78.

2. MAIZE RESPONSIVENESS TO AZOSPIRILLUM BRASILENSE: INSIGHTS INTO GENETIC CONTROL, HETEROSIS AND GENOMIC PREDICTION

ABSTRACT

Several studies have shown differences in the abilities of maize genotypes to facilitate or impede *Azospirillum brasilense* colonization and to receive benefits from this association. Hence, our aim was to study the genetic control, heterosis effect and the prediction accuracy of shoot and root traits related to the maize responsiveness to *A. brasilense* from 118 hybrids evaluated under N stress (control) and N stress plus *A. brasilense* inoculation. The diallel analyses were performed using mixed model equations, and the genomic prediction models accounted for the general and specific combining ability (GCA and SCA, respectively) in combination with parametric (G-BLUP) and semi-parametric (RKHS) kernels and the presence or not of G×E effects. The genotypes showed significant inoculation effect for five root traits, and the GCA and SCA were significant for both. However, the GCA in the inoculated treatment presented a greater magnitude than the control, whereas the opposite was observed for SCA. Heterosis was weakly influenced by the inoculation, and the heterozygosity and N status in the plant can have a role on the benefits that can be obtained from this PGPB. Prediction accuracies for N stress plus *A. brasilense* ranged from 0.42 to 0.78, depending on the scenario and trait, and were higher in the most cases than the non-inoculated treatment. Finally, our findings provide an understanding of the quantitative variation of maize responsiveness to *A. brasilense* and provide important insights to be applied in maize breeding aiming the development of superior hybrids for this association.

Keywords: Plant Growth-Promoting Bacteria (PGPB); Diallel analysis; Genomic prediction; Heterozygosity; Nitrogen stress; *Zea mays* L.

2.1. INTRODUCTION

In recent years, several Plant Growth-Promoting Bacteria (PGPB) have been isolated, and their beneficial effects, such as the production of phytohormones and biological nitrogen fixation (N) have been identified (Vandenberghe et al., 2017; Shameer & Prasad, 2018). The presence of these mechanisms allow the strains to be used commercially as inoculants, which is a sustainable alternative to the use of chemical fertilizers and to mitigate biotic and abiotic stress. In this context, one of the most studied genera is *Azospirillum* sp. (Cassán & Diaz-Zorita, 2016), which has excellent potential for response in association with cereal crops, such as maize. For this, increases up to 30% have been reported for grain yield and reductions up to 25% in N fertilizer needs (Hungria et al.,

2010; Fukami et al., 2016). Other beneficial effects include the ability to modulate the root architecture, leading to a greater exploration of the soil and root expansion to deeper soil layers to reach water and nutrients (Rozier et al., 2016; D'Angioli et al., 2017).

The establishment of the association of the plant-PGPB involves complex mechanisms, and the genotype of the host plant plays a crucial role in the regulation of this partnership. Genotypes can vary concerning the amount and composition of the substances released in the exudates, as well as in the composition of the genes related to the plant defense resulting on different degrees of beneficial results obtained with the inoculation (Zamioudis & Pieterse, 2012; Carvalho et al., 2014). In this context, previous studies have shown differential responses among plant genotypes to *Azospirillum* sp. inoculation (Cunha et al., 2016; Brusamarello-Santos et al., 2017).

Knowledge about the genetic control and inheritance of this association could help breeders establish selection strategies for the partnership-related plant traits, thereby aiming the development of new cultivars with better responsiveness to inoculation. For this, the diallel mating design can be a useful approach, since it determines the genetic control and the relative proportion of additive and non-additive genetic variation associated with the trait. Moreover, the genomic prediction of non-phenotyped genotypes has been routinely implemented in maize breeding programs and is the object of study of several authors (Sousa et al., 2017; Lyra et al., 2017). To our knowledge, there are no reports about the use of this approach for the traits related to the maize responsiveness to PGPB as *Azospirillum* sp., which are laborious and time-consuming for the mensuration.

Several studies have proposed the use of plant breeding to improve the interaction of plants with soil microorganisms (Gopal & Gupta, 2016; Kroll et al., 2017). So far, despite some progress being made in determining the molecular basis of the maize-*Azospirillum* sp. interaction (Fukami et al., 2017; Brusamarello-Santos et al., 2017), no studies about the maize genetic control for the responsiveness to the inoculation with this PGPR were reported, especially under N stress conditions, which is responsible for significant yield losses in many regions of the world (He et al., 2018). In addition, although some authors speculate on the influence of maize heterosis on the efficiency of microorganism association (Picard & Bosco, 2005, 2006), little is currently available about the effects of PGPB inoculation on this important phenomenon. Therefore, these knowledge could contribute to the selection of genotypes that are more efficient in the association with these microorganisms, thereby providing an effective technology for maize cultivation under low levels of N.

Hence, our objectives were (i) to identify the genetic control and inheritance of maize traits related to its responsiveness to *Azospirillum brasilense* under N stress, (ii) verify the possible influence of heterosis and heterozygosity of maize on the benefits obtained from the association with this PGPB, and (iii) compare the prediction accuracy of maize hybrids under inoculated and non-inoculated treatments through different prediction models.

2.2. MATERIALS AND METHODS

2.2.1. Plant material and *Azospirillum brasilense* inoculation

Nineteen inbred lines contrasting for Nitrogen Use Efficiency (NUE) were crossed in an incomplete diallel mating design (Fig. **S1a**), without the reciprocals, to generate 118 single-cross maize hybrids. More information about the parental lines are presented in Figs S2 and Morosini et al. (2017). The commercial strain Ab-V5 of the Plant Growth-Promoting Bacteria (PGPB) *A. brasilense* was grown in dextrose yeast glucose sucrose (DYGS) liquid medium (Rodrigues Neto et al.), while being shaken at 180 rpm, in the dark, at a temperature of 28ºC until reaching an optical density (OD) of 0.8. The bacterial cell concentration was adjusted to 10^{-8} UFC mL-1 and the inoculant was mixed with the maize seeds in plastic bags.

2.2.2. Experimental design and phenotyping

Experiments were carried out in November-December (2016) and February-March (2017) under greenhouse conditions at Allogamous Plant Breeding Laboratory, "Luiz de Queiroz" College of Agriculture, University of São Paulo, Brazil (22°42'39"S; 47°38'09"W, altitude 540 m). The maize plants were grown in 3-L plastic pots containing unsterilized loam soil (Table **S1**). To achieve optimal conditions for the bacterial biological N-fixation (low N condition), nitrogen fertilizer was not included (Kox et al., 2016). Potassium chloride and super simple phosphate inputs were added to the soil. In each pot, three seeds were sown and thinned to one after germination. The experimental design was a randomized complete block with three replications in each season. The two treatments consisted of N stress (control) and N stress plus *A. brasilense* inoculation. During the experiment, the average temperature was semi-controlled, with a maximum temperature of 33ºC, and the water supply was provided individually per pot every other day or when necessary to maintain a well-watered condition. Supplementary luminosity was done with fluorescent lamps to

establish a photoperiod of 12 hours of light. Parental inbred lines and hybrids were conducted under the same conditions but as individual experiments.

All evaluations were conducted in the V7 stage of development (seven expanded leaves), about 35 days after emergence. Plant height (PH, cm) was evaluated, and the harvested shoot (leaves and stem) was dried in a forced draft oven at 60°C for 72 h to determinate the shoot dry mass (SDM, g). The roots were extracted and carefully rinsed with water to remove soil particles before being stored individually in plastic pots with 25% ethanol solution for preservation. WinRHIZO™ software (Reagent Instruments Inc., Quebec, Canada) was used to analyze the root images acquired by an Epson LA2400 scanner (2,400 dpi resolution), providing the measures of root average diameter (RAD, mm), root volume (RV, cm^3), and length of a serial of root diameter classes. Lateral root length (roots formed from the axial roots - LRL, cm) and axial root length (comprising crow, seminal and primary roots - ARL, cm) were considered as roots fragments with a diameter class less than or equal to 0.5 mm and root fragments with a diameter class greater than 0.5 mm, respectively (Trachsel et al., 2013). After the image had been analyzed, the roots were dried in the same conditions of SDM to determine the root dry mass (RDM, g). Then, specific root length (SRL, cm g^{-1}) and specific root surface area (SRSA, cm^2 g^{-1}) were calculated through the division of the total root length and the superficial area by RDM, respectively. All the measures were recorded individually by plant, thereby resulting in six replications per genotype for a total of 1,644 analyzed roots.

2.2.3. Genotypic data

The genomic DNA of the parental inbred lines was extracted from leaf tissue at the V3 maize stage of development using a modified CTAB method (Murray & Thompson, 1980) and was genotyped with the Affymetrix Axiom® Maize Genotyping Array of 616,201 Single Nucleotide Polymorphism (SNP) markers (Unterseer et al., 2014). The markers were filtered for call rate 95% and those with heterozygous genotype of at least one individual were removed. Remaining missing data were inputted using the synbreed R package with the Beagle algorithm (Wimmer et al., 2012). The genomic matrix of each hybrid was obtained from the combination of the two parental genotypes. We discarded those markers with minor allele frequency (MAF) smaller than 0.05. Thus, a final SNP set of 65,225 and 52,215 for the inbred lines and hybrids, respectively.

2.2.4. Diallel analysis

Diallel joint analysis across both treatments was performed for each trait by fitting the following model:

$$y = X_E\beta_E + X_B\beta_B + X_C\beta_C + X_I\beta_I + X_{EI}\beta_{EI} + Z_G u_G + Z_H u_H + Z_{GE}u_{GE} + Z_{HE}u_{HE} + Z_{GI}u_{GI} + Z_{HI}u_{HI} + \varepsilon$$

where $\boldsymbol{y}$ is the vector of hybrids phenotypes; $\boldsymbol{\beta_E}$ is the vector of fixed effects of year; $\boldsymbol{\beta_B}$ is the vector of the block within the year effect, considered as fixed; $\boldsymbol{\beta_C}$ is the vector of the fixed effects of the countertop within block and year; $\boldsymbol{\beta_I}$ is the vector of the fixed effects of inoculation; $\boldsymbol{\beta_{IE}}$ is the vector of the fixed effect of the inoculation × year interaction; $\boldsymbol{u_G}$ is the vector of random effects of general combining ability (GCA), with $\boldsymbol{u_G} \sim N(\boldsymbol{0}, \sigma_G^2\boldsymbol{G})$, where σ_G^2 is the associated variance component and $\boldsymbol{G}$ is the associated additive relationship matrix from the parental inbred lines; $\boldsymbol{u_H}$ is a vector of random effects of specific combining ability (SCA), with $\boldsymbol{u_H} \sim N(\boldsymbol{0}, \sigma_H^2\boldsymbol{I_H})$, where σ_H^2 is the associated variance component; $\boldsymbol{u_{GE}}$ is the vector of random effects of GCA × year interaction, with $\boldsymbol{u_{GE}} \sim N(\boldsymbol{0}, \sigma_{GE}^2\boldsymbol{I_E} \otimes \boldsymbol{G})$, where σ_{GE}^2 is the associated variance component and ⊗ denotes the Kronecker product of matrices; $\boldsymbol{u_{HE}}$ is the vector of random effects of SCA × year interaction, with $\boldsymbol{u_{HE}} \sim N(\boldsymbol{0}, \sigma_{HE}^2\boldsymbol{I_E} \otimes \boldsymbol{I_H})$, where σ_{HE}^2 is the associated variance component; $\boldsymbol{u_{GI}}$ is the vector of random effects of GCA × inoculation interaction, with $\boldsymbol{u_{GI}} \sim N(\boldsymbol{0}, \sigma_{GI}^2\boldsymbol{I_I} \otimes \boldsymbol{G})$, where σ_{GI}^2 is the associated variance component; $\boldsymbol{u_{HI}}$ is the vector of random effects of SCA × year interaction, with $\boldsymbol{u_{HI}} \sim N(\boldsymbol{0}, \sigma_{HI}^2\boldsymbol{I_I} \otimes \boldsymbol{I_H})$, where σ_{HI}^2 is the associated variance component; $\boldsymbol{\varepsilon}$ is the vector of random residual effects, with $\boldsymbol{\varepsilon} \sim N(\boldsymbol{0}, \sigma_\varepsilon^2\boldsymbol{I})$. $\boldsymbol{X_E}$, $\boldsymbol{X_B}$, $\boldsymbol{X_C}$, $\boldsymbol{X_I}$, $\boldsymbol{X_{EI}}$, $\boldsymbol{Z_G}$, $\boldsymbol{Z_H}$, $\boldsymbol{Z_{GE}}$, $\boldsymbol{Z_{HE}}$, $\boldsymbol{Z_{GI}}$, and $\boldsymbol{Z_{HI}}$ are the respective incidence matrices and $\boldsymbol{I_H}, \boldsymbol{I_E}, \boldsymbol{I_H}$ are identity matrices of appropriate dimensions.

Individual diallel analyses for N stress and N stress plus *A. brasilense* inoculation were conducted employing the previous model disregarding the inoculation effect and its interactions effects with GCA and SCA. All analyses were carried out by the ASReml R package (Butler *et al.* 2009). The synbreed R package (Wimmer *et al.*, 2012) was used to obtain the $\boldsymbol{G}$ matrix according to VanRaden (2008) from the SNP set of inbred lines. This dense matrix was posteriorly formatted as a general inverse list (or G-inverse) as required by ASReml through a function included in MASS R package (Ripley *et al.* 2018).

The Wald test implemented in ASReml was used to test the significance of the fixed effects. In turn, the significance of random effects was determined by likelihood ratio test (LRT) by using asremlPlus R package (Brien 2016). The random effects from the diallel models were predicted as

Best Linear Unbiased Predictors (BLUPs), and their associated variance components were obtained using the Maximum Restricted Likelihood (REML) method.

Broad-sense heritability (H^2) and narrow-sense heritability (h^2) were estimated as:

$$H^2 = (\sigma_a^2 + \sigma_d^2)/(\sigma_a^2 + \sigma_d^2 + \sigma_\epsilon^2),$$

$$h^2 = \sigma_a^2 \ / (\sigma_a^2 + \sigma_d^2 + \sigma_\epsilon^2)$$

where σ_a^2 is the additive genetic variance, σ_d^2 is the dominance genetic variance, and σ_ϵ^2 is the residual variance. Genetic components were obtained as $\sigma_a^2 = 4\sigma_G^2$ and $\sigma_d^2 = 4\sigma_H^2$, where σ_G^2 and σ_H^2 are the GCA and SCA variances, respectively. Considering that the genetic variance between single-cross progeny is $2\sigma_a^2 + \sigma_d^2$, the relative importance of GCA and SCA for predicting the hybrid progeny performance was accessed by the Baker's ratio as follows (Baker, 1978):

$$BR = 2\sigma_G^2 \ / \ (2\sigma_G^2 + \sigma_H^2)$$

We dissected the relation between all measured traits, estimating the correlations among them. The igraph R package (Cesárd and Nepusz, 2018) was used to produce the network visualization plot from these results.

2.2.5. Heterosis and heterozygosity estimates

Adjusted means of the hybrids and inbred lines in each treatment were obtained using the following model:

$$y = X_E\beta_E + X_B\beta_B + X_C\beta_C + X_I\beta_I + X_{EI}\beta_{EI} + X_G\beta_G + X_{GE}\beta_{GE} + \varepsilon$$

where $\boldsymbol{y}$ is the phenotypic vector of hybrids or inbred lines; $\boldsymbol{\beta_E}$ is the vector of the fixed effects of year; $\boldsymbol{\beta_B}$ is the vector of the block within year effect, considered as fixed; $\boldsymbol{\beta_C}$ is the vector of the fixed effects of countertop within block and year; $\boldsymbol{\beta_I}$ is the vector of fixed effects of inoculation; $\boldsymbol{\beta_{IE}}$ is the vector of fixed effects of inoculation × year interactions; $\boldsymbol{\beta_G}$ is the vector of fixed effects of the genotype; $\boldsymbol{\beta_{GE}}$ is the fixed effects of genotype × year interaction; $\boldsymbol{\varepsilon}$ is the vector of random residual effects, with $\boldsymbol{\varepsilon} \sim N(\boldsymbol{0}, \sigma_\varepsilon^2 \boldsymbol{I})$. $\boldsymbol{X_E}$, $\boldsymbol{X_B}$, $\boldsymbol{X_C}$, $\boldsymbol{X_I}$, $\boldsymbol{X_{EI}}$, $\boldsymbol{X_G}$, and $\boldsymbol{X_{GE}}$ being the respective incidence matrices.

Mid-parent heterosis (MPH) and high-parent heterosis (HPH) were calculated for each hybrid for those traits with significant inoculation effect in the diallel joint analysis as:

$$MPH(\%) = [(F1 + MP)/MP] \times 100$$

$$HPH(\%) = [(F1 + BP)/BP] \times 100$$

where $F1$ is the mean performance of the hybrid; MP is the mid-parent value, given by $(P1 + P2)/2$, where $P1$ and $P2$ are the mean performance of parental inbred line 1 and parental inbred line 2; BP is the mean performance of the better parental inbred line.

Furthermore, the individual heterozygosity level through was calculated as the ratio of the number of heterozygous loci with the number of total markers from the genomic matrix. Posteriorly, these values were correlated with the performance of the hybrids in the N stress and N stress plus *A. brasilensis*, as well as with the difference of the hybrid performance in the two treatments (Δ), being $\Delta = T_2 - T_1$, where T_1 and T_2 are the hybrids adjusted means in N stress and N stress plus *A. brasilense*, respectively. Considering that the Δ in the biological sense is the change in the trait due to inoculation, this parameter for each hybrid was also correlated with the adjusted means in the N stress treatment.

2.2.6. Genomic prediction

Parametric (G-BLUP) and semi-parametric (RKHS) prediction methods accounting for the general and specific combining abilities (GCA and SCA) were used to predict the performance of the single-crosses in the N stress and N stress plus *A. brasilense* inoculation scenarios. The fitted prediction models accounted for the genotype by the environment interaction effects (multi-environment, only variance G×E deviation model) or not (across environments). For this, we used a two-stage approach (Massman *et al.*, 2013), where, in the first stage, the adjusted means were obtained from full fixed models by year and by treatment, including hybrids and blocks and assuming residuals with $\boldsymbol{\varepsilon} \sim N(\mathbf{0}, \sigma_{\varepsilon}^2 \boldsymbol{I})$. In the second stage, the prediction models were fitted only for the traits with significant inoculation effect in the diallel joint analysis.

Across-environment GCA and SCA effects model

The model assumes the fixed effect of the environment and the random effects of the GCA of the parental inbred line and the SCA of the hybrid (Technow *et al.*, 2014). Here, each year was considered as an environment, being:

$$y = Z_E \beta_E + Z_G g + Z_H h + \varepsilon,$$

where $\boldsymbol{y}$ is the vector of hybrid's adjusted phenotypes, obtained on stage one; $\boldsymbol{\beta}_E$ is the vector of environmental fixed effects; $\boldsymbol{g}$ is the vector of random effects of GCA with $\boldsymbol{g} \sim N(\boldsymbol{0}, \sigma_G^2 \boldsymbol{G})$, where σ_G^2 and $\boldsymbol{G}$ are the variance component and a variance covariance matrix associated with GCA, respectively; $\boldsymbol{h}$ is the vector of random effects of SCA with $\boldsymbol{h} \sim N(\boldsymbol{0}, \sigma_H^2 \boldsymbol{H})$, where σ_H^2 and $\boldsymbol{H}$ are the variance component and the relationship matrix associated with SCA, respectively; $\boldsymbol{Z_E}$, $\boldsymbol{Z_G}$, and $\boldsymbol{Z_H}$ are the respective incidence matrices; and $\boldsymbol{\varepsilon}$ is the vector of the residuals with $\boldsymbol{\varepsilon} \sim N(\boldsymbol{0}, \sigma_\varepsilon^2 \boldsymbol{I})$.

This model was initially proposed to account for the GCA effects from inbred lines of two distinct heterotic groups. However, in this study, we have the same inbred lines set composing the parental set one and two for the diallel mating design, and thus, only one GCA effect was modeled. For this, the incidence matrices for parental set one ($\boldsymbol{Z_{p1}}$) and two ($\boldsymbol{Z_{p2}}$) were computed separately, and $\boldsymbol{Z_G}$ was obtained as $\boldsymbol{Z_G} = \boldsymbol{Z_{p1}} + \boldsymbol{Z_{p2}}$.

We considered two variance covariance matrices: 1) $\boldsymbol{G} = \boldsymbol{WW'}/m$, where $\boldsymbol{W}$ is the centered and standardized matrix of the molecular markers for the inbreed lines, and m is the number of markers (Lopez-Cruz *et al.*, 2015); hereafter, we refer to the model that uses this matrix as GB; 2) $\boldsymbol{G}$ based on a Gaussian kernel, $\boldsymbol{G}(\boldsymbol{w_i}, \boldsymbol{w_j}) = exp(-hd_{ij}^2)$, where $\boldsymbol{w_i}$ and $\boldsymbol{w_j}$ are the genotype vectors of individuals i and j; d_{ij}^2 is the marker-based Euclidean distance between the individuals i and j; $h > 0$ is the bandwidth parameter that controls the rate of decay of the $\boldsymbol{G}$ values when the distance between the pairs of genotype vectors increases (Pérez-Rodríguez *et al.*, 2012). In this study, we considered $h = 1$ and the median of the distances as the scaling factor so that $\boldsymbol{K}(\boldsymbol{w_i}, \boldsymbol{w_j}) = exp(-hd_{ij}^2 / median(d_{ij}^2))$, and because this kernel potentially takes into account complex gene interactions (e.g., epistasis), we will refer to the model that uses this matrix as GK.

For both kernels, the relationship matrix H was computed as the product of the G_{p1} (parental set 1) and G_{p2} (parental set 2), following the equation $h_{ij} = g_{p1_i} \times g_{p2_j}$, where h_{ij} is the hybrid obtained by crossing the inbred lines i and j; g_{p1_i} is the ith element of G_{p1}; g_{p2_j} is the jth element of G_{p2} (Technow *et al.*, 2014; Acosta-Pech *et al.*, 2017). This derivation is readily performed because SCA can be represented as the interaction effect from a single cross between two inbred lines.

Multi-environment, single variance G×E deviation model

We fitted the extended previous model by adding GCA and SCA × environment interactions, as proposed by Acosta-Pech et al. (2017):

$$y = Z_E\beta_E + Z_G g + Z_H h + u_G + u_H + \varepsilon$$

where $\boldsymbol{u_G}$ is the vector of random interaction effects of GCA with the environment with $\boldsymbol{u_G} \sim N(\mathbf{0}, \sigma^2_{GE}\boldsymbol{V_G})$, where σ^2_{GE} and $\boldsymbol{V_G}$ are the relative variance component and the associated variance-covariance matrix; $\boldsymbol{u_H}$ is the vector of random interaction effects of SCA with the environment with $\boldsymbol{u_H} \sim N(\mathbf{0}, \sigma^2_{HE}\boldsymbol{V_H})$, where σ^2_{HE} and $\boldsymbol{V_H}$ are the relative variance component and the associated variance-covariance matrix.

The $\boldsymbol{V_G}$ and $\boldsymbol{V_H}$ matrices were derived as $\boldsymbol{V_G} = [\boldsymbol{Z_G G Z'_G}] \circ [\boldsymbol{Z_E Z_E}']$ and $\boldsymbol{V_H} = [\boldsymbol{Z_H H Z'_H}] \circ [\boldsymbol{Z_E Z_E}']$, where (°) is the Hadamard element-wise product of two matrices of the same dimensions that results in a block diagonal matrix. The model fitted using GBLUP (GB + G×E) is equivalent to Acosta-Pech *et al.* (2017). Furthermore, we also tested the Gaussian kernel and these results were reported as GK+G×E.

Variance components and prediction accuracy

All the variance components were estimated by fitting the models using the Bayesian Generalized Linear Regression (BGLR) R package (Pérez-Rodríguez & de los Campos, 2014). The results were based on 50,000 iterations after a burn-in period of 5,000 iterations.. The mean posterior of variance components and standard deviation for GCA (σ^2_G), SCA (σ^2_H), GCA and SCA x environment interactions (σ^2_{GE} and σ^2_{GH}), and residual variance (σ^2_ϵ) were reported, with σ^2_{GE} and σ^2_{GH} being considered only in the GB+G×E and GK+G×E models.

The comparisons between the models were based on their prediction accuracies from cross-validation (CV) schemes simulating two prediction problems, as proposed by Burgueño *et al.* (2012). First, we assessed the prediction accuracy of the models considering that a set of hybrids was not evaluated in any of the environments (CV1). Second, we considered the problem of incomplete trials, where a set of hybrids are conducted only in part but not in all of the target environments (CV2). For both CV procedures, the hybrids were divided randomly into five groups, and four of them were used as the training set (TS) to estimate marker effects and to predict the phenotypes of individuals assigned to the fifth fold, referred to as the validation set (VS). The process was repeated 100 times for each model. For each TS-VS partition, the Pearson correlation was estimated, and the prediction accuracy was reported as the average of these values.

2.3. RESULTS

2.3.1. Genetic correlations between traits

The different degrees of the genetic correlations among the traits were revealed by the network (Fig. **1**). However, few substantial differences were observed between the N stress and N stress plus *A. brasilense* treatments, as these differences were related more to the correlation's estimated magnitude than the direction. One example is the connections of the LRL with the RV, ARL, RSR, and RDM, which were weaker in the inoculated treatment than the N stress. In both treatments, strong positive correlations were observed within the group of RDM, RV, RAD, and ARL. Additionally, the SRL and SRSA revealed a strong positive correlation with the other but had negative correlations with RDM, RV, and RAD.

2.3.2. Relative importance of additive and non-additive gene action for the hybrid phenotype under the different treatments

In the diallel joint analysis performed across both treatments, the fixed effects of year and experimental design (block and countertop) were significant for most of the traits, indicating the importance of environmental control even in greenhouse conditions (Table **1**). In addition, the YxI effect (inoculation by year interaction) was not significant for any trait, suggesting that the responses of the genotypes to inoculation do not change differentially with the year. Among all of the evaluated traits, we observed significant effects of *A. brasilense* inoculation only for RDM, RV, RAD, SRL, and SRSA. Thus, all subsequent results and analyses were reported only for these five root traits.

The decomposition of the genotypic variance into GCA and SCA showed that most of the genetic variation between the genotypes was due to GCA (Table **1**). Different from the GCA, only SRL and SRSA showed a significant SCA effect. For these same two traits, significant effects of GCAxY and SCAxY were observed. Moreover, we verified significant GCAxI for all the traits, except for RV, whereas SCAxI was not detected for any trait. In this sense, the GCA values for the inbred lines were variable depending on the treatment.

Concerning the variance components from joint (Table **2**) and individual (Tables **S1** and **S2**) diallel analyses, we found that the GCA variance ($\hat{\sigma}_G^2$) contributed more significantly for the phenotypic variation in N stress plus *A. brasilense* than N stress (Fig. **2**, Tables **2** and **S4**). In turn, the estimates of SCA variance ($\hat{\sigma}_H^2$) displayed higher magnitudes for all traits under N stress in comparison to N stress plus *A. brasilense* (Table **2**). For example, differences between non-

inoculated and inoculated reached 95% for SRL, which was also evident from the distribution of the SCA values (Fig. **3a**, Table **S5**). The exception was RV, for which the values were 44.4% higher under *A. brasilense* inoculation. The first two principal components (PC1 and PC2) extracted from the 118 SCA values for each root trait explained more than 87% of the observed variance in both treatments (Fig. **3b**) and each trait contributed approximately form 15% to 25% in the variation of PC1 and PC2.

The Backer's ratios were higher than 0.74 and 0.95 under N stress and N stress plus *A. brasilense*, respectively (Table **2**). Considering that this proportion was close to one, this indicates a considerable influence of GCA variance for the phenotypes measured. The estimates of narrow-sense heritabilities were higher in the inoculated treatment, ranging from 0.44 (SRSA) to 0.60 (RAD), whereas these estimates in the non-inoculated ranged from 0.13 (RDM) to 0.34 (RAD). In turn, values of broad-sense heritability ($\widehat{H}^2$) were relatively close to narrow-sense heritability ($\hat{h}^2$), where the smallest estimates were 0.19 (RDM) under N stress and 0.48 (SRSA) under N stress plus *A. brasilense*.

2.3.3. Relation of heterosis and heterozygosity with root traits

Heterosis was expressed relative to mid-parent (MPH) and high-parent (HPH) (Figs **4a** and **4b**). The distribution of the MPH estimates illustrates that only SRL exhibited pronounced differences between N stress and N stress plus *A. brasilense*, with an average heterosis. For the other traits, no substantial variation was detected among the treatments. RDM and RV were the traits with greater heterosis over the mid-parent, with values approaching 250% and without negative values verified on the density plot. Concerning HPH estimates, the root traits displayed a similar density pattern of MPH, except for RAD and SRSA.

Heterozygosity across the hybrid loci varied from 0.17 to 0.39, with a mean of 0.32. The correlation of this measure of individual genetic diversity with the adjusted means from the *A. brasilense* treatment was of relatively low magnitude for all the traits (Fig. **4c**). The values of greater magnitude found were -0.36 and -0.28 for RDM and RV, respectively. Regarding N stress, all correlation values were less than 0.18. Changes due to inoculation (Δ) for each trait displayed low association with the genetic diversity of hybrids, as well as the 15% bottom and top Δ hybrids, which represent the groups with smaller and larger responsiveness to inoculation to *A. brasilense*. In turn, the correlation values between the Δ and N stress ranged from -0.25 to -0.47, indicating that hybrids with greater root traits values in N stress tend to have less modulation of root architecture by *A. brasilense* inoculation (Fig. **4d**).

2.3.4. Accuracy of predicting hybrid performance under inoculated and non-inoculated treatments

Results of the prediction accuracy varied according to the root traits and treatments (Fig. **5**). Concerning RDM and RV, the average prediction accuracy considering all the prediction models under N stress plus *A. brasilense*, were 36% and 10%, respectively, higher than N stress, for both CV methods. On the other hand, a small increase in prediction accuracy was found with the inoculation for SRL, with the percent change ranging from 1.8% to 8.6%. Additionally, the prediction accuracy of RAD under N stress plus *A. brasilense* was negatively affected, with a reduction of the approximately 12% for all the models and validation systems. The difference in predicting the SRSA in each treatment was variable depending on the CV method. For example, in CV1, an increase of 16% was observed for prediction accuracy when the GB model was employed for predicting the hybrid's performance when inoculated with *A. brasilense,* whereas in CV2, a reduction of 16% was observed.

Overall, high prediction accuracies were found under inoculated treatment, mainly for the traits more related to mitigation of N stress (RDM, RV, and RAD), ranging from 0.65 (RDM) to 0.78 (RV). Conversely, no substantial differences were observed between models with different kernel regression methods and with or without the incorporation of G×E effects. However, in general, the models with GBLUP displayed less residual variance that those with Gaussian kernel, thus indicating better adjustment of the models (Tables **S6**, **S7**, **S8**, **S9** and S**10**).

Concerning the cross-validations methods, CV2 differed slightly for the RDM, RV, RAD, and SRL, which suggests that the recovered information among the environments was small for these traits. The highest gains in prediction accuracy when employing the CV2 over CV1 were found for the SRSA under N stress, especially in combination with GBLUP. However, surprisingly, we found a modest reduction of the prediction accuracy for the same trait when using the GBLUP model for prediction under N stress plus *A. brasilense*. In addition, for the same treatment, the opposite was found when the relationship between individuals was modeled using Gaussian kernel.

2.4. DISCUSSION

2.4.1. Inheritable variance of root traits increases with *A. brasilense* inoculation

We performed individual and joint diallel analysis for 118 maize hybrids evaluated under N stress and N stress plus *A. brasilense* for a series of shoot and root traits. From a total of ten traits, the RDM, RV, RAD, SRL, and SRSA underlying the root traits were significantly affected by the

bacterial inoculation. These results are consistent with those found for D'Angioli *et al.* (2017) under similar conditions and using the same bacterial strain, indicating that the root growth promotion did not necessarily increase the shoot-related traits. In turn, the modification of the RDM, RV, and RAD reinforces the findings of the capacity of *A. brasilense* modulate essential root traits by the production of phytohormones increasing the exploration of the soil and allow growth into deep soil layers, thus helping to mitigate stress conditions (Cassán & Diaz-Zorita, 2016). However, negative genetic correlations were observed between these traits and SRL and SRSA, which are most related to phosphorus starvation tolerance (Chen *et al.*, 2018). Therefore, this indicate that the selection of genotypes with enhanced responsiveness to *A. brasilense* inoculation should be specific for each stress condition.

A key finding of our study is that the proportion of additive genetic under *A. brasilense* inoculation variance was higher than N stress, increasing the inheritable variance for all root traits. Considering this element is a determinant factor for the evolutionary potential of species in natural conditions (Hoffmann & Merilä, 1999), the maize-*A. brasilense* interactions would enhance the plant's ability to respond to environmental changes and persist over time. For example, in common bean this PGPB can be vertically transmit to successive plant generations demonstrating to be an effective inoculum in seed (Malinich & Bauer, 2018). Conversely, in the context of plant breeding, under N stress plus *A. brasilense* inoculation the genetic gain with the selection could be more significant than N stress. However, we should be cautious with these results because, although in the diallel analysis the absence of epistasis is assumed, epistasis can manifest in several plant traits (Luo *et al.*, 2017; Yang *et al.*, 2018). Moreover, according to Falconer and Mackay (1996), additive genetic variance and additive-by-additive epistasis variance are responsible for the genetic value of each parental line (GCA) while non-additive genetic variations are related to SCA. Thereby, a more substantial influence of GCA variance (and consequently the predominance of additive genetic variance) under inoculated treatment over non-inoculated possibly is due, in part, to the presence of an epistasis component. The importance of epistasis for underlying the complex genetic architecture of plant-pathogens interactions has been reported by several authors (Rybak *et al.*, 2017; Moellers *et al.*, 2017). In this sense, further studies as genome-wide epistasis studies (GWES) could promote an understanding of the role and the relative importance of the genetic loci interactions for the differential ability of maize genotypes to establish an association with *A. brasilense*.

We also found low to moderate heritability values, which suggest the maize–*A. brasilense* association has quantitative inheritance. This is consistent with the high number of genes that could be involved in the production of the root exudates, hormonal balance, and defense system that

would modulate the plant bacterial colonization (Fukami *et al.*, 2017; Brusamarello-Santos *et al.*, 2017). Additionally, although additive effects were greater than the dominance effects, both are involved in the genetic control of the maize root traits responsiveness to *A. brasilense* inoculation.

2.4.2. Heterosis is variable across root traits but is weakly influenced by the bacterial inoculation

Heterosis, or hybrid vigor, is a phenomenon in which the hybrids often outperform their parents in yield, growth rate, biomass or stress tolerance (Goulet *et al.*, 2017). Mid-parent heterosis (MPH) and high-parent heterosis (HPH) have been extensively exploited in several studies as a measure of heterosis (Seifert *et al.*, 2018; Feys *et al.*, 2018). A very similar pattern of MPH and HPH distribution was observed. Considering that high-parent and low-parent share close phenotypic values, similar estimates of mid-parent and high-parent are possible. This finding is consistent with a certain level of relatedness that can be observed in our set of inbred lines (Figs **S2**). Therefore, our discussion focusses on merely using the term heterosis.

Although present in a range of traits, the heterotic responses can display variable levels among them (Yang *et al.*, 2017; Li *et al.*, 2018). The highest estimates were for RDM and RV, with the maximum values reaching 250%, suggesting a high genetic divergence between the parental lines, which leads to the enhancement of the phenotypic expression. Furthermore, similarly to grain yield, RDM and RV can be the result of the multiplication of many others secondary traits, such as the average root diameter, total root length, and surface area. Hence, the combination of quantitative variations can interact to produce higher heterosis, exceeding by more than double the mid- or high-parent heterosis, whereas the majority of the other traits display no more than 50% (Flint-Garcia *et al.*, 2009).

The analyses of heterosis showed positive, negative, or the combination of both directions. The positive heterosis for RDM, RV, and RAD in hybrids might confer better nutritional and water status than parental lines, considering that an increase of root biomass and expansion is often the primary driver for plant performance (Zaidi *et al.*, 2016; Li *et al.*, 2016). Conversely, the prevalence of negative heterosis for SRL and SRSA suggests a low genetic divergence in our inbred lines set for these traits, where genes with unidirectional negative dominance effects are complementary at particular loci. It is not surprising given that SRL and SRSA are more related to phosphorus stress tolerance, and our parental lines contrast in NUE.

We found that the enhancement of growing conditions by the *A. brasilense* inoculation does not lead pronounced variations in heterosis for most of the evaluated traits. However, heterotic

responses in other maize traits, such as grain yield and leaf growth, can be correlated linearly with environmental quality (Munaro *et al.*, 2011; Amelong *et al.*, 2017). Under these considerations, some explanations about our results are possible. First, the internal changes in the plant caused by this PGPB might have a relatively small effect on the genetic factors that trigger heterosis in comparison to other possible external sources. Second, the heterosis over time may be relatively stable or variable during the plant lifecycle, depending on the trait (Feys *et al.*, 2018). Therefore, in stages of development other than V7 heterosis, the results could be different between the treatments.

Even though four of the five traits showed lower $\hat{\sigma}_d^2$ estimates in N stress plus *A. brasilense* than under the N stress, similar heterosis levels were observed under both treatments. Advances in genetic and genomic studies have revealed that, in addition to traditional dominance and overdominance hypotheses, multiple causal mechanisms contribute to heterosis, including epistasis, epigenetic modification and small RNA activity (Goulet *et al.*, 2017). As already mentioned above, additive-by-additive epistatic effects might be present in the GCA effects. Thus, even with lower $\hat{\sigma}_d^2$ estimates, heterosis levels remained consistent for inoculated treatment. Under these considerations, additive-by-additive epistatic effects can play a more prominent role in maize heterotic responsiveness under *A. brasilense* inoculation than dominance effects, such as observed in traits of bread wheat (Jiang *et al.*, 2017).

2.4.3. Individual heterozygosity and N status in the plant can regulate the maize- *A. brasilense* partnership

Relations between genomic heterozygosity and plant fitness have been explored in several species, and, when studied at the individual level, these relations serve as a measure of individual genetic diversity (Arct *et al.*, 2017; Eastwood *et al.*, 2017). Our analysis revealed modest negative correlations between heterozygosity and RDM and RV under N stress plus *A. brasilense* treatment. Most likely, the increase in the diversity of compounds released in the exudates because of high levels of heterozygosity results in an interaction with a more significant amount of soil microorganisms, leading to stimulation of other certain strains (Picard & Bosco, 2006; Peiffer *et al.*, 2013). Hence, the competition between *A. brasilense* and a wide range of other microorganisms that have little or no effect on the plant could have resulted in a lower benefit due to inoculation. In addition, regarding host-pathogen systems, the lower individual genetic diversity can increase the susceptibility to infection (Govindaraj *et al.*, 2015; Eastwood *et al.*, 2017). Similarly, this could happen with *A. brasilense*, where the allelic diversity among specific loci associated with plant immunity would actively control the extent of colonization by the bacteria and, consequently,

the degree of beneficial results. Moreover, further studies are needed to better understand why some traits under inoculation treatment are more affected by heterozygosity level than other. We can speculate that the *A. brasilense* inoculation can stimulate certain heterozygous loci, which may affect differently the plant traits.

We also found negative correlations between performance under N stress and Δ (difference between N stress plus *A. brasilense* and N stress treatments) for all evaluated traits. This correlation indicates that the average rate of increase due to inoculation tends to be higher in genotypes with worse performance under N stress effects. Thereby, traits related to NUE and the internal N status in the plant could be relevant for the development of more responsive maize hybrids to *A. brasilense* inoculation. Additionally, this observation reinforces the possible role of internal N metabolism regulating the association efficiency through the modulation of plant defense (Carvalho *et al.*, 2014). On the other hand, this may indicate that the plant breeding based on high N input can be indirectly selecting plants with less advantage in take benefits from the interaction with PGPB. Therefore, studies are needed to better understand the impact of plant breeding for N stress tolerance, for example, in the crosstalk and the efficiency association of *A. brasilense* and other PGPB.

2.4.4. Hybrid performance under *A. brasilense* inoculation can be predicted with high accuracy

Our results showed high prediction accuracies for the majority of the traits evaluated under *A. brasilense* treatment in comparison to those traits observed under N stress. The high heritability estimates found for the inoculation condition could be a reason for these findings. Moreover, these results are consistent with those observed by Sousa *et al.* (2017) and Zhang *et al.* (2015), in which the prediction accuracy under stress conditions tends to be lower than the non-limiting environments, especially for traits with more complex architecture.

Although predictions with medium-to-high accuracy were found for both treatments for all tested genomic models, no substantial differences were observed between the parametric and semi-parametric methods (GB and GK, respectively). However, the limitations due to the small number of hybrids and the relatedness among our parental set may have influenced our results. For instance, in studies with larger panels of hybrids, a superior overall performance of the nonlinear GK model relative to GBLUP has been observed (Lyra *et al.*, 2017; Cuevas *et al.*, 2018). In this sense, the use of GK proposed in our study, when applied to other data sets, could show better results in comparison to the use of GB, as initially proposed by Acosta-Pech *et al.* (2017) and

Massman *et al.* (2013). The same explanation may be valid for the incorporation of G×E effects in the prediction models. The reduced number of environments in which our hybrids were tested and the greenhouse conditions that reduce the action of environmental factors over the plant development, possibly resulted in high correlation among environments and led to a small occurrence of G×E interactions. In this sense, in our results, this modeling did not provide mainly an increase in the prediction accuracy for all traits and treatments. Our results reinforce the importance of prediction model-kernel combinations for both maize prediction under N stress plus *A. brasilense* and N stress, in addition to the possibility that they must be specific to each CV scheme for determined traits.

2.5. CONCLUSION

We verified a quantitative inheritance of the maize responsiveness to *A. brasilense*, and that both additive and dominance genetic effects are involved the genetic control of this association. Furthermore, the heterozygosity and N status in the plant could influence the regulation of *A. brasilense* benefits to the plant. In general, the prediction accuracies were higher under inoculated treatment than the non-inoculated and the results are encouraging for the application of this breeding methodology. Finally, our results may support possible plant breeding strategies to explore the genetic variability among maize genotypes relative to their differential ability to allow the colonization by *A. brasilense* and take advantage of this beneficial interaction.

REFERENCES

Acosta-Pech R, Crossa J, de los Campos G, Teyssèdre S, Claustres B, Pérez-Elizalde S, Pérez-Rodríguez P. 2017. Genomic models with genotype × environment interaction for predicting hybrid performance: an application in maize hybrids. Theoretical and Applied Genetics 130: 1431–1440.

Amelong A, Hernández F, Novoa AD, Borrás L. 2017. Maize stand density yield response of parental inbred lines and derived hybrids. Crop Science 57: 32–39.

Arct A, Sudyka J, Podmokła E, Drobniak SM, Gustafsson L, Cichoń M. 2017. Heterozygosity–fitness correlations in blue tit nestlings (Cyanistis caeruleus) under contrasting rearing conditions. Evolutionary Ecology 31: 803–814.

Baker RJ. 1978. Issues in diallel analysis. Crop Science 18: 533.

Brien C. 2016. asremlPlus: augments the use of 'asreml' in fitting mixed models. R package version 2.0-9. [WWW document] URL https://CRAN.R-project.org/package=asremlPlus. [accessed 20 August 2018].

Brusamarello-Santos LC, Gilard F, Brulé L, Quilleré I, Gourion B, Ratet P, Maltempi de Souza E, Lea PJ, Hirel B. 2017. Metabolic profiling of two maize (Zea mays L.) inbred lines inoculated with the nitrogen fixing plant-interacting bacteria Herbaspirillum seropedicae and Azospirillum brasilense (R Aroca, Ed.). PLOS ONE 12: e0174576.

Burgueño J, de los Campos G, Weigel K, Crossa J. 2012. Genomic prediction of breeding values when modeling genotype × environment interaction using pedigree and dense molecular markers. Crop Science 52: 707.

Butler DG, Cullis, BR, Gilmour AR, Gogel BJ. 2009. ASReml-R reference manual. R package version 3.0. [WWW document] URL https://www.vsni.co.uk. [accessed 31 August 2018].

Carvalho TLG, Balsemao-Pires E, Saraiva RM, Ferreira PCG, Hemerly AS. 2014. Nitrogen signalling in plant interactions with associative and endophytic diazotrophic bacteria. Journal of Experimental Botany 65: 5631–5642.

Cassán F, Diaz-Zorita M. 2016. Azospirillum sp. in current agriculture: From the laboratory to the field. Soil Biology and Biochemistry 103: 117–130.

Chen Y, Hong T, Nguyen N, Qin J, Jiao Y, Li Z, Ding S, Lu Y, Liu Q, Luo Z. 2018. Running head : Phosphorus assimilation in Chinese fir. Environmental and Experimental Botany.

Csárdi G, Nepusz T. 2018. Network Analysis and Visualization. R package version 1.2.1. [WWW document] URL https://cran.r-project.org/web/packages/igraph/igraph.pdf. [accessed 31 August 2018].

Cuevas J, Granato I, Fritsche-Neto R, Montesinos-Lopez OA, Burgueño J, Sousa MB e., Crossa J. 2018. Genomic-enabled prediction kernel models with random intercepts for multi-environment trials. G3: Genes/Genomes/Genetics 8: g3.300454.2017.

Cunha FN, Silva NF da, Ribeiro Rodrigues C, Alves Morais W, Ferreira Gomes FH, Lopes Filho, Luiz C, Cabral LB dos S, Marconi BT, Gustavo da SV, Cicero TSC. 2016. Performance of different genotypes of maize subjected to inoculation with Azospirillum brasilense. African Journal of Agricultural Research 11: 3853–3862.

D'Angioli AM, Viani RAG, Lambers H, Sawaya ACHF, Oliveira RS. 2017. Inoculation with Azospirillum brasilense (Ab-V4, Ab-V5) increases Zea mays root carboxylate-exudation rates, dependent on soil phosphorus supply. Plant and Soil 410: 499–507.

Eastwood JR, Ribot RFH, Rollins LA, Buchanan KL, Walder K, Bennett ATD, Berg ML. 2017. Host heterozygosity and genotype rarity affect viral dynamics in an avian subspecies complex. Scientific Reports 7: 13310.

Falconer DS, Mackay T F C. 1996. Introduction to quantitative genetics. Edinburgh: Longman Group Limited.

Feys K, Demuynck K, De Block J, Bisht A, De Vliegher A, Inzé D, Nelissen H. 2018. Growth rate rather than growth duration drives growth heterosis in maize B104 hybrids. Plant, Cell & Environment 41: 374–382.

Flint-Garcia SA, Buckler ES, Tiffin P, Ersoz E, Springer NM. 2009. Heterosis is prevalent for multiple traits in diverse maize germplasm. PLoS ONE 4: e7433.

Fukami J, Nogueira MA, Araujo RS, Hungria M. 2016. Accessing inoculation methods of maize and wheat with Azospirillum brasilense. AMB Express 6: 3.

Fukami J, Ollero FJ, Megías M, Hungria M. 2017. Phytohormones and induction of plant-stress tolerance and defense genes by seed and foliar inoculation with Azospirillum brasilense cells and metabolites promote maize growth. AMB Express 7:1.

Gopal M, Gupta A. 2016. Microbiome selection could spur next-generation plant breeding strategies. Frontiers in Microbiology 7: 1–10.

Goulet BE, Roda F, Hopkins R. 2017. Hybridization in plants: old ideas, new techniques. Plant Physiology 173: 65–78.

Govindaraj M, Vetriventhan M, Srinivasan M. 2015. Importance of genetic diversity assessment in crop plants and its recent advances: An overview of its analytical perspectives. Genetics Research International 2015.

He K, Chang L, Dong Y, Cui T, Qu J, Liu X, Xu S, Xue J, Liu J. 2018. Identification of quantitative trait loci for agronomic and physiological traits in maize (Zea mays L.) under high-nitrogen and low-nitrogen conditions. Euphytica 214: 15.

Hoffmann AA, Merilä J. 1999. Heritable variation and evolution under favourable and unfavourable conditions. Trends in Ecology & Evolution 14: 96–101.

Hungria M, Campo RJ, Souza EM, Pedrosa FO. 2010. Inoculation with selected strains of Azospirillum brasilense and A. lipoferum improves yields of maize and wheat in Brazil. Plant and Soil 331: 413–425.

Jiang Y, Schmidt RH, Zhao Y, Reif JC. 2017. Quantitative genetic framework highlights the role of epistatic effects for grain-yield heterosis in bread wheat. Nature Genetics 49: 1741–1746.

Kox MAR, Lüke C, Fritz C, van den Elzen E, van Alen T, Op den Camp HJM, Lamers LPM, Jetten MSM, Ettwig KF. 2016. Effects of nitrogen fertilization on diazotrophic activity of microorganisms associated with Sphagnum magellanicum. Plant and Soil 406: 83–100.

Kroll S, Agler MT, Kemen E. 2017. Genomic dissection of host–microbe and microbe–microbe interactions for advanced plant breeding. Current Opinion in Plant Biology 36: 71–78.

Li Z, Coffey L, Garfin J, Miller ND, White MR, Spalding EP, de Leon N, Kaeppler SM, Schnable PS, Springer NM, et al. 2018. Genotype-by-environment interactions affecting heterosis in maize. PLoS ONE 13: e0191321.

Li P, Zhuang Z, Cai H, Cheng S, Soomro AA, Liu Z, Gu R, Mi G, Yuan L, Chen F. 2016. Use of genotype-environment interactions to elucidate the pattern of maize root plasticity to nitrogen deficiency. Journal of Integrative Plant Biology 58: 242–253.

Lopez-Cruz M, Crossa J, Bonnett D, Dreisigacker S, Poland J, Jannink J-L, Singh RP, Autrique E, de los Campos G. 2015. Increased Prediction Accuracy in Wheat Breeding Trials Using a Marker × Environment Interaction Genomic Selection Model. G3: Genes/Genomes/Genetics 5: 569–582.

Luo X, Ding Y, Zhang L, Yue Y, Snyder JH, Ma C, Zhu J. 2017. Genomic Prediction of Genotypic Effects with Epistasis and Environment Interactions for Yield-Related Traits of Rapeseed (Brassica napus L.). Frontiers in Genetics 8: 1–9.

Lyra DH, de Freitas Mendonça L, Galli G, Alves FC, Granato ÍSC, Fritsche-Neto R. 2017. Multi-trait genomic prediction for nitrogen response indices in tropical maize hybrids. Molecular Breeding 37: 80.

Malinich EA, Bauer CE. 2018. The plant growth promoting bacterium Azospirillum brasilense is vertically transmitted in Phaseolus vulgaris (common bean). Symbiosis 76: 97–108.

Massman JM, Gordillo A, Lorenzana RE, Bernardo R. 2013. Genomewide predictions from maize single-cross data. Theoretical and Applied Genetics 126: 13–22.

Moellers TC, Singh A, Zhang J, Brungardt J, Kabbage M, Mueller DS, Grau CR, Ranjan A, Smith DL, Chowda-Reddy R V., et al. 2017. Main and epistatic loci studies in soybean for Sclerotinia sclerotiorum resistance reveal multiple modes of resistance in multi-environments. Scientific Reports 7: 3554.

Morosini JS, Mendonça LDF, Lyra DH, Galli G, Vidotti MS, Fritsche-Neto R. 2017. Association mapping for traits related to nitrogen use efficiency in tropical maize lines under field conditions. Plant and Soil 421: 453–463.

Munaro EM, Eyhérabide GH, D'Andrea KE, Cirilo AG, Otegui ME. 2011. Heterosis×environment interaction in maize: What drives heterosis for grain yield? Field Crops Research 124: 441–449.

Peiffer JA, Spor A, Koren O, Jin Z, Tringe SG, Dangl JL, Buckler ES, Ley RE. 2013. Diversity and heritability of the maize rhizosphere microbiome under field conditions. Proceedings of the National Academy of Sciences of the United States of America 110: 6548–53.

Pérez-Rodríguez P, Gianola D, González-Camacho JM, Crossa J, Manès Y, Dreisigacker S. 2012. Comparison between linear and non-parametric regression models for genome-enabled prediction in wheat. G3: Genes/Genomes/Genetics 2: 1595–1605.

Pérez-Rodríguez P, de los Campos G. 2014. Genome-wide regression and prediction with the BGLR statistical package. Genetics 198: 483–495.

Picard C, Bosco M. 2005. Maize heterosis affects the structure and dynamics of indigenous rhizospheric auxins-producing Pseudomonas populations. FEMS Microbiology Ecology 53: 349–357.

Picard C, Bosco M. 2006. Heterozygosis drives maize hybrids to select elite 2,4-diacethylphloroglucinol-producing Pseudomonas strains among resident soil populations. FEMS Microbiology Ecology 58: 193–204.

Ripley B, Venables B, Bates D M, Hornik K, Gebhardt A, Firth D. 2018. MASS. Support functions and datasets for Venables and Ripley's MASS. [WWW document] URL http://cran.r-project.org/web/packages/MASS/MASS.pdf. [accessed 25 August 2018].

Rodrigues Neto J, Malavolta V A, Victor O. 1986. Meio simples para o isolamento e cultivo 828 de Xanthomonas campestris pv. citri tipo B. Summa Phytopathol 12:32.

Rosier A, Bishnoi U, Lakshmanan V, Sherrier DJ, Bais HP. 2016. A perspective on inter-kingdom signaling in plant–beneficial microbe interactions. Plant Molecular Biology 90: 537–548.

Rozier C, Erban A, Hamzaoui J, Prigent-Combaret C, Comte G, Kopka J, Czarnes S, Legendre L. 2016. Xylem Sap Metabolite Profile Changes During Phytostimulation of Maize by the Plant Growth-Promoting Rhizobacterium, Azospirillum lipoferum CRT1. Journal of Postgenomics Drug & Biomarker Development 6: 1–10.

Rybak K, See PT, Phan HTT, Syme RA, Moffat CS, Oliver RP, Tan KC. 2017. A functionally conserved Zn2Cys6binuclear cluster transcription factor class regulates necrotrophic effector gene expression and host-specific virulence of two major Pleosporales fungal pathogens of wheat. Molecular Plant Pathology 18: 420–434.

Seifert F, Thiemann A, Grant-Downton R, Edelmann S, Rybka D, Schrag TA, Frisch M, Dickinson HG, Melchinger AE, Scholten S. 2018. Parental expression variation of small RNAs is negatively correlated with grain yield heterosis in a maize breeding population. Frontiers in Plant Science 9:13.

Shameer S, Prasad TNVK V. 2018. Plant growth promoting rhizobacteria for sustainable agricultural practices with special reference to biotic and abiotic stresses. Plant Growth Regulation 84: 603–615.

Sousa MB, Cuevas J, Couto EG de O, Pérez-Rodríguez P, Jarquín D, Fritsche-Neto R, Burgueño J, Crossa J. 2017. Genomic-enabled prediction in maize using kernel models with genotype × environment interaction. G3: Genes/Genomes/Genetics 7: g3.117.042341.

Technow F, Schrag TA, Schipprack W, Bauer E, Simianer H, Melchinger AE. 2014. Genome properties and prospects of genomic prediction of hybrid performance in a breeding program of maize. Genetics 197: 1343–1355.

Trachsel S, Kaeppler SM, Brown KM, Lynch JP. 2013. Maize root growth angles become steeper under low N conditions. Field Crops Research 140: 18–31.

Unterseer S, Bauer E, Haberer G, Seidel M, Knaak C, Ouzunova M, Meitinger T, Strom TM, Fries R, Pausch H, et al. 2014. A powerful tool for genome analysis in maize: development and evaluation of the high density 600 k SNP genotyping array. BMC Genomics 15: 823.

Van Raden PM. 2008. Efficient methods to compute genomic predictions. Journal of Dairy Science 91: 4414–4423.

Vandenberghe LP de S, Marcela Blandon Garcia L, Rodrigues C, Cândido Camara M, Vinícius de Melo Pereira G, de Oliveira J, Ricardo Soccol C. 2017. Potential applications of plant probiotic microorganisms in agriculture and forestry. AIMS Microbiology 3: 629–648.

Wimmer V, Albrecht T, Auinger H-J, Schön C-C. 2012. synbreed: a framework for the analysis of genomic prediction data using R. Bioinformatics 28: 2086–2087.

Yang Z, Jin L, Zhu H, Wang S, Zhang G, Liu G. 2018. Analysis of epistasis among QTLs on heading date based on single segment substitution lines in Rice. Scientific Reports 8: 3059.

Yang J, Mezmouk S, Baumgarten A, Buckler ES, Guill KE, McMullen MD, Mumm RH, Ross-Ibarra J. 2017. Incomplete dominance of deleterious alleles contributes substantially to trait variation and heterosis in maize. PLoS Genetics 13: e1007019.

Zaidi PH, Seetharam K, Krishna G, Krishnamurthy L, Gajanan S, Babu R, Zerka M, Vinayan MT, Vivek BS. 2016. Genomic regions associated with root traits under drought stress in tropical maize (Zea mays L.). PLoS ONE 11: 1–18.

Zamioudis C, Pieterse CMJ. 2012. Modulation of host immunity by beneficial microbes. Molecular Plant-Microbe Interactions 25: 139–150.

Zhang X, Pérez-Rodríguez P, Semagn K, Beyene Y, Babu R, López-Cruz MA, San Vicente F, Olsen M, Buckler E, Jannink J-L, et al. 2015. Genomic prediction in biparental tropical maize populations in water-stressed and well-watered environments using low-density and GBS SNPs. Heredity 114: 291–299.

TABLES

Table 1 Wald test for fixed effects and Likelihood Ratio Test for random effects from the joint diallel analysis of 118 maize hybrids evaluated under N stress and N stress plus *Azospirillum brasilense* treatments.

Effects	PH	SDM	RDM	LRL	ARL	RV	RAD	SRL	SRSA	RSR
Fixed										
Year (Y)	1,484.0**	576.1**	29.3**	42.5**	1.6	11.6**	116.0**	11.7**	103.6**	818.5**
Block/Year	73.0**	4.0**	18.5**	27.8**	13.0*	63.4**	223.0**	88.0**	58.4**	22.8**
Countertop/Block	530.0**	164.8**	159.2**	185.6**	205.2**	182.6**	9.0	14.9*	20.5**	67.2**
Inoculation (I)	0	0.1	8.8**	0.2	1.2	10.3**	25.0**	11.7**	8.6**	3.4
Y x I	0	0.1	0.5	1.0	0	0	1.0	1.7	1.1	1.3
Random										
GCA	2.7	0.5	7.5**	12.4**	17.5**	16.4**	11.6**	7.9**	6.3*	6.1*
GCA x Y	-4.5×10^{-7}	-3.5×10^{-7}	0.9	7.4×10^{-2}	1.8	1,6	2.1	4.3*	5.4*	19.8**
GCA x I	1.1×10^{-2}	-2.3×10^{-5}	5.0*	1.3×10^{-5}	1.4	3.3	11.1**	6.9**	5.2*	1.7
SCA	0.3	2.1	1.0	-3.1×10^{-6}	4.3*	3.1	3.2	6.3*	6.2*	2.8
SCA x Y	15.0**	7.8**	1.0	3.5	6.3×10^{-2}	5.7×10^{-3}	0.2	-1.1×10^{-6}	8.4×10^{-2}	0.2
SCA x I	-3.0×10^{-5}	-1.5×10^{-5}	-4.4×10^{-5}	8.1×10^{-6}	-3.2×10^{-5}	-3.9×10^{-5}	-4.3×10^{-5}	-1.6×10^{-5}	-4.0×10^{-5}	-3.9×10^{-5}

PH: plant height, SDM: shot dry mass, RDM: root dry mass, LRL: lateral root length, ARL: axial root length, RV: root volume, RAD: root average diameter, SRL: specific root length, SRSA: specific root surface area, and RSR: root shoot ratio. Significant at 5% (*) or 1% (**) level.

Table 2 Estimates of genetic parameters from individual and joint diallel analysis of maize hybrids evaluated under N stress and N stress plus *Azospirillum brasilense* treatments.

Analysis	$\hat{\sigma}^2_G$	$\hat{\sigma}^2_{GY}$	$\hat{\sigma}^2_{GI}$	$\hat{\sigma}^2_H$	$\hat{\sigma}^2_{HY}$	$\hat{\sigma}^2_{HI}$	$\hat{\sigma}^2_\epsilon$	$\hat{\sigma}^2_a$	$\hat{\sigma}^2_d$	$\hat{h}^2$	$\hat{H}^2$	BR
RDM												
N stress	6.24	1.62 x 10^{-5}	-	3.06	2.31 x 10^{-5}	-	159.74	24.95	12.22	0.13	0.19	0.80
N stress + *Azospirillum*	31.17	7.50	-	1.84	1.95 x 10^{-5}	-	13.87	126.83	7.38	0.46	0.49	0.97
Joint	15.05	2.20	3.87	3.07	3.73	6.3 x 10^{-5}	145.76	60.18	12.29	0.28	0.33	0.91
RV												
N stress	2.4	1.89 x 10^{-6}	-	0.35	9.04 x 10^{-7}	-	18.75	9.54	1.39	0.32	0.36	0.93
N stress + *Azospirillum*	6.40	0.70	-	0.63	1.05 x 10^{-5}	-	16.99	25.62	2.55	0.56	0.62	0.95
Joint	3.92	0.27	0.40	0.63	3.12 x 10^{-2}	1.12 x 10^{-5}	17.75	15.66	2.53	0.44	0.51	0.92
RAD												
N stress	4.28	0.40	-	0.86	2.89 x 10^{-6}	-	28.61	17.12	3.43	0.34	0.41	0.90
N stress + *Azospirillum*	11.86	0.39	-	0.35	1.33	-	30.74	47.44	1.40	0.60	0.61	0.99
Joint	6.51	0.71	1.49	1.16	0.30	1.37 x 10^{-5}	29.78	26.04	4.62	0.43	0.50	0.92
SRL												
N stress	84.81	43.98	-	50.23	3.04 x 10^{-4}	-	1,019.22	339.25	200.90	0.22	0.35	0.77
N stress + *Azospirillum*	260.43	0.40	-	2.50	9.33 x 10^{-5}	-	1,077.83	1,041.70	10.00	0.51	0.51	1.00
Joint	134.40	32.84	32.49	50.39	4.60 x 10^{-5}	1.01 x 10^{-4}	993.97	537.60	201.55	0.31	0.42	0.84
SRSA												
N stress	1,529.70	1,085.88	-	1,024.40	7.00 x 10^{-4}	-	17,058.29	6,118.79	4,097.59	0.22	0.37	0.74
N stress + *Azospirillum*	3,587.74	61.92	-	357.63	7.98 x 10^{-4}	-	16,801.18	14,351.97	1,430.50	0.44	0.48	0.95
Joint	2,034.36	723.48	443.77	960.39	120.99	5.33 x 10^{-3}	16,729.18	8,137.46	3,841.57	0.28	0.41	0.81

$\hat{\sigma}^2_G$: GCA variance; $\hat{\sigma}^2_{GY}$: GCA x year variance; $\hat{\sigma}^2_{GI}$: GCA x inoculation variance; $\hat{\sigma}^2_H$: SCA variance; $\hat{\sigma}^2_{HY}$: SCA x year variance, $\hat{\sigma}^2_{HI}$: SCA x inoculation variance; $\hat{\sigma}^2_\epsilon$: residual error variance; $\hat{\sigma}^2_a$: additive genetic variance and $\hat{\sigma}^2_d$: dominance genetic variance, narrow-sense heritability ($\hat{h}^2$), broad-sense heritability ($\hat{H}^2$), and Baker's ratio (BR) for root dry mass (RDM), root volume (RV), root average diameter (RAD), specific root length (SRL) and specific root surface area (SRSA). Variance components of RDM, RAD and SRL must be multiplied by 10^{-3}, 10^{-4} and 10^{3}, respectively, to return to its correct magnitude.

FIGURES

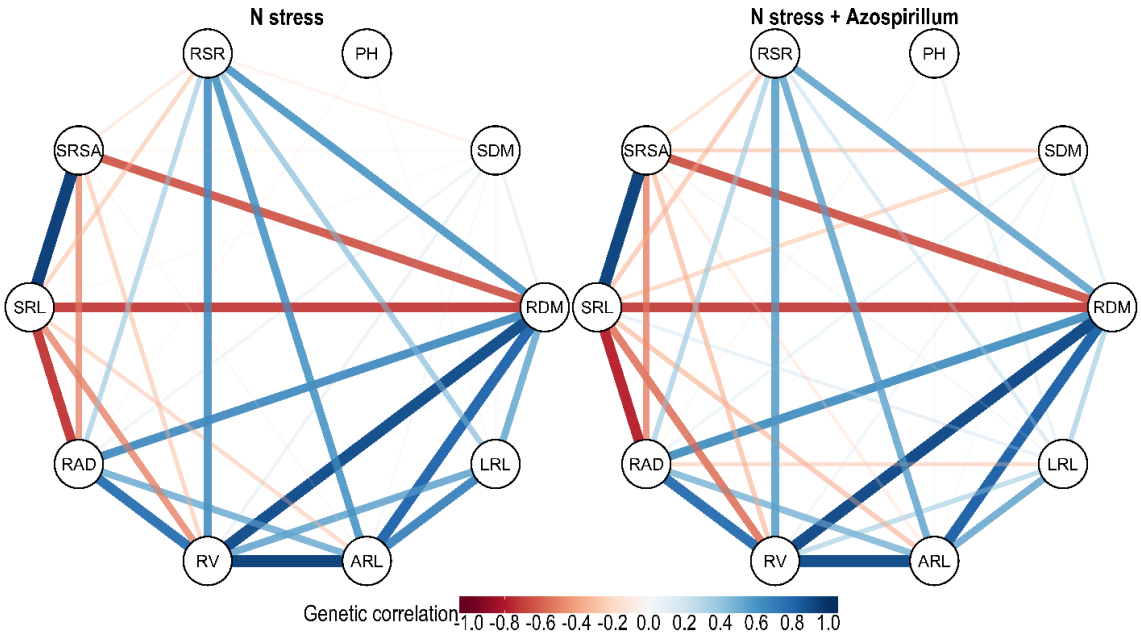

Fig. 1 Network visualization of the genetic correlations between traits evaluated in hybrids under N stress and N stress plus *Azospirillum brasilense*. PH: plant height, SDM: shot dry mass, RDM: root dry mass, LRL: lateral root length, ARL: axial root length, RV: root volume, RAD: root average diameter, SRL: specific root length, SRSA: specific root surface area, and RSR: root shoot ratio.

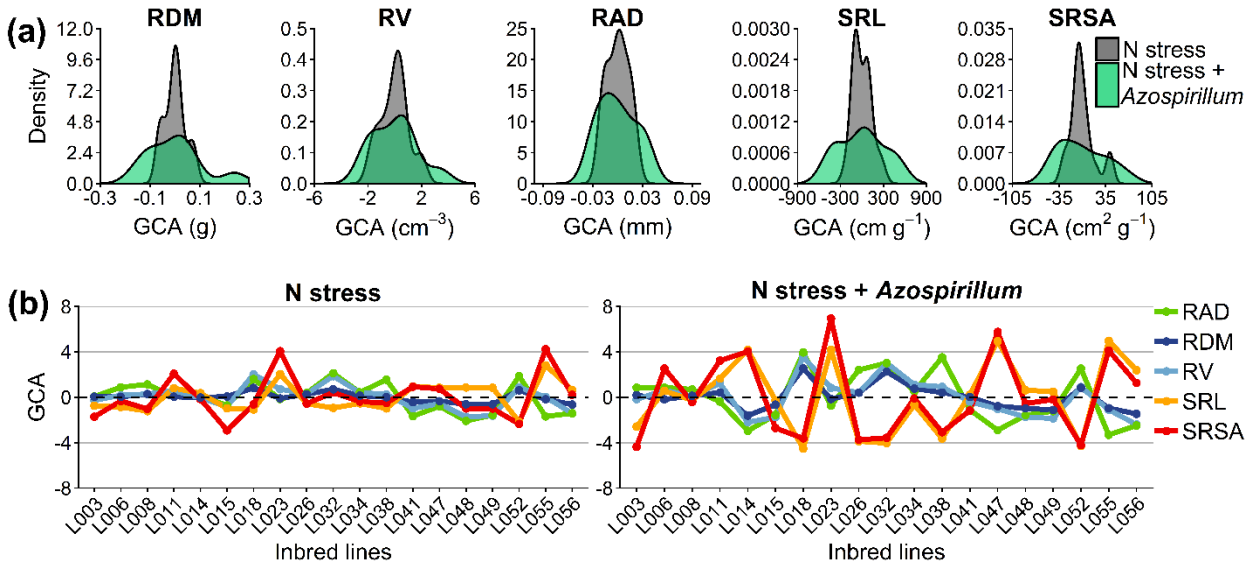

Fig. 2 General Combining Ability (GCA) of the 19 parental inbred lines obtained via Best Linear Unbiased Predictior (BLUP) for N stress and N stress plus *Azospirillum brasilense* treatments. **(a)** Density plots by trait. **(b)** Distribuition by inbred lines (for this plot, the values of RDM, RAD, SRL and SRSA must be multiplied by 10^{-1}, 10^{-2}, 10^{2} and 10, respectively, to return to its correct magnitude). RDM: root dry mass, RV: root volume, RAD: root average diameter, SRL: specific root length, and SRSA: specific root surface area.

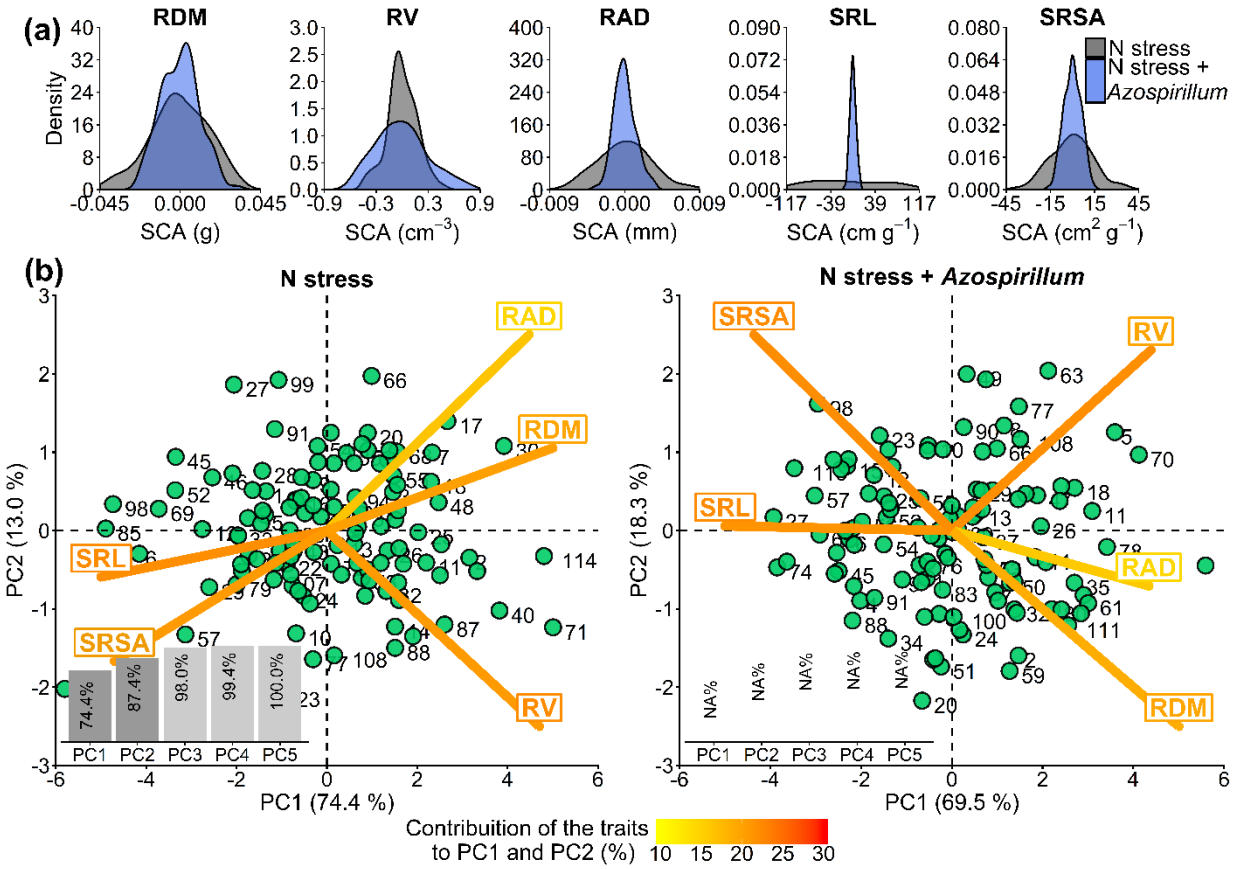

Fig. 3 Specific Combining Ability (SCA) of the 118 maize hybrids obtained via Best Linear Unbiased Predictior (BLUP) for N stress and N stress plus *Azospirillum brasilense* treatments. **(a)** Density plots by trait. **(b)** Principal Components (PC), where each number corresponds to a different hybrid (more details are given in the Table **S5**). RDM: root dry mass, RV: root volume, RAD: root average diameter, SRL: specific root length, and SRSA: specific root surface area.

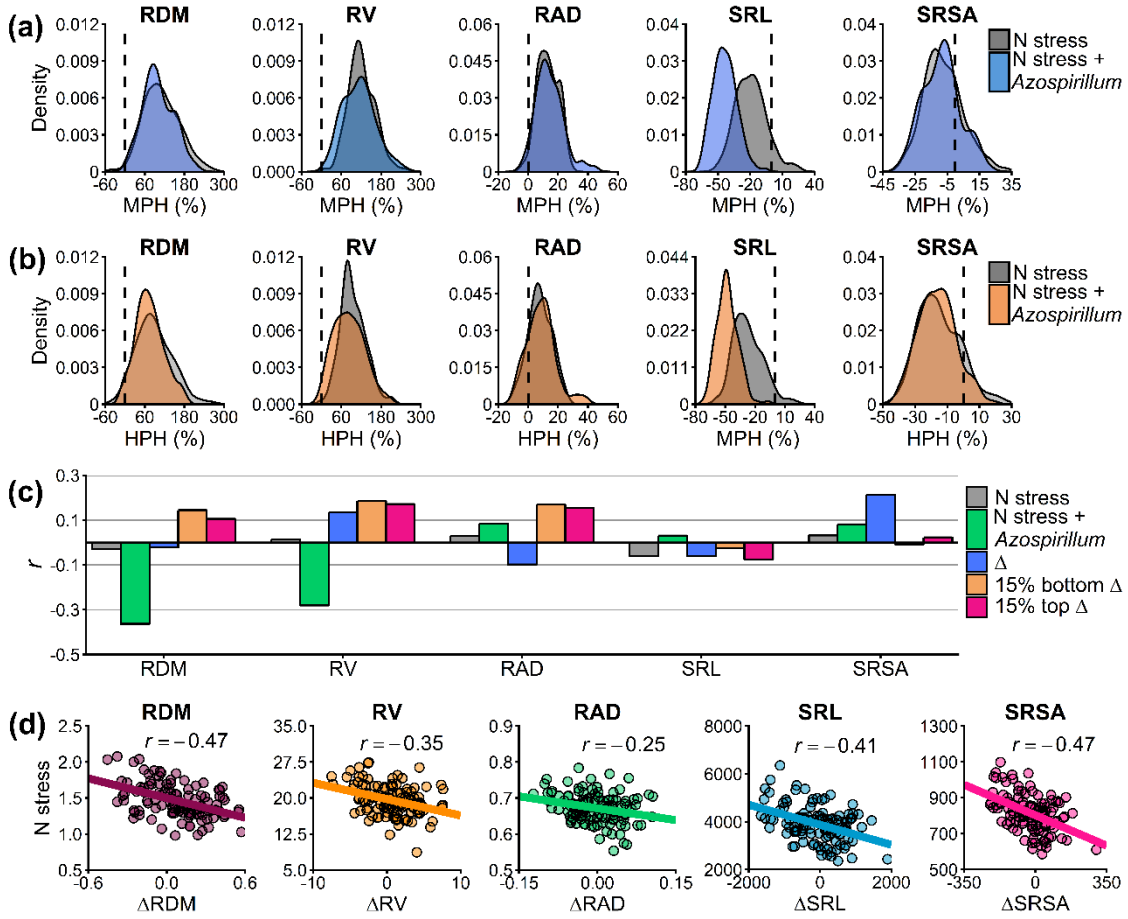

Fig. 4 Heterosis effect and relationship with intrinsic root growth rates. **(a)** and **(b)** show the Mid-Parente Heterosis (MPH %) and the High-Parent Heterosis (HPH %), respectively. Black dashed line indicate the point where y is equal to zero. **(c)** Pearson correlation between hybrids adjusted means and genomic heterosigosity. Delta (Δ) is the change in root traits due the inoculation (difference between N stress plus *Azospirillum brasilense* inoculation and N stress) and thus, 15% bottom Δ and 15% top Δ represents the hybrids with smaller and higher responsiveness to inoculation, respectively. **(d)** Pearson correlation between hybrids adjusted means of N stress and delta. RDM: root dry mass, RV: root volume, RAD: root average diameter, SRL: specific root length, and SRSA: specific root surface area.

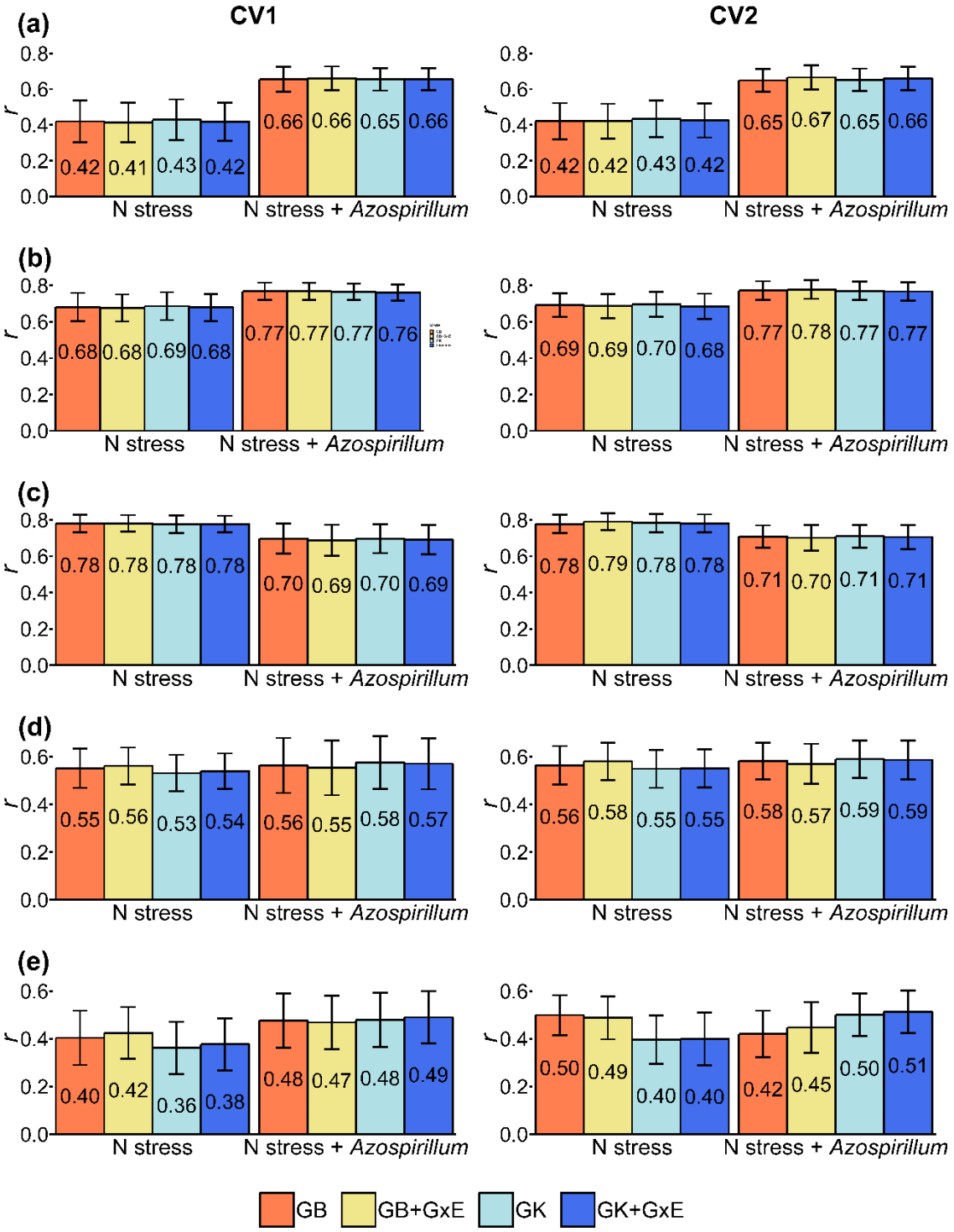

Fig. 5 Prediction accuracy of GB, GB + G×E, GK and GK +G×E models via cross-validation methods 1 and 2 for maize traits evaluated under N stress and N stress plus *Azospirillum brasilense* treatments. **(a)** root dry mass (RDM), **(b)** root volume (RV), **(c)** root average diameter (RAD), **(d)** specific root length (SRL), and **(e)** specific root surface area (SRSA).

SUPPLEMENTARY TABLES

Table S1 Soil chemical and physic characteristics.

Parameters	Unity	Value
Soil pH (H_2O)	-	5.6
Soil pH ($CaCl_2$)	-	4.7
P (Mehlich)	$mg.dm^{-3}$	72.5
K	$mg.dm^{-3}$	118.0
Ca^{+2}	$cmolc.dm^{-3}$	3.4
Mg^{+2}	$cmolc.dm^{-3}$	1.0
Al^{+3} (KCl)	$cmolc.dm^{-3}$	0.1
Aluminium saturation (m)	%	2.1
Organic matter	$g.dm^{-3}$	25.7
Cation-exchange capacity (CEC)	$cmolc.dm^{-3}$	8.6
Clay	$g\ kg^{-1}$	226
Silt	$g\ kg^{-1}$	167
Sandy	$g\ kg^{-1}$	607
Classification: *sandy loam soil*		

Table S2 Wald test for fixed effects and Likelihood Ratio Test (LRT) for random effects from the diallel analysis of 118 maize hybrids evaluated under N stress.

Effects	PH	SDM	RDM	LRL	ARL	RV	RAD	SRL	SRSA	RSR
Fixed										
Year (Y)	1,102.0**	363.0**	12.8**	31.9**	0.9	5.2*	74.0**	2.4	43.3**	436.1**
Block/Year	32.0**	4.4	11.9*	16.6**	8.6	38.2**	140.0**	73.3**	54.8**	6.6
Countertop/Block	241.00**	86.0**	75.0**	92.6**	104.6**	92.1**	9.0*	12.5	14.3*	24.9**
Random										
GCA	4.3×10^{-2}	-4.0×10^{-7}	3.3	7.2**	13.5**	11.0**	8.7**	3.1	2.8	0.5
GCA x Y	-6.7×10^{-7}	6.0×10^{-2}	-2.4×10^{-6}	-1.3×10^{-5}	-7.7×10^{-6}	-1.8×10^{-6}	0.3	2.5	4.5*	22.9**
SCA	0.4	8.3×10^{-7}	0.5	-1.5×10^{-5}	4.0×10^{-2}	0.5	1.2	3.10.8	3.5	0.4
SCA x Y	-1.9×10^{-6}	0.8	-7.8×10^{-7}	2.2×10^{-5}	-1.3×10^{-6}	-2.3×10^{-7}	-7.0×10^{-6}	-1.6×10^{-5}	-1.1×10^{-6}	-9.7×10^{-7}

PH: plant height, SDM: shot dry mass, RDM: root dry mass, LRL: lateral root length, ARL: axial root length, RV: root volume, RAD: root average diameter, SRL: specific root length, SRSA: specific root surface area, and RSR: root shoot ratio. Significant at 5% (*) or 1% (**) level.

Table S3 Wald test for fixed effects and Likelihood Ratio Test for random effects from the diallel analysis of 118 maize hybrids evaluated under N stress plus *Azospirillum brasilense*.

Effects	PH	SDM	RDM	LRL	ARL	RV	RAD	SRL	SRSA	RSR
Fixed										
Year (Y)	1068.0**	376.9**	20.5**	18.4**	0.5	6.7**	47.0**	11.9**	69.4**	432.3**
Block/Year	30.0**	1.3	9.8*	19.1**	5.9	27.4**	109.0**	36.0**	22.1**	24.0**
Countertop/Block	297.0**	90.9**	89.3**	100.4**	107.7**	95.9**	3.0	7.8	13.5*	55.9**
Random										
GCA	3.7*	0.4	9.3**	7.0**	10.9**	16.0**	18.0**	16.9**	13.7**	12.5**
GCA x Y	0.4	-3.6×10^{-6}	2.8	3.9*	9.5**	2.6	0.2	3.2×10^{-7}	2.4×10^{-2}	2.3
SCA	0.3	-1.5×10^{-5}	0.2	3.1×10^{-3}	3.2	1.5	7.7×10^{-2}	9.0×10^{-7}	0.5	3.5×10^{-2}
SCA x Y	-1.3×10^{-6}	-1.3×10^{-5}	-1.1×10^{-6}	4.1×10^{-4}	-9.9×10^{-7}	-1.5×10^{-5}	0.6	-6.4×10^{-7}	-7.3×10^{-7}	0.5

PH: plant height, SDM: shot dry mass, RDM: root dry mass, LRL: lateral root length, ARL: axial root length, RV: root volume, RAD: root average diameter, SRL: specific root length, SRSA: specific root surface area, and RSR: root shoot ratio. Significant at 5% (*) or 1% (**) level.

Table S4 Estimates of General Combining Ability (GCA) for 19 maize parental inbred lines in conditions of N stress and N stress plus *Azospirillum brasilense*.

Inbred line	N stress					N stress + *Azospirillum*				
	RDM	**VR**	**RAD**	**SRL**	**SRSA**	**RDM**	**VR**	**RAD**	**SRL**	**SRSA**
L003	0.004	-0.27	0.001	-74.82	-17.21	0.019	-0.18	0.008	-258.51	-43.66
L006	0.003	0.18	0.009	-86.54	-3.32	-0.019	0.62	0.008	56.02	25.26
L008	0.028	0.29	0.011	-122.72	-10.33	0.012	0.10	0.007	-25.98	-4.32
L011	0.005	0.57	0.000	78.87	20.68	0.042	1.22	-0.004	163.96	32.23
L014	-0.003	-0.07	0.001	35.23	-1.75	-0.162	-2.20	-0.030	417.11	40.13
L015	0.007	-0.82	-0.007	-98.56	-29.21	-0.065	-1.75	-0.016	-26.48	-27.20
L018	0.081	2.03	0.016	-107.85	-6.29	0.253	3.56	0.039	-452.66	-36.25
L023	-0.010	0.71	-0.002	203.84	40.57	-0.016	0.82	-0.007	418.92	69.34
L026	0.026	0.29	0.004	-56.39	-5.67	0.040	0.41	0.024	-387.77	-37.47
L032	0.070	1.86	0.021	-94.41	4.11	0.226	3.02	0.030	-404.32	-35.81
L034	0.014	0.41	0.004	-54.20	-3.88	0.076	1.11	0.005	-67.22	-1.06
L038	0.000	0.26	0.015	-98.82	-5.19	0.041	0.92	0.035	-364.43	-30.76
L041	-0.044	-0.98	-0.017	93.93	9.27	0.002	-0.40	-0.011	22.27	-11.78
L047	-0.035	-0.57	-0.008	83.80	7.31	-0.079	-1.03	-0.029	493.33	57.48
L048	-0.061	-1.73	-0.021	85.85	-9.91	-0.098	-1.73	-0.016	61.92	-5.54
L049	-0.062	-1.63	-0.016	83.58	-10.07	-0.112	-1.87	-0.012	48.57	-2.09
L052	0.061	0.87	0.018	-217.20	-23.56	0.084	0.90	0.025	-430.26	-42.22
L055	-0.018	0.01	-0.017	280.99	42.31	-0.096	-1.10	-0.033	497.19	41.08
L056	-0.065	-1.42	-0.014	65.43	2.13	-0.147	-2.41	-0.025	238.34	12.63

RDM: root dry mass, RV: root volume, RAD: root average diameter, SRL: specific root length, and SRSA: specific root surface area.

Table S5 Estimates of Specific Combining Ability (SCA) for 118 maize hybrids in conditions of N stress and N stress plus *Azospirillum brasilense*.

Nº	Cross	N stress					N stress + *Azospirillum*				
		RDM	VR	RAD	SRL	SRSA	RDM	VR	RAD	SRL	SRSA
1	L003xL006	-0.013	-0.15	-0.0024	59.52	3.25	-0.006	-0.22	-0.0001	-0.25	-0.61
2	L003xL008	0.030	0.27	0.0039	-149.88	-20.47	0.015	-0.03	-0.0012	-6.35	-9.19
3	L003xL014	0.011	0.07	0.0011	-114.43	-15.03	-0.006	-0.20	-0.0005	-2.24	-3.04
4	L003xL015	0.000	-0.02	-0.0011	-1.69	-1.60	-0.017	-0.43	-0.0011	1.68	2.52
5	L003xL018	-0.001	-0.05	0.0015	-34.71	-0.35	0.021	0.59	0.0031	-6.54	-3.64
6	L003xL023	-0.028	-0.32	-0.0050	266.52	32.57	-0.003	-0.22	-0.0027	6.73	4.78
7	L003xL026	0.012	0.06	0.0036	-185.83	-24.36	0.006	-0.05	0.0001	-3.66	-5.05
8	L003xL032	0.026	0.28	0.0067	-167.35	-15.59	0.005	0.39	0.0015	-1.13	2.53
9	L003xL034	0.004	-0.07	-0.0041	-7.48	-8.22	-0.007	-0.25	-0.0008	1.73	0.10
10	L003xL041	-0.001	0.11	-0.0006	102.98	16.35	-0.005	0.21	0.0005	8.09	0.40
11	L003xL047	0.014	0.19	0.0052	-127.45	-7.04	0.006	0.30	0.0036	-9.60	-5.25
12	L003xL049	-0.026	-0.18	-0.0039	132.59	20.49	-0.006	-0.07	-0.0011	5.21	7.52
13	L003xL052	0.008	0.01	0.0001	-9.82	1.92	0.005	0.15	-0.0001	-0.49	-0.86
14	L006xL008	0.014	0.26	0.0032	-33.40	1.76	-0.001	0.15	-0.0002	2.49	5.79
15	L006xL011	-0.014	-0.14	-0.0029	89.90	10.47	-0.015	-0.24	-0.0001	6.37	9.68
16	L006xL014	-0.016	-0.11	0.0015	-7.56	6.67	-0.008	-0.11	-0.0013	8.03	8.94
17	L006xL015	0.019	0.03	0.0026	-209.15	-32.68	0.005	-0.10	0.0005	-4.03	-5.65
18	L006xL023	0.020	0.12	0.0013	-151.28	-25.06	0.015	0.51	0.0014	-5.45	-5.29
19	L006xL026	0.001	-0.05	-0.0025	38.46	-2.47	0.007	0.04	-0.0004	-2.80	-4.42
20	L006xL038	0.005	-0.06	-0.0007	-108.49	-20.04	-0.009	-0.54	-0.0007	-3.10	-6.03
21	L006xL047	-0.008	-0.09	-0.0013	10.56	2.19	0.018	0.55	0.0005	-3.91	-5.03
22	L006xL049	-0.016	-0.03	0.0021	41.97	16.07	-0.001	0.02	0.0011	-1.10	-0.31
23	L006xL052	-0.005	0.16	0.0012	122.75	30.58	-0.008	0.02	-0.0004	5.51	8.97
24	L008xL011	0.005	0.09	-0.0033	70.71	7.76	0.006	-0.11	-0.0016	-2.39	-5.96
25	L008xL015	0.019	0.15	0.0021	-109.56	-15.00	0.000	0.03	-0.0016	11.88	-0.72
26	L008xL018	0.020	0.09	0.0012	-69.32	-5.38	0.002	0.15	0.0027	-5.53	-4.52
27	L008xL023	-0.032	-0.39	-0.0008	11.18	1.96	-0.021	-0.59	-0.0015	9.53	11.62
28	L008xL026	-0.008	-0.18	-0.0045	52.87	-0.22	0.004	0.16	0.0004	-0.85	-0.97
29	L008xL032	-0.017	-0.15	-0.0026	169.02	28.36	0.006	0.08	0.0008	0.03	1.03
30	L008xL034	0.032	0.15	0.0048	-250.99	-39.26	-0.005	0.12	0.0009	0.84	5.38
31	L008xL041	-0.017	-0.11	-0.0003	110.73	17.67	-0.017	-0.32	-0.0005	3.67	6.69
32	L008xL047	0.016	0.22	0.0003	-35.98	-5.22	0.005	0.04	0.0001	-6.40	-6.76
33	L008xL048	-0.012	-0.10	-0.0051	120.45	10.48	0.019	0.91	0.0015	0.84	6.13
34	L008xL049	-0.003	-0.07	-0.0026	-5.10	-0.04	-0.011	-0.44	-0.0012	-0.06	-1.11
35	L008xL052	-0.021	-0.13	0.0076	-103.83	-1.19	0.009	0.19	0.0019	-8.07	-9.46
36	L008xL056	-0.021	-0.17	-0.0015	74.36	6.41	-0.018	-0.49	-0.0006	2.71	3.61
37	L011xL014	0.009	0.03	-0.0002	-53.98	-7.92	0.000	0.00	0.0011	-2.65	-1.44
38	L011xL015	0.020	0.32	0.0027	-52.17	-1.14	0.002	-0.09	0.0012	-6.52	-6.79
39	L011xL018	-0.002	-0.05	-0.0027	80.11	7.97	0.004	0.04	-0.0004	-0.01	-0.26
40	L011xL023	0.026	0.38	0.0086	-175.46	-13.68	-0.008	-0.18	-0.0003	3.38	5.13

(The table continues on the next page)

(Continuation of the previous table)

Nº	Cross	N stress					N stress + *Azospirillum*				
		RDM	**VR**	**RAD**	**SRL**	**SRSA**	**RDM**	**VR**	**RAD**	**SRL**	**SRSA**
41	L011xL026	0.006	0.06	0.0034	-79.23	-5.73	0.022	0.47	0.0001	-3.51	-5.39
42	L011xL032	0.016	0.16	-0.0001	-4.46	0.13	-0.002	0.04	-0.0010	6.20	7.15
43	L011xL034	-0.010	-0.04	0.0007	47.02	9.18	0.005	0.79	0.0018	2.04	9.32
44	L011xL038	0.008	0.06	0.0003	-11.51	-4.52	0.016	0.23	-0.0001	-4.28	-6.10
45	L011xL047	-0.038	-0.40	-0.0017	136.45	19.73	-0.020	-0.52	-0.0005	4.77	4.54
46	L011xL056	-0.020	-0.28	-0.0043	130.19	9.47	-0.006	-0.15	-0.0007	0.84	-1.69
47	L014xL015	0.014	0.15	0.0021	-94.72	-7.79	0.005	0.32	0.0018	-4.61	-2.95
48	L014xL018	0.021	0.14	0.0029	-174.22	-18.86	-0.001	-0.03	-0.0003	0.76	0.74
49	L014xL023	-0.004	0.00	0.0003	54.56	16.17	0.004	0.42	0.0010	3.07	6.57
50	L014xL026	0.013	0.06	-0.0016	-50.97	-6.73	0.002	0.02	0.0009	-5.37	-5.27
51	L014xL032	-0.005	-0.01	0.0044	-87.42	-0.23	-0.002	-0.31	-0.0012	-2.86	-5.81
52	L014xL034	-0.034	-0.33	-0.0030	141.72	23.45	-0.008	-0.17	-0.0007	3.90	4.31
53	L014xL038	0.000	0.14	0.0029	-49.25	4.39	0.003	0.02	0.0002	-4.00	-2.60
54	L014xL041	-0.003	-0.10	-0.0030	-35.09	-12.39	-0.001	-0.19	-0.0018	5.27	2.28
55	L014xL047	0.008	0.05	0.0015	-142.03	-15.03	0.002	0.07	-0.0011	4.89	1.47
56	L014xL048	-0.006	-0.12	-0.0059	137.01	8.95	-0.009	-0.19	-0.0013	6.26	4.27
57	L014xL049	-0.011	-0.11	-0.0036	511.42	6.68	-0.019	-0.43	-0.0005	7.98	9.85
58	L014xL056	-0.004	0.09	0.0007	57.41	12.41	0.009	0.20	0.0018	-10.07	-9.78
59	L015xL018	0.009	0.08	0.0032	-100.46	-9.54	0.004	-0.15	-0.0001	-6.97	-9.67
60	L015xL023	-0.007	-0.06	-0.0011	56.60	4.66	-0.016	-0.45	-0.0014	5.34	4.27
61	L015xL032	0.012	-0.07	-0.0006	-83.48	-17.97	0.018	0.24	0.0008	-9.07	-10.80
62	L015xL034	-0.001	-0.12	-0.0051	78.77	4.01	0.002	0.07	-0.0001	-0.24	0.68
63	L015xL038	-0.004	-0.02	-0.0012	44.24	8.39	0.017	0.70	0.0014	-1.60	2.64
64	L015xL041	-0.012	-0.14	0.0018	-76.95	-9.23	-0.008	-0.18	-0.0003	3.42	5.03
65	L015xL047	-0.013	-0.10	-0.0028	68.11	8.93	-0.011	-0.19	-0.0010	7.91	8.97
66	L015xL052	0.007	-0.16	-0.0011	-145.53	-26.78	0.010	0.39	0.0003	0.21	0.85
67	L015xL055	-0.034	-0.24	-0.0074	453.79	57.75	-0.010	-0.14	-0.0003	2.73	5.72
68	L015xL056	-0.001	-0.01	0.0045	-156.95	-15.67	-0.008	-0.35	-0.0007	-3.63	-4.31
69	L018xL023	-0.018	-0.30	-0.0091	211.21	18.97	-0.012	-0.36	-0.0022	7.56	7.06
70	L018xL032	-0.009	0.18	0.0041	-34.74	-1.60	0.021	0.65	0.0034	-7.54	-7.37
71	L018xL038	0.052	0.49	0.0070	-203.86	-24.98	-0.009	-0.02	-0.0002	3.46	7.10
72	L018xL041	0.007	0.06	-0.0011	13.13	2.34	0.010	0.11	-0.0008	-1.83	-3.34
73	L018xL055	-0.008	-0.06	0.0005	41.82	9.89	0.001	0.14	0.0003	-1.92	0.61
74	L018xL056	0.000	-0.05	-0.0026	101.48	9.68	-0.014	-0.49	-0.0035	10.70	6.57
75	L023xL026	0.026	0.21	0.0023	-122.39	-18.55	-0.011	-0.30	0.0008	-0.09	0.81
76	L023xL032	0.005	0.16	0.0025	-61.93	-3.50	-0.004	-0.12	-0.0005	0.21	-0.04
77	L023xL034	0.002	0.15	0.0014	95.02	18.88	0.009	0.46	0.0018	-0.36	2.03
78	L023xL038	0.001	0.13	0.0044	-30.13	2.76	0.011	0.40	0.0025	-10.19	-9.03
79	L023xL041	-0.010	-0.04	-0.0046	164.99	15.48	0.004	0.22	0.0007	-1.95	0.12
80	L023xL047	-0.004	-0.09	0.0005	-63.12	-6.97	0.013	0.18	0.0002	-6.92	-9.87
81	L023xL048	0.002	0.10	0.0010	-2.42	3.88	0.006	0.10	0.0003	-5.00	-5.88
82	L023xL049	0.023	0.24	0.0043	-102.42	-12.49	0.006	-0.05	-0.0010	1.54	-1.38

(The table continues on the next page)

(Continuation of the previous table)

Nº	Cross	N stress					N stress + *Azospirillum*				
		RDM	VR	RAD	SRL	SRSA	RDM	VR	RAD	SRL	SRSA
83	L023xL055	-0.005	0.03	0.0008	71.91	13.23	-0.005	-0.24	0.0002	-2.44	-1.03
84	L023xL056	-0.004	-0.04	-0.0061	156.55	10.96	0.011	0.48	0.0007	2.94	4.85
85	L026xL032	-0.037	-0.44	-0.0051	276.27	38.26	-0.004	0.13	0.0016	-1.35	0.15
86	L026xL038	-0.013	0.00	0.0015	52.56	14.87	-0.011	-0.12	-0.0009	4.48	6.81
87	L026xL047	0.026	0.33	0.0040	-91.90	-7.16	-0.012	-0.32	-0.0012	5.07	4.70
88	L032xL034	0.023	0.28	0.0017	-6.85	1.98	-0.009	-0.49	-0.0021	3.90	1.03
89	L032xL038	0.019	0.06	-0.0031	-15.86	-9.39	-0.003	-0.07	0.0000	0.21	0.50
90	L032xL047	0.017	0.19	0.0023	-60.52	-4.51	0.007	0.34	-0.0001	1.81	4.48
91	L032xL052	-0.004	-0.24	-0.0045	4.53	-5.33	-0.007	-0.34	-0.0018	3.04	0.76
92	L034xL041	0.003	0.00	0.0027	-124.11	-16.57	0.014	0.16	0.0005	-7.81	-9.71
93	L034xL047	0.010	0.18	0.0057	-52.15	1.36	0.007	0.01	0.0009	-4.01	-4.81
94	L034xL049	0.011	0.03	-0.0024	-61.56	-11.21	-0.013	-0.35	-0.0017	6.29	4.71
95	L034xL052	0.010	0.11	-0.0001	-24.22	-1.33	0.002	0.04	0.0027	-6.76	-6.18
96	L034xL055	0.001	0.02	-0.0012	34.19	3.07	0.006	-0.12	-0.0016	-1.83	-5.65
97	L034xL056	-0.025	-0.15	0.0016	47.91	13.06	0.008	0.04	-0.0010	1.15	-0.39
98	L038xL047	-0.043	-0.42	-0.0048	254.59	32.53	-0.010	-0.16	-0.0009	10.32	14.46
99	L038xL049	-0.025	-0.32	0.0006	-66.78	-3.80	0.004	0.26	0.0018	-4.26	-1.80
100	L038xL052	0.001	-0.03	-0.0022	64.69	7.75	0.001	-0.20	-0.0007	-1.73	-4.26
101	L038xL055	-0.011	-0.04	0.0021	-43.52	-2.86	-0.020	-0.54	-0.0017	13.47	3.08
102	L038xL056	0.013	0.08	0.0003	-114.70	-18.78	0.011	0.16	0.0015	-9.71	-10.86
103	L041xL047	-0.004	-0.06	-0.0062	155.91	10.10	0.000	-0.31	-0.0013	-2.04	-0.60
104	L041xL049	-0.018	-0.10	0.0016	13.85	7.38	0.002	0.23	0.0017	-4.22	-1.58
105	L041xL056	0.005	0.01	0.0014	-119.51	-21.25	-0.004	-0.09	0.0002	-0.99	-0.90
106	L047xL048	-0.011	-0.08	-0.0004	-46.53	-6.22	0.000	-0.08	-0.0011	0.94	-1.45
107	L047xL052	-0.009	-0.03	-0.0005	88.53	16.16	-0.001	0.00	0.0003	-0.19	1.20
108	L047xL055	0.020	0.20	-0.0021	127.78	4.91	0.017	0.53	0.0000	-0.09	-0.39
109	L047xL056	0.003	-0.03	-0.0008	-74.99	-14.11	-0.018	-0.30	0.0003	8.37	9.82
110	L048xL049	-0.001	-0.05	0.0005	-118.39	-14.36	-0.010	-0.40	0.0000	-3.60	-4.51
111	L048xL052	0.022	0.11	-0.0012	-90.27	-17.92	0.017	0.14	0.0003	-7.73	-11.23
112	L048xL055	-0.021	-0.23	-0.0032	98.14	5.72	-0.011	-0.22	0.0010	0.21	3.31
113	L048xL056	-0.018	-0.06	-0.0005	100.22	15.31	-0.011	-0.27	-0.0023	12.19	10.50
114	L049xL052	0.033	0.39	0.0091	-275.25	-26.60	0.001	0.16	-0.0004	1.25	0.13
115	L049xL056	-0.008	-0.02	-0.0007	-16.57	-0.61	0.032	0.69	0.0024	-14.58	-15.72
116	L052xL055	0.013	0.02	-0.0015	-92.51	-21.00	0.001	-0.07	-0.0006	0.77	1.50
117	L052xL056	-0.007	-0.11	-0.0013	-6.35	-2.06	-0.022	-0.41	0.0001	3.77	6.97
118	L055xL056	0.012	0.20	0.0024	-66.53	-10.20	0.008	0.33	0.0001	0.53	1.93

RDM: root dry mass, RV: root volume, RAD: root average diameter, SRL: specific root length, and SRSA: specific root surface area.

Table S6 Estimates of variance components and standard deviation (in parentheses) from prediction models for root dry mass (RDM). The values must be multiplied by 10^{-3} to return to its correct magnitude.

Treatment	σ_G^2	σ_H^2	σ_{GE}^2	σ_{HE}^2	σ_ϵ^2
GB					
N stress	6.03 (2.32)	10.95 (3.59)	-	-	5.25 (5.65)
N stress + *Azospirillum*	18.12 (6.53)	10.77 (3.16)	-	-	47.76 (5.07)
GB + G×E					
N stress	4.33 (1.94)	8.48 (3.26)	3.78 (1.55)	8.98 (3.92)	45.58 (6.11)
N stress + *Azospirillum*	13.36 (5.98)	8.48 (2.96)	6.97 (3.03)	9.02 (3.23)	37.91 (5.08)
GK					
N stress	0.856 (0.75)	10.45 (4.53)	-	-	54.96 (5.82)
N stress + *Azospirillum*	15.77 (8.16)	11.49 (6.34)	-	-	49.30 (5.16)
GK + G×E					
N stress	0.52 (0.55)	6.88 (3.74)	0.84 (0.64)	8.81 (4.06)	51.42 (6.04)
N stress + *Azospirillum*	9.88 (8.79)	10.74 (7.33)	3.32 (4.89)	12.39 (5.68)	41.64 (5.49)

σ_G^2: General Combining Ability (GCA), σ_H^2: Specific Combining Ability (SCA), σ_{GE}^2: GCA x environment interaction, σ_{HE}^2: SCA x environment interaction, and σ_ϵ^2: residual. Prediction models: GB: GBLUP , GB + G×E: GBLUP + G×E, GK: Gaussian Kernel, and GK + G×E: Gaussian Kernel + G×E.

Table S7 Estimates of variance components and standard deviation (in parentheses) from prediction models for root volume (RV).

Treatment	σ_G^2	σ_H^2	σ_{GE}^2	σ_{HE}^2	σ_ϵ^2
GB					
N stress	1.49 (0.56)	1.55 (0.45)	-	-	6.04 (0.65)
N stress + *Azospirillum*	3.49 (1.23)	1.74 (0.47)	-	-	5.68 (0.61)
GB + G×E					
N stress	1.05 (0.45)	1.20 (0.41)	0.68 (0.28)	1.40 (0.41)	4.93 (0.72)
N stress + *Azospirillum*	2.69 (1.14)	1.37 (0.43)	0.92 (0.40)	1.36 (0.43)	4.67 (0.63)
GK					
N stress	0.46 (0.47)	2.24 (0.92)	-	-	6.12 (0.66)
N stress + *Azospirillum*	3.39 (1.44)	1.64 (0.77)	-	-	6.06 (0.64)
GK + G×E					
N stress	0.20 (0.29)	1.75 (0.83)	0.19 (0.17)	1.51 (0.70)	5.52 (0.71)
N stress + *Azospirillum*	2.95 (1.47)	1.35 (0.91)	0.24 (0.22)	1.39 (0.52)	5.45 (0.67)

σ_G^2: General Combining Ability (GCA), σ_H^2: Specific Combining Ability (SCA), σ_{GE}^2: GCA x environment interaction, σ_{HE}^2: SCA x environment interaction, and σ_ϵ^2: residual. Prediction models: GB: GBLUP , GB + G×E: GBLUP + G×E, GK: Gaussian Kernel, and GK + G×E: Gaussian Kernel + G×E.

Table S8 Estimates of variance components and standard deviation (in parentheses) from prediction models for root average diameter (RAD). The values must be multiplied by 10^{-4} to return to its correct magnitude.

Treatment	σ_G^2	σ_H^2	σ_{GE}^2	σ_{HE}^2	σ_ϵ^2
GB					
N stress	2.75 (1.01)	2.90 (0.78)	-	-	8.38 (0.93)
N stress + *Azospirillum*	5.69 (2.00)	2.94 (0.84)	-	-	11.30 (1.23)
GB + G×E					
N stress	2.00 (0.87)	2.29 (0.72)	1.12 (0.48)	2.21 (0.72)	2.20 (0.96)
N stress + *Azospirillum*	4.55 (1.90)	2.26 (0.76)	1.41 (0.63)	2.30 (0.81)	9.77 (1.30)
GK					
N stress	0.72 (0.76)	4.16 (0.15)	-	-	8.75 (0.99)
N stress + *Azospirillum*	6.21 (2.66)	2.60 (1.14)	-	-	11.90 (1.25)
GK + G×E					
N stress	0.34 (0.47)	3.39 (1.50)	0.36 (0.31)	2.89 (1.25)	7.36 (1.07)
N stress + *Azospirillum*	5.83 (2.69)	2.00 (1.24)	0.30 (0.30)	2.62 (1.06)	10.70 (1.27)

σ_G^2: General Combining Ability (GCA), σ_H^2: Specific Combining Ability (SCA), σ_{GE}^2: GCA x environment interaction, σ_{HE}^2: SCA x environment interaction, and σ_ϵ^2: residual. Prediction models: GB: GBLUP , GB + G×E: GBLUP + G×E, GK: Gaussian Kernel, and GK + G×E: Gaussian Kernel + G×E.

Table S9 Estimates of variance components and standard deviation (in parentheses) from prediction models for specific root length (SRL).

Treatment	σ_G^2	σ_H^2	σ_{GE}^2	σ_{HE}^2	σ_ϵ^2
GB					
N stress	61,037.77	91,452.32	-	-	324,387.30
	(23,836.21)	(29,164.38)			(36,455.43)
N stress + *Azospirillum*	120,392.80	65,691.42	-	-	338,562.50
	(44,514.44)	(20,210.64)			(35,389.73)
GB + G×E					
N stress	42,513.56	75,563.97	37,032.54	64,311.60	259,269.70
	(20,385.99)	(28,490.71)	(15,235.62)	(27,011.56)	(38,145.20)
N stress + *Azospirillum*	94,805.63	49,074.92	32,478.37	51,116.82	307,349.20
	(41,581.98)	(17,461.34)	(15,162.41)	(18,632.54)	(37,073.20)
GK					
N stress	9,464.56	120,500.50	-	-	346,739.90
	(11,067.73)	(48,872.90)			(39794.01)
N stress + *Azospirillum*	116,164.40	69,702.99	-	-	339,307.00
	(57,104.10)	(37,091.26)			(34,874.36)
GK + G×E					
N stress	4,960.72	90,530.97	9,794.91	82,924.39	301,820.00
	(6,914.57)	(47,986.61)	(10,272.81)	(42,624.66)	(43,569.28)
N stress + *Azospirillum*	95,988.61	57,835.98	8,357.87	70,370.65	306,469.00
	(59,673.97)	(43,314.62)	(12,662.27)	(31,853.05)	(36,979.57)

σ_G^2: General Combining Ability (GCA), σ_H^2: Specific Combining Ability (SCA), σ_{GE}^2: GCA x environment interaction, σ_{HE}^2: SCA x environment interaction, and σ_ϵ^2: residual. Prediction models: GB: GBLUP , GB + G×E: GBLUP + G×E, GK: Gaussian Kernel, and GK + G×E: Gaussian Kernel + G×E.

Table S10 Estimates of variance components and standard deviation (in parentheses) from prediction models for specific root surface area (SRSA).

Treatment	σ_G^2	σ_H^2	σ_{GE}^2	σ_{HE}^2	σ_ϵ^2
GB					
N stress	1,080.95	1,534.69	-	-	5,978.15
	(431.33)	(510.57)			(678.94)
N stress + *Azospirillum*	1,686.55	1,181.45	-	-	5,880.65
	(638.28)	(384.32)			(627.51)
GB + G×E					
N stress	737.93	1,298.24	662.90	1,145.74	4,686.34
	(359.18)	(517.81)	(283.02)	(532.77)	(736.71)
N stress + *Azospirillum*	1,255.95	900.37	563.04	895.94	5,235.78
	(560.06)	(340.85)	(260.06)	(353.42)	(652.94)
GK					
N stress	218.47	2,071.81	-	-	6,414.06
	(281.13)	(939.79)			(740.90)
N stress + *Azospirillum*	1,170.52	1,592.55	-	-	5,960.32
	(834.35)	(947.50)			(636.99)
GK + G×E					
N stress	94.04	1,563.91	195.77	1,495.18	5,561.40
	(137.57)	(918.66)	(229.63)	(813.64)	(816.83)
N stress + *Azospirillum*	659.47	1,511.83	137.79	1,578.95	5,062.23
	(725.73)	(968.94)	(188.96)	(762.81)	(699.39)

σ_G^2: General Combining Ability (GCA), σ_H^2: Specific Combining Ability (SCA), σ_{GE}^2: GCA x environment interaction, σ_{HE}^2: SCA x environment interaction, and σ_ϵ^2: residual. Prediction models: GB: GBLUP , GB + G×E: GBLUP + G×E, GK: Gaussian Kernel, and GK + G×E: Gaussian Kernel + G×E.

SUPPLEMENTARY FIGURES

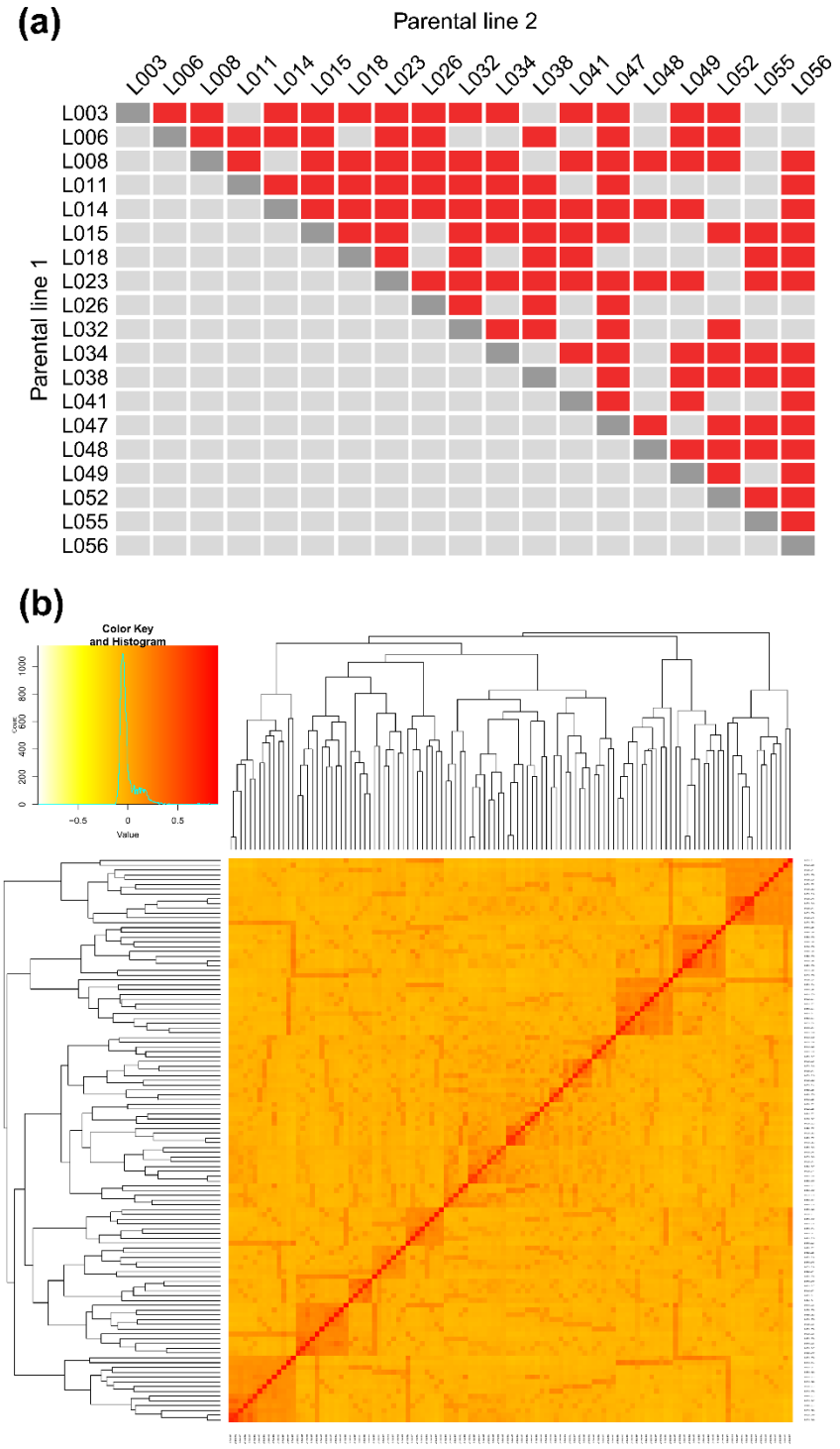

Fig. S1 Information about the panel of 118 maize hybrids. **(a)** Scheme of obtaining from the crossing of 19 parental inbred lines in an incomplete diallel design (without the reciprocals), where the red squares indicate the hybrids evaluated and the gray squares represent the unrealized crosses. **(b)** Heatmap and dendogram of a kinship matrix estimated using Van Randen method based on 59,215 SNPs markers.

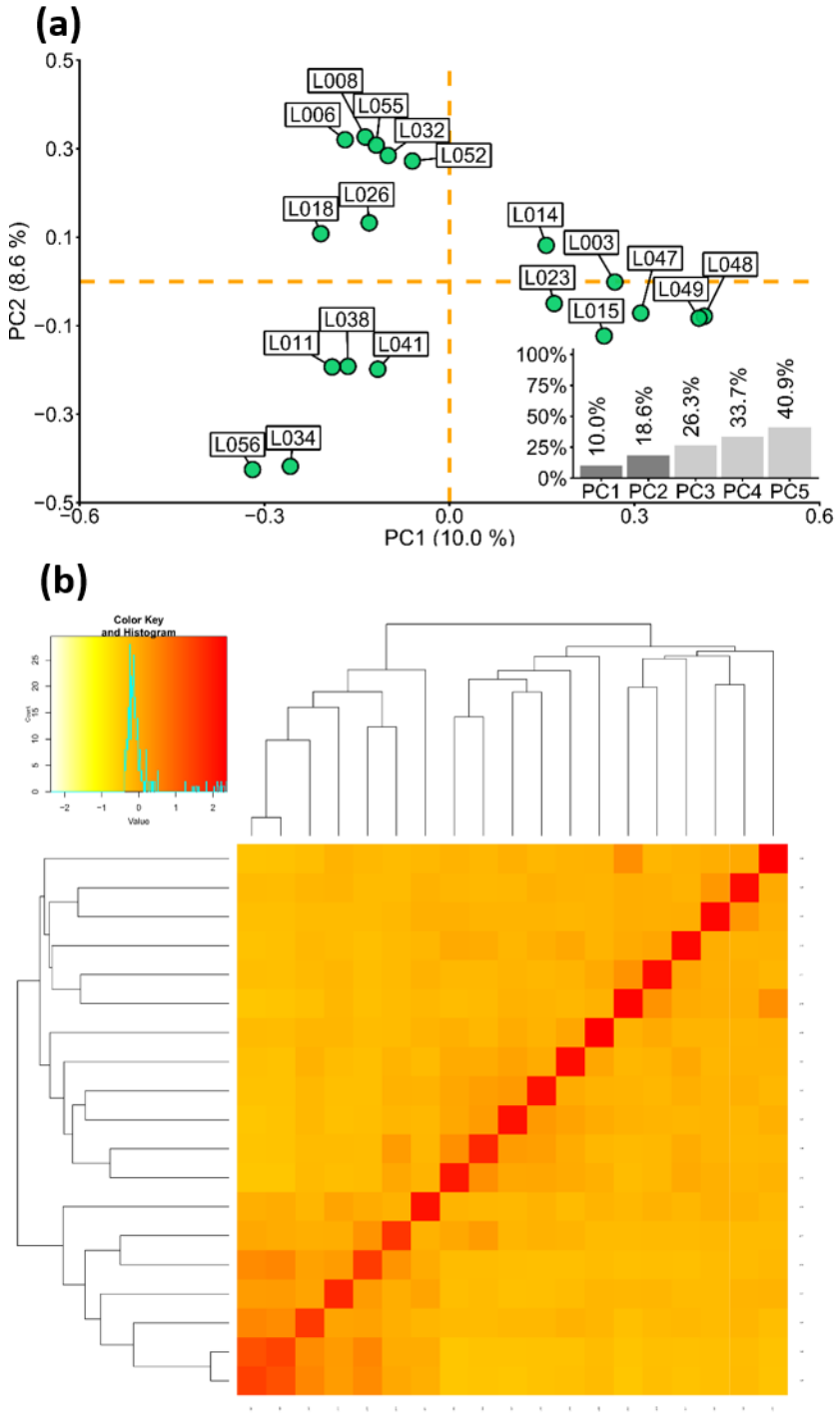

Fig. S2 Panel structure analysis of the 19 maize parental inbred lines. Based on 65,225 SNPs markers, **(a)** the first two principal components, and **(b)** heatmap and dendogram of the kinship matrix estimated using the Van Randen method.

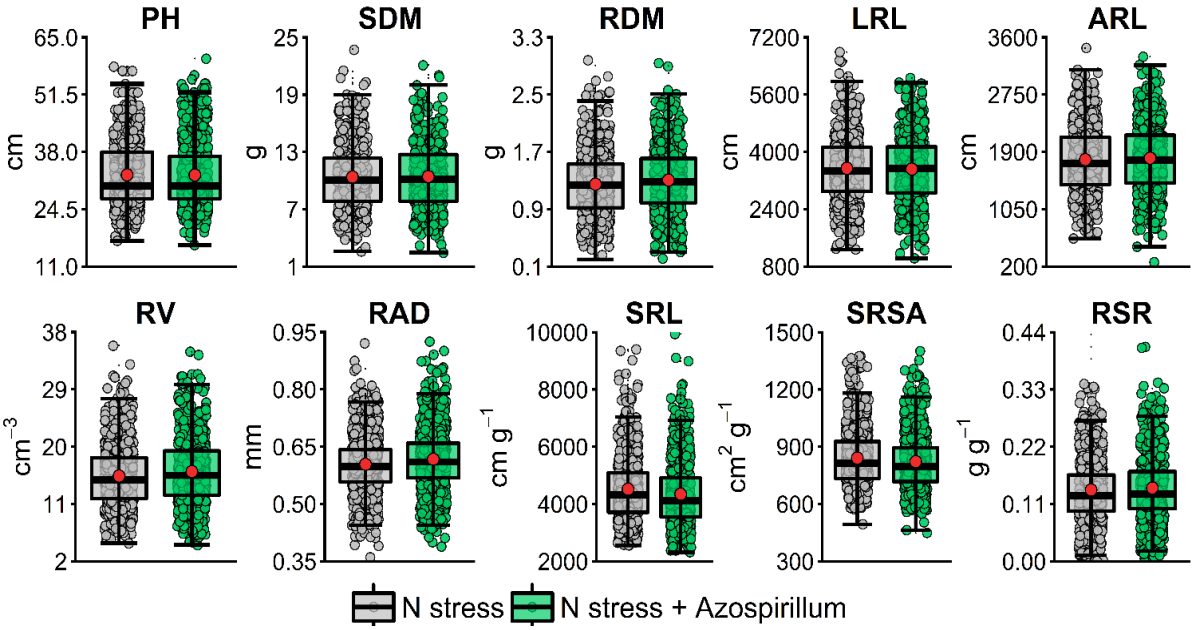

Fig. S3 Box plot showing the phenotypic variation of traits evaluated in 118 maize hybrids under conditions of N stress and N stress plus *Azospirillum brasilense*. PH: plant height, SDM: shot dry mass, RDM: root dry mass, LRL: lateral root length, ARL: axial root length, RV: root volume, RAD: root average diameter, SRL: specific root length, SRSA: specific root surface area, and RSR: root shoot ratio.

3. ADDITIVE AND HETEROZYGOUS (DIS)ADVANTAGE GWAS MODELS REVEAL CANDIDATE GENES INVOLVED IN GENOTYPIC VARIATION OF MAIZE HYBRIDS TO AZOSPIRILLUM BRASILENSE

ABSTRACT

The maize genotypes can show different responsiveness to the inoculation with the *A. brasilense*. An intriguing issue is what genes of the plant are involved in the recognition and growth promotion by this Plant Growth-Promoting Bacteria (PGPB). Here, we conducted Genome-Wide Association Study (GWAS) using additive and heterozygous (dis)advantage models to find candidate genes involved in the genotypic differences of maize to *A. brasilense*. For this, a panel of 118 maize hybrids was evaluated for root and shoot traits under N stress and N stress plus *A. brasilense* and 52,215 Single Nucleotide Polymorphism (SNP) markers were used for GWAS analyses. For the six root traits with significant inoculation effect, the GWAS analyses revealed 25 significant SNPs for the N stress plus *A. brasilense* treatment, in which only two were coincident to 22 found in N stress. Most of them were found by heterozygous (dis)advantage model and were more related to exclusive Gene Ontology terms. In general, the candidate genes around the significant SNPs found for maize-*A. brasilense* association are involved in different functions previously described to PGPB in plants, as in signaling pathways of the plant's defense system and phytohormone biosynthesis. Our findings are a benchmark towards the understanding of the genetic variation among maize hybrids for the association with *A. brasilense* and revel the potential for further enhancement of maize concerning this association.

Keywords: Plant Growth-Promoting Bacteria (PGPB); Non-additive effects; Nitrogen stress; Association mapping; *Zea mays*

3.1. INTRODUCTION

Currently, major agro-systems are highly dependent of chemical fertilizers and pesticides inputs. One of the main strategies to develop sustainable agriculture in face of natural resources scarcity and environmental impacts caused by the application of these products is the use of Plant Growth-Promoting Bacteria (PGPB) inoculants. These bacteria in association with plants may generate several benefits to the host, such as phytohormone biosynthesis, biological nitrogen fixation (FBN), and induction of mechanisms of resistance. In turn, there are positive effects on the enhancement of root traits, tolerance to abiotic stress, and defense against pathogens (Fukami *et al.*, 2017, 2018a).

Azospirillum brasilense is a well-known PGPB, which is marketed by several companies in South America countries as Brazil, Argentina, and Uruguay. It is used as a nitrogen fixing bacterium in some cereal crops as maize and wheat (Cassán & Diaz-Zorita, 2016). Some studies have reported the influence of plant genotype on the degree of beneficial responses to PGPBs inoculation, including *A. brasilense* (Carvalho *et al.*, 2016; Kazi *et al.*, 2016; Cunha *et al.*, 2016; Brusamarello-Santos *et al.*, 2017). In this context, *Genome-wide Association Studies* (GWAS) is a powerful approach for the identification of genomic regions significantly associated with phenotypic traits variation and has been widely applied to study the genetic basis of plant-microbes interactions, including pathogens (Rosas *et al.*, 2017; Genissel *et al.*, 2017), arbuscular mycorrhizal fungi (Lehnert *et al.*, 2017; De Vita *et al.*, 2018), and endogenous microbiome (Wallace *et al.*, 2018). As far as we know, only two GWAS studies were reported to PGPB. The first, (Kamfwa *et al.*, 2015) explored traits related to FBN of *Rhizobium tropici* in a panel of 259 common bean. The second, Wintermans *et al.*(2016) evaluated shoot and root traits of 302 accessions of *Arabidopsis thaliana* inoculated with *Pseudomonas simiae* WCS417r. However, even its potential, studies of GWAS related to the cereals genetic basis for the responsiveness to PGPB keeps insipient, particularly for those with N-fixing ability.

Moreover, the growing of plants on soil conditions should be considered for the studies concerning plants-PGPB. The soil characteristics might influence this association, specially due to the interaction of inoculated strain with soil microbiome. For instance, they might compete for resources and site, or show antagonist effects (Pieterse *et al.*, 2016). The understanding of the plant genetic basis related with PGPB and nitrogen (N) starvation is also crucial. It is known that the change on the diversity and the amount of the compounds released by the roots depending on the nutritional status, with consequences on the transcription of PGPB genes (Carvalhais *et al.*, 2013), and the composition of plant-associated microbiome (Castrillo *et al.*, 2017; Gomes *et al.*, 2018). Furthermore, in tropical areas as Africa and part of South America, the soils are often N-limited and a significant proportion of maize production occurs in these conditions.

Another challenge is the heterosis (or hybrid vigor) for several maize traits (Li *et al.*, 2017, 2018; Yang *et al.*, 2017). Therefore, GWAS analyses should consider not only the additive marker effects but also the non-additive ones that might explain an important proportion of the variation on complex traits (Bonnafous *et al.*, 2018; Monir & Zhu, 2018). In this way, some authors speculate that maize root colonization by beneficial microbes could be regulated by heterosis due to hybrids plants support more and numerous strains than their parental inbred lines (Picard & Bosco, 2005, 2006). However, it was not clearly elucidated. Thus, heterozygous (dis)advantage GWAS models (Goyette *et al.*, 2015; Tsepilov *et al.*, 2015) applied on plant-related traits to the responsiveness to

PGPB could provide additional information about the influence of heterosis concerning this association and help to identify candidate genes with heterotic performance under the inoculation conditions.

The knowledge about the genetic variation available and the genetic architecture of the traits involved in maize–*A. brasilense* interaction is unknown. However, this information can contribute to understanding its genetic base and how to apply it in plant breeding programs aiming to improve the germplasm for this association. Hence, we aimed with this study *(i)* understand the maize genetic variation in response to *A. brasilense* inoculation under low-N soil conditions, and *(ii)* perform GWAS analyses using additive and heterozygous (dis)advantage models to identify Single Nucleotides Polymorphisms (SNPs) significantly associated with traits related to this association, the underlying candidate genes, and the importance of non-additive effects on the maize- *A. brasilense* association.

3.2. MATERIALS AND METHODS

3.2.1. Bacterial strain and inoculum

The bacterial strain *A. brasilense* Ab-V5 was selected from maize roots in Brazil and is registered in the Brazilian Ministry of Agriculture, Livestock and Food Supply (MAPA) for the inoculant production for maize, rice and wheat (Hungria *et al.*, 2010; Cassán & Diaz-Zorita, 2016). In addition, it is part of the Culture Collection of Diazotrophic and PGPR of Embrapa Soybean (Londrina, Paraná, Brazil). The bacterial inoculum of *A. brasilense* Ab-V5 was prepared in the Laboratory of Genetics of Microorganisms "Prof. João Lúcio de Azevedo," at ESALQ/USP, Piracicaba-SP, Brazil, and take immediately to the experimental area. Bacterial inoculum were prepared by growing Ab-V5 in Dextrose Yeast Glucose Sucrose (DYGS) liquid medium (Rodrigues Neto *et al.*, 1986) at 28 °C with 150 rpm agitation. The inoculum concentration was adjusted to approximately $1x10^8$ UFC mL^{-1}. Posteriorly, the inoculum was transferred with a pipette for plastic bags containing the maize seeds and the sowing was made about thirty minutes later the inoculation.

3.2.2. Plant material and greenhouse experiments

The association panel was comprised of 118 single-cross hybrids from a diallel mating design among 19 tropical maize inbred lines with genetic diversity to nitrogen use efficiency

(Morosini *et al.*, 2017). The plants were grown under semi-controlled conditions in a greenhouse located at the University of São Paulo, Brazil (22°42'39"S; 47°38'09"W, altitude 540 m), in two seasons: November-December (2016) and February-March (2017).

A randomized complete block experimental design with three replications spatially arranged under two countertops was adopted in each season. Two main treatments were evaluated: N stress without bacterial inoculation and N stress plus *A. brasilense* inoculation. The decision of non-input N fertilizer was due to its negative effects reported on N-fixation by diazothophic bacteria (Kox *et al.*, 2016). In each plot, three seeds were sown with 3 cm depth in plastic pots of 3L capacity containing unsterilized loam soil from an area without any agricultural use. After the germination, the seedlings were thinned to one. Only potassium chloride and super simple phosphate fertilizers were added to soil according to the general crop demand. The average temperature was semi-controlled (between 20ºC-33ºC), and a supplementation of luminosity was done with fluorescent lamps to simulate a photoperiod of 12 hours. Furthermore, the water supply was provided manually by pot, with the same amount applied for all of them and always maintaining a well-watered condition. During the conduction of the experiments, no insect or pathogens attack was detected, and pesticides were not used.

Approximately 35 days after the emergency, when most of the hybrids reached the V7 stage (seven expanded leaves), plant height (PH, cm) was measured from the soil level to the insertion of the least expanded leaf. In addition, the shoot was harvested and dried in a forced draft oven at 60°C for 72 h to determine the shoot dry mass (SDM, g). The soil particles of each root system were carefully removed with water and the individual storage was performed in plastic pots with 25% ethanol solution for preservation. The root images acquired by an Epson LA2400 scanner (2,400 dpi resolution) were analyzed by WinRHIZO™ (Reagent Instruments Inc., Quebec, Canada). This software provided the measures of root average diameter (RAD, mm), root volume (RV, cm^3), and the total length of a series of root diameter classes. The fragments with a diameter class less than or equal to 0.5 mm were considered as the lateral root length (roots from the axial roots - LRL, cm), while that with diameter classes greater than 0.5 mm were considered as axial root length (comprising crow, seminal and primary roots - ARL, cm) (Trachsel *et al.*, 2013). We determined the root dry mass (RDM, g) after drying the roots under the same conditions used for SDM. This trait was used to calculate the specific root length (SRL, cm g^{-1}) and specific root surface area (SRSA, cm^2 g^{-1}) dividing the total root length and the superficial area by RDM, respectively. Furthermore, the root to shoot ratio (RSR, g g^{-1}) was obtained by dividing the RDM by SDM. In total, 10 traits were evaluated and approximately 1,416 root systems were analyzed.

3.2.3. Phenotypic analyses

The analyses were conducted using Restricted Maximum Likelihood/Best Linear Unbiased Predictor (REML/BLUP) mixed models, by ASReml R package (Gilmour *et al.*, 2015), considering the following model:

$$\boldsymbol{y} = \boldsymbol{X_E\beta_E} + \boldsymbol{X_B\beta_B} + \boldsymbol{X_C\beta_C} + \boldsymbol{X_I\beta_I} + \boldsymbol{X_{EI}\beta_{EI}} + \boldsymbol{Z_G u_G} + \boldsymbol{Z_{GE}u_{GE}} + \boldsymbol{Z_{GI}u_{GI}} + \boldsymbol{Z_{GEI}u_{GEI}} + \boldsymbol{\varepsilon}$$

where $\boldsymbol{y}$ is the vector of phenotypic observations of the traits evaluated on maize hybrids; $\boldsymbol{\beta_E}$ is the vector of fixed effects of year; $\boldsymbol{\beta_B}$ is the vector of fixed effects of block within year; $\boldsymbol{\beta_C}$ is the vector of fixed effects of countertop within block and year; $\boldsymbol{\beta_I}$ is the vector of fixed effects of inoculation; $\boldsymbol{\beta_{EI}}$ is the vector of fixed effects of inoculation × year interaction; $\boldsymbol{u_G}$ is the vector of random effects of genotype, where $\boldsymbol{u_G} \sim N(0, I\sigma_G^2)$; $\boldsymbol{u_{GE}}$ is the vector of random effects of genotype × year interaction, where $\boldsymbol{u_{GE}} \sim N(0, \sigma_{GE}^2)$; $\boldsymbol{u_{GI}}$ is the vector of random effects of genotype × inoculation interaction, where $\boldsymbol{u_{GI}} \sim N(0, \sigma_{GI}^2)$; $\boldsymbol{u_{GEI}}$ is the vector of random effects of genotype × year × inoculation interaction, where $\boldsymbol{u_{GEI}} \sim N(0, \sigma_{GEI}^2)$; $\boldsymbol{\varepsilon}$ is the vector of errors, where $\boldsymbol{\varepsilon} \sim N(0, \sigma_\varepsilon^2)$. $\boldsymbol{X_E}$, $\boldsymbol{X_B}$, $\boldsymbol{X_C}$, $\boldsymbol{X_I}$, $\boldsymbol{X_{EI}}$, $\boldsymbol{Z_G}$, $\boldsymbol{Z_{GE}}$, $\boldsymbol{Z_{GI}}$, and $\boldsymbol{Z_{GEI}}$ are the respective incidence matrices related to each vector. The significance of fixed effects was tested using the Wald test implemented in the ASReml R package, while the significance of random effects was assessed by Likelihood Ratio Test (LTR) from asremlPlus R package (Brien, 2016). The variance components by treatment were estimated through reduced models from that disregarding the inoculation effect and its interaction with genotype. Posteriorly, broad-sense heritabilities were estimated as $H^2 = \sigma_G^2/(\sigma_G^2 + \sigma_{GE}^2/j + \sigma_\varepsilon^2/rj)$, where the σ_G^2 is the genetic variance; σ_{GE}^2 is the genotype-by-year variance; σ_ε^2 is the error variance; j and r are the number of years and replications in each experiment, respectively.

3.2.4. Genotypic data

The Affymetrix® Axiom® Maize Genotyping Array (Unterseer *et al.*, 2014) of 616,201 Single Nucleotide Polymorphism (SNP) markers were used to genotype the parental inbred lines. Markers with call rate < 95% and heterozygous loci on at least one individual were removed. Remaining missing data were imputed based on the algorithms from Beagle 4.0 (Browning and Browning 2009) using the codeGeno function from Synbreed R package (Wimmer et al. 2012). Posteriorly, the hybrid genotypes were obtained *in silico* from the genotypes of the corresponding parental

inbred lines. After that, we applied one more filter on the matrix eliminating SNPs with Minor Allele Frequency (MAF) ≤ 0.05. A final SNP set of 59,215 was obtained and used for the subsequent analyses.

3.2.5. GWAS analyses

Marker-trait association analyses were performed for the traits with significant inoculation effect. For these traits, the adjusted means for each hybrid were calculated by treatment (inoculated and non-inoculated), separately, considering the following model:

$$\boldsymbol{y} = \boldsymbol{X_E\beta_E} + \boldsymbol{X_B\beta_B} + \boldsymbol{X_C\beta_C} + \boldsymbol{X_G\beta_G} + \boldsymbol{X_{GE}\beta_{GE}} + \boldsymbol{\varepsilon}$$

where $\boldsymbol{y}$ is the vector of phenotypic observations of the traits evaluated on maize hybrids; $\boldsymbol{\beta_E}$ is the vector of fixed effects of year; $\boldsymbol{\beta_B}$ is the vector of fixed effects of block within year; $\boldsymbol{\beta_C}$ is the vector of fixed effects of countertop within block and year; $\boldsymbol{\beta_G}$ is the vector of fixed effects of the genotype; $\boldsymbol{\beta_{GE}}$ is the vector of fixed effects of genotype × year interaction; $\boldsymbol{\varepsilon}$ is the vector of errors, where $\boldsymbol{\varepsilon} \sim N(0, \sigma^2_{\boldsymbol{\varepsilon}})$. $\boldsymbol{X_E}, \boldsymbol{X_B}, \boldsymbol{X_C}, \boldsymbol{X_G}$, and $\boldsymbol{X_{GE}}$ are the respective incidence matrices for each vector. Density and box plots were used to compare the means between both treatments. In addition, we calculated the changes due to *A. brasilense* inoculation on the hybrids traits by $\Delta = M1 - M2$, where $M1$ is the adjusted mean under N stress plus *A. brasilense* and $M2$ is the adjusted mean under N stress.

Population structure was estimated by principal components analysis (PCA) using the genomic matrix through SNPRelate R package (Zheng *et al.*, 2012). The GWAS analyses were conducted in a Fixed and Random Model Circulating Probability Unification method thought the FarmCPU R package (Liu *et al.*, 2016). This statistical procedure considers the confounding among the testing marker and both kinship (K) and population structure (Q) as covariates for minimizing the problem of false positive and false negative SNPs. FarmCPU R package uses the FaST-LMM algorithm to calculate the K from selected pseudo-QTNs (Quantitative Trait Nucleotides) and not from the total SNP set, as the standard K. The thresholds values were calculated by the p.threshold function of FarmCPU. It permutes the phenotypes to break the spurious relationship with the genotype. After the obtention of a vector of the minimum p-values of each experiment, the 95% quantile value of the vector is recommended for p.threshold. Finally, quantile-quantile (Q-Q) plots were used to verify the goodness of the model considering population structure and kinship as factors.

The additive and heterozygous (dis)advantage models were applied in GWAS analyses by using specifics encodings for the SNP matrix. Concerning the additive SNP effect with two alleles

(A_1 and A_2), the SNP matrix was coded by 0 (A_1A_1), 1(A_1A_2), and 2 (A_2 A_2), considering the A_2 as the minor allele. In this context, the additive GWAS model assumes there is a linear change in the phenotype regarding the minor allele number of copies. On the other hand, in the heterozygous (dis)advantage GWAS model, the homozygous genotypes (A_1A_1 or A_2A_2) were assumed to have the same effect while the heterozygous genotypes have a different one, implying an increase or decrease effect on the trait. Therefore, the SNP matrix was coded by 0 (A_1A_1), 1 (A_1A_2), and 0 (A_2A_2) (Goyette *et al.*, 2015; Tsepilov *et al.*, 2015). Posteriorly, box plots were used to show the phenotype values by genotypes of the SNPs significantly associated with the traits.

The average linkage disequilibrium (LD) in the hybrid panel was investigated using the square allele frequency correlation coefficient r^2 between all pairs of SNPs across the chromosomes using PLINK v.1.9 software (Purcell *et al.*, 2007). The extension of LD decay was verified by plotting the r^2 values against the physical distance of the SNPs. Moreover, the heterozygosity by hybrid and by SNP marker was estimated dividing the number of heterozygous loci by the total of SNP markers and maize genotypes, respectively.

3.2.6. Identification of candidate genes

The candidate genes associated with the significant SNPs were obtained from the B73 genome reference (version 4) in the MaizeGDB genome browser (http://www. maizegdb.org/). Complementary information was collected from the U.S. National Center for Biotechnology Information (http://www.ncbi.nlm.nih.gov/) and the Universal Protein Resource (http://www.uniprot.org/). Venn diagrams were constructed to summarize the number of candidates genes identified using the VennDiagram R package (Chen & Boutros, 2011).

In addition, the sequences of the candidate genes were functionally categorized by Gene Ontology (GO) terms (Ashburner *et al.*, 2000), disregarding those with hypothetical function. The terms were obtained using the Blast2GO software with the default parameters specified by the program (Conesa *et al.*, 2005) and were previously simplified using the GO Slim feature.

3.3. MATERIALS AND METHODS

3.3.1. The phenotypic effect of *A. brasilense* inoculation on the maize hybrids

Significant genotypic differences among the 118 maize hybrids were observed for all traits evaluated, except for PH and SDM (Table **1**). Furthermore, the genotypic performance for RDM,

RV, RAD, SRL, SRSA, and RSR were significantly affected by the inoculation with *A. brasilense*, thus, just these traits were considered for the subsequent analyses. The interactions of genotype × year and genotype × inoculation were not significant for most of the traits, indicating these factors varied independently.

In general, the correlation between adjusted means of both treatments showed moderate magnitude varying from 0.41 to 0.56, except for RAD, whose value was 0.12 (Fig. **1a**). Moreover, we found higher genetic variances under inoculated treatment than non-inoculated. In this context, the estimates of broad-sense heritability ranged from 0.16 (SRL) to 0.42 (SRSA) under N stress and varied from 0.42 (RDM) to 0.68 (RAD) under N stress plus *A. brasilense* (Fig. **1b**).

Regarding the density distribution of the adjusted means for all traits, larger phenotypic variances were found in the inoculated condition compared with the non-inoculated (Fig. **2a**). Overall, the inoculation increased the RDM, RV, RAD, and RSR while the conversely was observed for SRL and SRSA. Concerning the change due to inoculation (Δ), for all the traits, a distribution close to normal was observed (Fig. **2b**). In this sense, most hybrids had low responsiveness to *A. brasilense*. Moreover, a considerable portion of the genotypes showed negative responsiveness to *A. brasilense*, that is a worse performance than the non-inoculated. The correlation between the ΔRDM and ΔRV with ΔRSR varied were of 0.41 and 0.35, respectively (Fig. **2c**).

3.3.2. Population structure and LD decay

The genetic structure of the hybrid panel was accessed by PC analysis using 59,215 SNP markers (Fig. **3a**). The first two PCs captured a small percentage of the total variance (20.8%). In addition, the individuals had a wide distribution throughout the projection space. It indicates a weak structure among the genotypes. Moreover, a rapid decline in LD was observed (Fig. **3b**), with 121.7 kb extent when r^2 reached 0.23 (half of the maximum value).

The average heterozygosity of hybrids was 0.32, ranging from 0.03 to 0.38 with most of the individuals presenting about 0.35 (Fig. **3c**). The low values found for some individuals indicate that some inbred lines used in the diallel crosses have high genetic similarity. For the heterozygosity of markers, this value was also 0.32, varying from 0.10 to 0.61 (Fig. **3d**).

3.3.3. Marker-trait associations

The additive and heterozygous (dis)advantage GWAS models were used to dissect the genetic basis of the traits RDM, RV, RAD, SRL, SRSA, and RSR under N stress and N stress plus *A. brasilense* condition since for these traits the genotypes showed a differential performance due to the inoculation effect. Only the genetic relatedness (K matrix) was used as a covariate in all GWAS analyses, being it automatically incorporated by FarmCPU package. Thus, we did not include the population structure information due to the increase of the deviation from expected *p*-values showed by Q-Q plots (not presented. Furthermore, based on the LD decay for this hybrid panel, the gene annotation was performed within a 50 kb sliding window around each significant SNP.

Concerning the additive GWAS model, 8 significant SNP-trait associations were revealed from the maize hybrids evaluated under N stress plus *A. brasilense* treatment (Table **2**, Fig. **S1**, **S5a**). In general, at least one candidate gene was identified for each trait, which were located on the chromosomes 2, 4, 6, 7, and 9. In addition, using the same model but for N stress treatment, we detected one significant association for each trait, totalizing 5 candidate genes, which were located on chromosomes 2, 5, and 6 (Table **2**, Fig. **S2**, **S5b**). However, for chromosome 5, position 149998432, no candidate gene was found within the window considered. The results for RSR in both treatments were disregarded due to poor adjustment with the expected values showed by the Q-Q plots.

Two candidate genes identified in the inoculated treatment were similar to those identified under N-stress treatment, but for different traits (Fig. **4a**). In this sense, the candidate genes Zm00001d013098 and Zm00001d005892 were related to RAD and SRL under *A. brasilense* treatment, and to RDM and RAD under non-inoculated treatment, respectively.

A higher number of significant associations were revealed using heterozygous (dis)advantage GWAS model. We found17 significant SNPs associated with traits under N stress plus *A. brasilense* treatment located on chromosomes 1, 2, 3, 7, and 8 (Table **3**, Fig. **S3**, **S6**). Several common candidate genes were found among the traits: Zm00001d029115 (RDM, RV, and RSR), Zm00001d037182 (RDM and RV), Zm00001d003312 (RV and RAD), and Zm00001d030590 (RAD and SRL). Under N stress, 17 significant associations were identified throughout the chromosomes 1, 2, 3, 4, 5, 6, and 9 (Table **3**, Fig. **S4**, **S7**). For this model, any of the candidate genes were simultaneously detected for both inoculated and non-inoculated treatments (Fig. **4b**). No candidate genes were detected for chromosome 1 position 251090900 (RAD, inoculated treatment) and chromosome 3 position 165642810 (RDM, non-inoculated treatment).

In total, 47 significant SNP-trait associations were found, where 25 related to traits under N stress plus *A. brasilense* and 22 for N stress. Regarding the models, 13 significant associations were identified by using additive GWAS model and 34 by the heterozygous (dis)advantage model. There was no candidate gene shared between them (Fig. **4c**). Finally, the nature of the SNP effect on the traits, positive or negative, was independent of the treatment or GWAS model (**S5**, **S6**, and **S7**).

The categorization of candidate genes sequences according to biological process using the Blast2GO software showed that just one category was present in all treatments biosynthetic process (Fig **5**). Moreover, in general, the candidate genes found by additive GWAS model tended to be mainly enriched for terms as "DNA metabolic process" and "lipid metabolic process". In turn, those found by to heterozygous (dis)advantage model showed more exclusive biological functions, for example, "catabolic process", "cellular component organization", "response to stress", and "secondary metabolic process". Comparing the inoculated and non-inoculated treatments, a different pattern of categorization was verified between both, especially for the candidates genes found by heterozygous (dis)advantage model.

3.4. DISCUSSION

3.4.1. Genotypic variation of maize to *A. brasilense* under nitrogen stress

One of the aims was to evaluate the genetic variability of 118 maize hybrids responsiveness to the inoculation with the PGPB *A. brasilense* and the genetic control of related traits to this effect. The few previous studies reporting the differential responsiveness among maize genotypes to *A. brasilense* inoculation are based on a smaller number of hybrids or inbreed lines (Rozier *et al.*, 2016; Cunha *et al.*, 2016; Brusamarello-Santos *et al.*, 2017). Moreover, as far as we know, our report has evaluated the biggest number of maize genotypes for the association with PGPB. The inoculation of *A. brasilense* under N stress promoted significant change on the maize performance for six root-related traits: RDM, RV, RAD, SRL, SRSA, and RSR. These results are in agreement with the findings of Rozier *et al.* (2016) and D'Angioli *et al.* (2017), in which effects of inoculation respectively of *A. lipoferum* and *A. brasilense* were observed in root traits but not in shoot ones. In addition, some studies have shown the positive effect of the inoculation of *Azospirlillum* spp. on RDM, RV, and promotion of thinner roots growth (Spaepen *et al.*, 2014; Chamam *et al.*, 2015). Similarly, we also observed the improvement of RDM, RV. Conversely, no studies are reporting the effect of *Azospirlillum* spp. inoculation on SRL and SRSA in maize.

Our results did not show pronounced differences among the distributions of adjusted means of the hybrids under N stress and N stress plus *A. brasilense*. However, regarding the delta (the difference between inoculated and non-inoculated treatments), an expressive variation was found, including part of the maize hybrids with negative effects on the traits due to the inoculation. This result shows that adding only one PGPB in the microbiome is enough to expand the range of maize plants responses under low N stress. The may be because microbes alter the plant functioning and confer different characteristics to the host plant. It reinforces the emerging idea of holobiont as a unit of selection, which possess a larger variability to be explored in the plant breeding (Nogales *et al.*, 2016; Gopal & Gupta, 2016; Hohmann & Messmer, 2017).

Studies reporting a decrease in the phenotypic traits of host plants due to the inoculation with PGPBs, such as *A. brasilense,* are not common in the literature (Fukami *et al.*, 2016). One possibility is that the genotypes with negative response to the inoculation can have more unfavorable alleles related to the association with *A. brasilense*. For example, triggering plant defense responses requires an energetic cost (Rosier *et al.*, 2016), which may lead to a reduction of resources to root system development causing a worse growth than only the N stress condition would already entail. In addition, similarly to the plant-endophytic interactions, the "balanced antagonism theory" has occurred in the relationships plant-PGPB (Schulz & Boyle, 2005; Fesel & Zuccaro, 2016). Then, phenotypic plasticity on the host plants may vary from mutualism to antagonism depending on the plant genotype, the environmental conditions, and the bacterial strain.

Another explanation for the negative responsiveness is because the effect of *A. brasilense* on the plant can vary according to the concentration of the inoculant (German *et al.*, 2000; Fukami *et al.*, 2016). In general, plant hormones are stimulatory only at certain concentrations, which should not exceed the stimulatory threshold specific to each plant genotype (Duca *et al.*, 2018). The higher concentration of *A. brasilense* under the root environment might increase the release of plant hormones that consequently inhibit the root growth (Fukami *et al.*, 2016). Thus, considering the number of genotypes evaluated, the concentration of the inoculant used in our experiment could be unfavorable for some of them, even using the recommended dose.

On the other hand, the reduction in root traits due to inoculation would not necessarily be a negative factor for the plant. Under abiotic stress conditions, such as low N supply and drought, it is common high root-shoot ratios (Wang *et al.*, 2014; Xu *et al.*, 2015). In this sense, we found moderate positive correlations between the ΔRDM and ΔRV root traits and ΔRSR. It indicates that under *A. brasilense* inoculation some plant genotypes could reduce the investment on root growth in order to allocate it in the shoot development. However, further studies are needed to better

understand the influence of the inoculation with this PRPB on the distribution of dry matter between roots and shoots.

The continuous phenotypic variation and the moderate estimates of heritability for the traits related to the maize responsiveness to *A. brasilense* suggest the influence of several genes of small effect and a strong environmental influence. In summary, these results reinforce the complex interactions between PGPB × plant × environment. Furthermore, they show the possibility of improving plants to be more efficient in the association with PGPB.

3.4.2. Candidate genes related to the maize responsiveness to *A. brasilense*

To the best of our knowledge, this is the first report employing GWAS to assess the genetic architecture of the association of maize with *A. brasilense*. We detected several candidate genes related to the maize responsiveness to *A. brasilense*. Considering the panel size used in our study, possibly due to the power of our GWAS analyses has been low and only the SNPs with more effect have been identified (Yan *et al.*, 2011). Korte & Farlow (2013) suggest that a way to mitigate the small sample effect is to account for large phenotypic variability. Thus, as we used hybrids rather than inbred lines, a series of different allelic combinations can occur, increasing the genetic variants with heterozygous loci and thereby allowing to find better results in GWAS analysis (Wang *et al.*, 2017). This reflected in the number of significant SNPs identified by heterozygous (dis)advantage model, which was about three times higher than the additive model. Consequently, given the great number of candidate genes found, we focused our discussion mainly on those with functions more related to the treatments of this study.

In general, it is known that the colonization of host plants by beneficial microbes depends on their ability to manipulate defense-related pathways (Carvalho *et al.*, 2016). In this study, the candidate gene Zm00001d051881 (additive model) was found, which codes the protein Binding to ToMV RNA 1 (BTR1). It is involved in the defense of Tomato Mosaic Virus (TOMV) RNA, with possible indirect effect in the host innate immunity (Huh & Paek, 2013). In addition, the Zm00001d052221 (additive model) codes the tetratricopeptide repeat (TPR) like superfamily protein, which is determinant for signal transduction of mediated by plant hormones signals and able to activate the plant defense response. For example, TPR is related to the quantitative resistance of soybean to *Fusarium graminearum* (Cheng *et al.*, 2017). Another candidate gene is the ethylene-responsive transcription factor ERF109 (Zm00001d005892, additive model), which besides being involved in abiotic stress responses ethylene-activated (Klay *et al.*, 2018), it induces the expression of defense-related genes promoting a positive modulation of the response against

pathogen infections (Sun *et al.*, 2018). The Zm00001d029115 identified for two traits using the heterozygous (dis)advantage model codes the protein strictosidine synthase-like, known to play a key role in the alkaloids biosynthesis pathway. These chemical compounds function as protection against pathogenic microorganisms and herbivorous animals. In addition, the improvement of alkaloid content in the roots has been observed with *A. brasilense* inoculation in medicinal plants (Rai *et al.*, 2017), but there are no reports about its induction in cereal crops.

The modulation of plant hormones and related signaling pathways by *A. brasilense* are also aspects frequently reported (Spaepen *et al.*, 2014; Fukami *et al.*, 2018b). For example, we found the Zm00001d013098 (additive model) corresponding to the Aldehyde oxidase 2, which is a key enzyme in the final step abscisic acid (ABA) biosynthesis. In addition, it makes the final catalytic conversion of indole-3-acetaldehyde (IAAld) in indole-3-acetic acid (AIA) in different tryptophan-dependent auxin biosynthesis pathways (Tivendale *et al.*, 2014). Moreover, we found the candidate gene 12-oxo-phytodienoic acid reductases (Zm00001d037182, heterozygous model) that are key enzymes in the control jasmonates (JA) biosynthesis in plants as maize (Wang *et al.*, 2016) and wheat (Wang *et al.*, 2016). Among other functions, this phytohormone orchestrates defense and growth responses (Koo, 2018).

Some studies show the modulation of the induction and emission of plant volatiles by the plant-associated microorganisms, including PGPBs and Rhizobia (Dicke, 2016; Sharifi *et al.*, 2017). In turn, these chemicals have an important role especially on the induction of resistance in plants against insects and pathogens (Ding *et al.*, 2017; Disi *et al.*, 2018). We found the Zm00001d046604 candidate gene (additive model) corresponding to the (Z)-3-hexen-1-ol acetyltransferase. This enzyme is involved in the green leaf volatile biosynthetic process that is derived from the lipoxygenase pathway (D'Auria *et al.*, 2007). In agreement with this finding, *A. brasilense* negatively affect the attraction of the pest insect *Diabrotica speciose* in maize by inducing higher emissions of the volatile (E)-β-caryophyllene. Therefore, the validation of this candidate gene and further studies could help to better understand the role of plant defense against pests induced by *A. brasilense*.

Regarding the candidate genes related to abiotic stress mitigation, we found the Zm00001d020747 (additive model) encoding the Aquaporin TIP4-1. Under N deficiency, this plant transporter is up-regulated in Arabidopsis (Liu *et al.*, 2003) and it is induced by rhizobial and arbuscular mycorrhizal fungi symbiosis (Ding *et al.*, 2018). In both cases, its function is related to the N delivery among plant compartments.

Directly involved in the plant root growth, we found a candidate gene encoding hydroxyproline-rich glycoprotein family protein (Zm00001d006108, additive model), a protein family from plant cell wall classified of arabinogalactan-proteins (AGPs), extensins (EXTs), and

proline-rich proteins (PRPs). It plays a key role in several processes of plant development, as root elongation and root biomass, especially in the stress conditions (Kavi Kishor, 2015). Additionally, AGPs are exuded in the rhizosphere and help in communicating with soil microbes, participate of the signaling cascade modulating the plant immune system and are required to root colonization by symbiotic bacteria (Nguema-Ona *et al.*, 2013). Another, LOC103636767 (heterozygous model), corresponds to a formin-like protein 20, which is involved in cytoskeleton movement and secondary cell wall formation (Oda & Hasezawa, 2006).

The major part of N in the leaf is allocated in the chloroplast proteins, and the deficiency of this nutrient leads to a reduction of photosynthetic efficiency (Ding *et al.*, 2005). The Zm00001d035859 candidate gene (additive model) found in our study is related to the Plastocyanin homolog 1, a protein involved in the transfer of electron in the photosystem I. In accordance with this result, the inoculation of the PGPB *Burkholderia* sp. in *Arabidopsis thaliana* led to the modification in this protein expression (Timm *et al.*, 2016). Moreover, it is involved in the response of maize to N deficiency (Luo *et al.*, 2015).

Although the candidate genes found for the N stress treatment were not the main focus of this study, many of them were previously described due their direct or indirect relation with plant responses to abiotic stress conditions. The LOC109941493 (heterozygous model) encodes the plasma membrane ATPase 2-like being this ion pump in the plant cell membrane important for root growth and architecture during different nitrogen regimes (Młodzińska *et al.*, 2015). In addition, Zm00001d006722 (heterozygous model) is related to arabinosylation of extensin proteins that contribute to root cell hairs growth, being these specialized in the absorption of nutrients (Velasquez *et al.*, 2011). The Zm00001d013098 and Zm00001d038300 (additive model) corresponding to Aldehyde oxidase2 and Ethylene-responsive transcription factor ERF109, respectively, were the only candidate genes shared between both treatments. Their functions that were above described as related to ABA and AIA biosynthesis and ethylene-activated signaling pathway, are also frequently reported for the N availability and hormones interactions (Khan *et al.*, 2015; Ristova *et al.*, 2016). Moreover, this suggests the regulation and signalization of these hormones in the plant can be involved on the cross talk between the *A. brasilense* and N stress on maize. Therefore, besides these results indicate that the stress applied in our experiment was effective, they also could be helpful for further studies better understand the genetic control of root traits under N stress in early stages of plant development for improving tolerance in maize.

Some of the candidate genes found by heterozygous (dis)advantage GWAS model were identified for more than one trait, what was not observed using the additive model. For these, the effect on phenotypes always was in the same direction, for example, the candidate gene

Zm00001d029115 (protein strictosidine synthase-like) had a negative effect for both RDM and RV. Possibly, it occurred because these pleiotropic candidate genes were only found between RDM, RV, and RAD that showed a positive correlation among them.

3.4.3. Additive and heterozygous (dis)advantage GWAS models

GWAS analyses using non-additive models are common in humans and animals studies (Lee *et al.*, 2018; Abri *et al.*, 2018; Tsairidou *et al.*, 2018). However, few studies have been reported using plant species (Bonnafous *et al.*, 2018; Monir & Zhu, 2018). In our study, most of significant SNPs were identified by heterozygous (dis)advantage GWAS analyses and none of them were detected by the additive model. It demonstrates how important is to study the non-additive effects on the genetic variability of maize responsiveness for both *A. brasilense* and N stress. This was also evident through the results of GO terms, where an increase of exclusive biological functions was verified. These results suggest that the PGPB provides the plant with a broader spectrum of internal activities, which may be an advantage for growth in stressful environments, such as N deficiency, with possible consequences in plant evolutionary potential.

Furthermore, our results showed that heterozygous genotypes can have advantage or disadvantage on the root traits (both treatments) depending on the allelic combinations that are formed by the parental crossing. Thus, the strategy of use of SNP–trait associations found by heterozygous loci in breeding programs depends on the effect of the heterozygous genotype. This is a challenge to plant breeders because during hybrid development the allele combination should be predicted by selecting parents in order to benefit its association with PGPB. In this sense, further studies underlying these candidate genes are required to better understand the biological mechanisms of heterotic performance in comparison to homozygous in the presence of this PGPB. For those providing an advantage, the alleles should be improved separately in different heterotic groups for their subsequent combination in the mating process. On the other hand, when for the heterozygous genotypes are a disadvantage, one or other allele should be improved simultaneously in both heterotic groups in order to obtain homozygous genotypes in hybrids.

3.5. CONCLUSION

Our study modeling additive and heterozygous (dis)advantage effects in GWAS analyses revealed 25 candidate genes for the maize responsiveness to *A. brasilense* with key roles specially in

plant defense, hormonal biosynthesis, signaling pathways, and root growth providing insights about their complex genetic architecture. In this context, the non-additive effects contribute substantially for the maize phenotypic variation in response to the inoculation, which is related to a larger spectrum of biological functions. Together, these findings allow starting the marker-assisted selection and genome editing in breeding programs for the development of maize hybrids more efficient to take benefits of this association. Finally, our results also represent a benchmark towards the identification of homologous genes in important related species, such as rice and wheat, besides advance the understanding of the genetic basis of plant-PGPB interactions.

REFERENCES

Abri MA, Posbergh C, Palermo K, Sutter NB, Eberth J, Hoffman GE, Brooks SA. 2018. Genome-Wide Scans Reveal a Quantitative Trait Locus for Withers Height in Horses Near the ANKRD1 Gene. Journal of Equine Veterinary Science 60: 67–73.e1.

Ashburner M, Ball CA, Blake JA, Botstein D, Butler H, Cherry JM, et al. 2000. Gene Ontology: tool for the unification of biology. the geneontology consortium. Nature Genetics 25: 25–29.

Bonnafous F, Fievet G, Blanchet N, Boniface MC, Carrère S, Gouzy J, Legrand L, Marage G, Bret-Mestries E, Munos S, et al. 2018. Comparison of GWAS models to identify non-additive genetic control of flowering time in sunflower hybrids. Theoretical and Applied Genetics 131: 319–332.

Brien C. 2016. asremlPlus: augments the use of 'asreml' in fitting mixed models. R package version 2.0-9. [WWW document] URL https://CRAN.R-project.org/package=asremlPlus. [accessed 15 April 2018].

Brusamarello-Santos LC, Gilard F, Brulé L, Quilleré I, Gourion B, Ratet P, Maltempi de Souza E, Lea PJ, Hirel B. 2017. Metabolic profiling of two maize (Zea mays L.) inbred lines inoculated with the nitrogen fixing plant-interacting bacteria Herbaspirillum seropedicae and Azospirillum brasilense (R Aroca, Ed.). PLoS ONE 12: e0174576.

Carvalhais LC, Dennis PG, Fan B, Fedoseyenko D, Kierul K, Becker A, von Wiren N, Borriss R. 2013. Linking Plant Nutritional Status to Plant-Microbe Interactions. PLoS ONE 8: e68555.

Carvalho TLG, Ballesteros HGF, Thiebaut F, Ferreira PCG, Hemerly AS. 2016. Nice to meet you: genetic, epigenetic and metabolic controls of plant perception of beneficial associative and endophytic diazotrophic bacteria in non-leguminous plants. Plant Molecular Biology 90: 561–574.

Cassán F, Diaz-Zorita M. 2016. Azospirillum sp. in current agriculture: From the laboratory to the field. Soil Biology and Biochemistry 103: 117–130.

Castrillo G, Teixeira PJPL, Paredes SH, Law TF, De Lorenzo L, Feltcher ME, Finkel OM, Breakfield NW, Mieczkowski P, Jones CD, et al. 2017. Root microbiota drive direct integration of phosphate stress and immunity. Nature 543: 513–518.

Chamam A, Wisniewski-Dyé F, Comte G, Bertrand C, Prigent-Combaret C. 2015. Differential responses of Oryza sativa secondary metabolism to biotic interactions with cooperative, commensal and phytopathogenic bacteria. Planta 242: 1439–1452.

Chen H, Boutros PC. 2011. VennDiagram: a package for the generation of highly-customizable Venn and Euler diagrams in R. BMC Bioinformatics 12: 35.

Cheng P, Gedling CR, Patil G, Vuong TD, Shannon JG, Dorrance AE, Nguyen HT. 2017. Genetic mapping and haplotype analysis of a locus for quantitative resistance to Fusarium graminearum in soybean accession PI 567516C. Theoretical and Applied Genetics 130: 999–1010.

Conesa A, Götz S, García-Gómez JM, Terol J, Talón M, Robles M. 2005. Blast2GO: A universal tool for annotation, visualization and analysis in functional genomics research. Bioinformatics 21: 3674– 3676.

Cunha FN, Silva NF da, Ribeiro Rodrigues C, Alves Morais W, Ferreira Gomes FH, Lopes Filho, Luiz C, Cabral LB dos S, Marconi BT, Gustavo da SV, Cicero TSC. 2016. Performance of different genotypes of maize subjected to inoculation with Azospirillum brasilense. African Journal of Agricultural Research 11: 3853–3862.

D'Angioli AM, Viani RAG, Lambers H, Sawaya ACHF, Oliveira RS. 2017. Inoculation with Azospirillum brasilense (Ab-V4, Ab-V5) increases Zea mays root carboxylate-exudation rates, dependent on soil phosphorus supply. Plant and Soil 410: 499–507.

D'Auria JC, Pichersky E, Schaub A, Hansel A, Gershenzon J. 2007. Characterization of a BAHD acyltransferase responsible for producing the green leaf volatile (Z)-3-hexen-1-yl acetate in Arabidopsis thaliana. The Plant Journal 49: 194–207.

Dicke M. 2016. Plant phenotypic plasticity in the phytobiome: a volatile issue. Current Opinion in Plant Biology 32: 17–23.

Ding Y, Huffaker A, Köllner TG, Weckwerth P, Robert CAM, Spencer JL, Lipka AE, Schmelz EA. 2017. Selinene Volatiles Are Essential Precursors for Maize Defense Promoting Fungal Pathogen Resistance. Plant Physiology 175: 1455–1468.

Ding L, Lu Z, Gao L, Guo S, Shen Q. 2018. Is Nitrogen a Key Determinant of Water Transport and Photosynthesis in Higher Plants Upon Drought Stress? Frontiers in Plant Science 9: 1–12.

Ding L, Wang KJ, Jiang GM, Biswas DK, Xu H, Li LF, Li YH. 2005. Effects of Nitrogen Deficiency on Photosynthetic Traits of Maize Hybrids Released in Different Years. Annals of Botany 96: 925–930.

Disi JO, Zebelo S, Kloepper JW, Fadamiro H. 2018. Seed inoculation with beneficial rhizobacteria affects European corn borer (Lepidoptera: Pyralidae) oviposition on maize plants. Entomological Science 21: 48–58.

Duca DR, Rose DR, Glick BR. 2018. Indole acetic acid overproduction transformants of the rhizobacterium Pseudomonas sp. UW4. Antonie van Leeuwenhoek 111: 1645–1660.

Fesel PH, Zuccaro A. 2016. Dissecting endophytic lifestyle along the parasitism/mutualism continuum in Arabidopsis. Current Opinion in Microbiology 32: 103–112.

Fukami J, Cerezini P, Hungria M. 2018a. Azospirillum: benefits that go far beyond biological nitrogen fixation. AMB Express 8: 1–12.

Fukami J, Nogueira MA, Araujo RS, Hungria M. 2016. Accessing inoculation methods of maize and wheat with Azospirillum brasilense. AMB Express 6: 3.

Fukami J, Ollero FJ, de la Osa C, Valderrama-Fernández R, Nogueira MA, Megías M, Hungria M. 2018b. Antioxidant activity and induction of mechanisms of resistance to stresses related to the inoculation with Azospirillum brasilense. Archives of Microbiology 200: 1191–1203.

Fukami J, Ollero FJ, Megías M, Hungria M. 2017. Phytohormones and induction of plant-stress tolerance and defense genes by seed and foliar inoculation with Azospirillum brasilense cells and metabolites promote maize growth. AMB Express 7: 153.

Genissel A, Confais J, Lebrun M-H, Gout L. 2017. Association Genetics in Plant Pathogens: Minding the Gap between the Natural Variation and the Molecular Function. Frontiers in Plant Science 8: 8–11.

German MA, Burdman S, Okon Y, Kigel J. 2000. Effects of Azospirillum brasilense on root morphology of common bean (Phaseolus vulgaris L.) under different water regimes. Biology and Fertility of Soils 32: 259–264.

Gilmour a R, Gogel BJ, Cullis BR, Welham SJ, Thompson R. 2015. Summary for Policymakers. In: Intergovernmental Panel on Climate Change, ed. Climate Change 2013 - The Physical Science Basis. Cambridge: Cambridge University Press, 1–30.

Gomes EA, Lana UGP, Quensen JF, Oliveira CA, Guo J, Guimar LJM, Tiedje JM, Maize E, Lagoas S, E-mail B, et al. 2018. Root-associated microbiome of maize genotypes with contrasting phosphorus use efficiency 2: 129-137.

Gopal M, Gupta A. 2016. Microbiome selection could spur next-generation plant breeding strategies. Frontiers in Microbiology 7: 1–10.

Goyette P, Boucher G, Mallon D, Ellinghaus E, Jostins L, Huang H, Ripke S, Gusareva ES, Annese V, Hauser SL, et al. 2015. High-density mapping of the MHC identifies a shared role for HLA-DRB1*01:03 in inflammatory bowel diseases and heterozygous advantage in ulcerative colitis. Nature genetics 47: 172–9.

Hohmann P, Messmer MM. 2017. Breeding for mycorrhizal symbiosis: focus on disease resistance. Euphytica 213: 1–11.

Huh SU, Paek K-H. 2013. Plant RNA binding proteins for control of RNA virus infection. Frontiers in Physiology 4: 1–5.

Hungria M, Campo RJ, Souza EM, Pedrosa FO. 2010. Inoculation with selected strains of Azospirillum brasilense and A. lipoferum improves yields of maize and wheat in Brazil. Plant and Soil 331: 413–425.

Kamfwa K, Cichy KA, Kelly JD. 2015. Genome-wide association analysis of symbiotic nitrogen fixation in common bean. Theoretical and Applied Genetics 128: 1999–2017.

Kavi Kishor PB. 2015. Role of proline in cell wall synthesis and plant development and its implications in plant ontogeny. Frontiers in Plant Science 6: 1–17.

Kazi N, Deaker R, Wilson N, Muhammad K, Trethowan R. 2016. The response of wheat genotypes to inoculation with Azospirillum brasilense in the field. Field Crops Research 196: 368–378.

Khan MIR, Trivellini A, Fatma M, Masood A, Francini A, Iqbal N, Ferrante A, Khan NA. 2015. Role of ethylene in responses of plants to nitrogen availability. Frontiers in Plant Science 6: 1–15.

Klay I, Gouia S, Liu M, Mila I, Khoudi H, Bernadac A, Bouzayen M, Pirrello J. 2018. Ethylene Response Factors (ERF) are differentially regulated by different abiotic stress types in tomato plants. Plant Science 274: 137–145.

Koo AJ. 2018. Metabolism of the plant hormone jasmonate: a sentinel for tissue damage and master regulator of stress response. Phytochemistry Reviews 17: 51–80.

Korte A, Farlow A. 2013. The advantages and limitations of trait analysis with GWAS: a review. Plant Methods 9: 29.

Kox MAR, Lüke C, Fritz C, van den Elzen E, van Alen T, Op den Camp HJM, Lamers LPM, Jetten MSM, Ettwig KF. 2016. Effects of nitrogen fertilization on diazotrophic activity of microorganisms associated with Sphagnum magellanicum. Plant and Soil 406: 83–100.

Lanes ECM, Viana JMS, Paes GP, Paula MFB, Maia C, Caixeta ET, Miranda GV. 2014. Population structure and genetic diversity of maize inbreds derived from tropical hybrids. Genetics and Molecular Research 13: 7365–7376.

Lee Y-S, Shin D, Song K-D. 2018. Dominance effects of ion transport and ion transport regulator genes on the final weight and backfat thickness of Landrace pigs by dominance deviation analysis. Genes & Genomics 0: 0.

Lehnert H, Serfling A, Enders M, Friedt W, Ordon F. 2017. Genetics of mycorrhizal symbiosis in winter wheat (Triticum aestivum). New Phytologist 215: 779–791.

Li Z, Coffey L, Garfin J, Miller ND, White MR, Spalding EP, de Leon N, Kaeppler SM, Schnable PS, Springer NM, et al. 2018. Genotype-by-environment interactions affecting heterosis in maize (L Lukens, Ed.). PLOS ONE 13: e0191321.

Li H, Yang Q, Gao L, Zhang M, Ni Z, Zhang Y. 2017. Identification of Heterosis-Associated Stable QTLs for Ear-Weight-Related Traits in an Elite Maize Hybrid Zhengdan 958 by Design III. Frontiers in Plant Science 8: 1–10.

Liu X, Huang M, Fan B, Buckler ES, Zhang Z. 2016. Iterative Usage of Fixed and Random Effect Models for Powerful and Efficient Genome-Wide Association Studies. PLoS Genetics 12: 100.

Liu L-H, Ludewig U, Gassert B, Frommer WBF, Wirén N Von. 2003. Urea Transport by Nitrogen-Regulated Tonoplast Intrinsic Proteins in Arabidopsis. Plant Physiology 133: 1220–1228.

Luo B, Tang H, Liu H, Shunzong S, Zhang S, Wu L, Liu D, Gao S. 2015. Mining for low-nitrogen tolerance genes by integrating meta-analysis and large-scale gene expression data from maize. Euphytica 206: 117–131.

Mendonça LDF, Granato ÍSC, Alves FC, Morais PPP, Vidotti MS, Fritsche-Neto R. 2017. Accuracy and simultaneous selection gains for N-stress tolerance and N-use efficiency in maize tropical lines. Scientia Agricola 74: 481–488.

Młodzińska E, Kłobus G, Christensen MD, Fuglsang AT. 2015. The plasma membrane H + -ATPase AHA2 contributes to the root architecture in response to different nitrogen supply. Physiologia Plantarum 154: 270–282.

Monir MM, Zhu J. 2018. Dominance and Epistasis Interactions Revealed as Important Variants for Leaf Traits of Maize NAM Population. Frontiers in Plant Science 9: 1–10.

Morosini JS, Mendonça LDF, Lyra DH, Galli G, Vidotti MS, Fritsche-Neto R. 2017. Association mapping for traits related to nitrogen use efficiency in tropical maize lines under field conditions. Plant and Soil 421: 453–463.

Nguema-Ona E, Vicré-Gibouin M, Cannesan M-A, Driouich A. 2013. Arabinogalactan proteins in root–microbe interactions. Trends in Plant Science 18: 440–449.

Nogales A, Nobre T, Valadas V, Ragonezi C, Döring M, Polidoros A, Arnholdt-Schmitt B. 2016. Can functional hologenomics aid tackling current challenges in plant breeding? Briefings in Functional Genomics 15: 288–297.

Oda Y, Hasezawa S. 2006. Cytoskeletal organization during xylem cell differentiation. Journal of Plant Research 119: 167–177.

Picard C, Bosco M. 2005. Maize heterosis affects the structure and dynamics of indigenous rhizospheric auxins-producing Pseudomonas populations. FEMS Microbiology Ecology 53: 349–357.

Picard C, Bosco M. 2006. Heterozygosis drives maize hybrids to select elite 2,4-diacethylphloroglucinol-producing Pseudomonas strains among resident soil populations. FEMS Microbiology Ecology 58: 193–204.

Pieterse CMJ, de Jonge R, Berendsen RL. 2016. The Soil-Borne Supremacy. Trends in Plant Science 21: 171–173.

Purcell S, Neale B, Todd-Brown K, Thomas L, Ferreira MAR, Bender D, Maller J, Sklar P, de Bakker PIW, Daly MJ, et al. 2007. PLINK: A Tool Set for Whole-Genome Association and Population-Based Linkage Analyses. The American Journal of Human Genetics 81: 559–575.

Rai A, Kumar S, Bauddh K, Singh N, Singh RP. 2017. Improvement in growth and alkaloid content of Rauwolfia serpentina on application of organic matrix entrapped biofertilizers (Azotobacter chroococcum, Azospirillum brasilense and Pseudomonas putida). Journal of Plant Nutrition 40: 2237–2247.

Ristova D, Carré C, Pervent M, Medici A, Kim GJ, Scalia D, Ruffel S, Birnbaum KD, Lacombe B, Busch W, et al. 2016. Combinatorial interaction network of transcriptomic and phenotypic responses to nitrogen and hormones in the Arabidopsis thaliana root. Science Signaling 9.

Rodrigues Neto J, Malavolta V A, Victor O. 1986. Meio simples para o isolamento e cultivo 828 de Xanthomonas campestris pv. citri tipo B. Summa Phytopathol 12:32.

Rosas JE, Martínez S, Blanco P, Pérez de Vida F, Bonnecarrère V, Mosquera G, Cruz M, Garaycochea S, Monteverde E, McCouch S, et al. 2017. Resistance to Multiple Temperate and Tropical Stem and Sheath Diseases of Rice. The Plant Genome 0: 0.

Rosier A, Bishnoi U, Lakshmanan V, Sherrier DJ, Bais HP. 2016. A perspective on inter-kingdom signaling in plant–beneficial microbe interactions. Plant Molecular Biology 90: 537–548.

Rozier C, Erban A, Hamzaoui J, Prigent-Combaret C, Comte G, Kopka J, Czarnes S, Legendre L. 2016. Xylem Sap Metabolite Profile Changes During Phytostimulation of Maize by the Plant Growth-Promoting Rhizobacterium, Azospirillum lipoferum CRT1. Journal of Postgenomics Drug & Biomarker Development 6: 1–10.

Schulz B, Boyle C. 2005. The endophytic continuum. Mycological Research 109: 661–686.

Sharifi R, Lee S-M, Ryu C-M. 2017. Microbe-induced plant volatiles. New Phytologist 220: 684-691.

Spaepen S, Bossuyt S, Engelen K, Marchal K, Vanderleyden J. 2014. Phenotypical and molecular responses of Arabidopsis thaliana roots as a result of inoculation with the auxin-producing bacterium Azospirillum brasilense. New Phytologist 201: 850–861.

Sun X, Yu G, Li J, Liu J, Wang X, Zhu G, Zhang X, Pan H. 2018. AcERF2, an ethylene-responsive factor of Atriplex canescens, positively modulates osmotic and disease resistance in Arabidopsis thaliana. Plant Science 274: 32–43.

Timm CM, Pelletier DA, Jawdy SS, Gunter LE, Henning JA, Engle N, Aufrecht J, Gee E, Nookaew I, Yang Z, et al. 2016. Two Poplar-Associated Bacterial Isolates Induce Additive Favorable Responses in a Constructed Plant-Microbiome System. Frontiers in Plant Science Front. Plant Sci 7: 10.

Tivendale ND, Ross JJ, Cohen JD. 2014. The shifting paradigms of auxin biosynthesis. Trends in Plant Science 19: 44–51.

Trachsel S, Kaeppler SM, Brown KM, Lynch JP. 2013. Maize root growth angles become steeper under low N conditions. Field Crops Research 140: 18–31.

Tsairidou S, Allen AR, Pong-Wong R, McBride SH, Wright DM, Matika O, Pooley CM, McDowell SWJ, Glass EJ, Skuce RA, et al. 2018. An analysis of effects of heterozygosity in dairy cattle for bovine tuberculosis resistance. Animal Genetics 49: 103–109.

Tsepilov YA, Shin S-Y, Soranzo N, Spector TD, Prehn C, Adamski J, Kastenmüller G, Wang-Sattler R, Strauch K, Gieger C, et al. 2015. Nonadditive Effects of Genes in Human Metabolomics. Genetics 200: 707–718.

Unterseer S, Bauer E, Haberer G, Seidel M, Knaak C, Ouzunova M, Meitinger T, Strom TM, Fries R, Pausch H, et al. 2014. A powerful tool for genome analysis in maize: development and evaluation of the high density 600 k SNP genotyping array. BMC Genomics 15: 823.

Velasquez SM, Ricardi MM, Dorosz JG, Fernandez P V., Nadra AD, Pol-Fachin L, Egelund J, Gille S, Harholt J, Ciancia M, et al. 2011. O-Glycosylated Cell Wall Proteins Are Essential in Root Hair Growth. Science 332: 1401–1403.

De Vita P, Avio L, Sbrana C, Laidò G, Marone D, Mastrangelo AM, Cattivelli L, Giovannetti M. 2018. Genetic markers associated to arbuscular mycorrhizal colonization in durum wheat. Scientific Reports 8: 10612.

Wallace JG, Kremling KA, Kovar LL, Buckler ES. 2018. Quantitative Genetic Analysis of the Maize Leaf Microbiome. BioRxiv: 268532.

Wang C, Liu W, Li Q, Ma D, Lu H, Feng W, Xie Y, Zhu Y, Guo T. 2014. Effects of different irrigation and nitrogen regimes on root growth and its correlation with above-ground plant parts in high-yielding wheat under field conditions. Field Crops Research 165: 138–149.

Wang H, Xu C, Liu X, Guo Z, Xu X, Wang S, Xie C, Li W-X, Zou C, Xu Y. 2017. Development of a multiple-hybrid population for genome-wide association studies: theoretical consideration and genetic mapping of flowering traits in maize. Scientific Reports 7: 40239.

Wang Y, Yuan G, Yuan S, Duan W, Wang P, Bai J, Zhang F, Gao S, Zhang L, Zhao C. 2016. TaOPR2 encodes a 12-oxo-phytodienoic acid reductase involved in the biosynthesis of jasmonic acid in wheat (Triticum aestivum L.). Biochemical and Biophysical Research Communications 470: 233–238.

Xu W, Cui K, Xu A, Nie L, Huang J, Peng S. 2015. Drought stress condition increases root to shoot ratio via alteration of carbohydrate partitioning and enzymatic activity in rice seedlings. Acta Physiologiae Plantarum 37.

Yan J, Warburton M, Crouch J. 2011. Association Mapping for Enhancing Maize (L.) Genetic Improvement. Crop Science 51: 433.

Yang J, Mezmouk S, Baumgarten A, Buckler ES, Guill KE, McMullen MD, Mumm RH, Ross-Ibarra J. 2017. Incomplete dominance of deleterious alleles contributes substantially to trait variation and heterosis in maize (JC Fay, Ed.). PLOS Genetics 13: e1007019.

Zheng X, Levine D, Shen J, Gogarten SM, Laurie C, Weir BS. 2012. A high-performance computing toolset for relatedness and principal component analysis of SNP data. Bioinformatics 28: 3326–3328.

TABLES

Table 1 Wald test for fixed effects and Likelihood Ratio Test for random effects from the joint diallel analysis of 118 maize hybrids evaluated under N stress and N stress plus *Azospirillum brasilense* treatments.

Variation source	PH	SDM	RDM	LRL	ARL	RAD	RV	SRL	SRSA	RSR
Fixed										
Year (Y)	1533.0**	576.9**	29.5**	41.0**	2.2	107.0**	9.3**	11.8**	95.0**	575.5**
Block (B)/Y	69.0**	4.0	17.9**	27.8**	13.2*	219.0**	61.4**	85.8**	57.3**	21.7**
Countertop/B/Y	505.0**	165.6**	152.4**	177.9**	191.1**	10.0	10.4**	12.4	17.2**	63.3**
Inoculation (I)	0	0.1	8.3**	0.2	1.1	19.0**	165.4**	11.8**	7.0**	5.1*
Y x I	0	0.1	0.7	1.1	0	1.0	0	1.7	1.1	0.5
Random										
Genotype (G)	3.7	0.1	16.9**	7.8**	49.9**	37.6**	39.4**	28.6**	23.0**	115.0**
G x Y	12.1**	8.8**	1.5	4.5*	0.8	1.3	0.5	0.7	2.8	10.7**
G x I	0	0	0	0	0	0.3	0.1	0	0	0
G x Y x I	0	0	0	0	0	0	0	0	0	0

PH: plant height, SDM: shot dry mass, RDM: root dry mass, LRL: lateral root length, ARL: axial root length, RV: root volume, RAD: root average diameter, SRL: specific root length, SRSA: specific root surface area, and RSR: root shoot ratio. Significant at 5% (*) or 1% (**) level.

Table 2 List of candidate genes around of significant SNPs identified by additive GWAS model and their description from maizeGDB (www.maizegdb.org) and NCBI database for root dry mass (RDM), root volume (RV), root average diameter (RAD), specific root length (SRL), and specific root surface area (SRSA) evaluated in maize hybrids under N stress and N stress plus *Azospirillum brasilense*.

Trait	Candidate gene	SNP	Chr.[1]	Position	MAF[2]	Effect	*P*-value	Gene annotation
	N stress plus Azospirillum brasilense							
RDM	Zm00001d051881	T/C	4	173317340	0.14	0.20	5.50×10^{-10}	Protein BTR1
RDM	Zm00001d035859	T/C	6	56793578	0.42	-0.20	1.31×10^{-16}	Plastocyanin homolog 1
RV	Zm00001d006108	C/G	2	198321726	0.43	-3.61	1.61×10^{-21}	Hydroxyproline-rich glycoprotein family protein
RAD	Zm00001d013098	A/G	5	4668442	0.46	0.04	3.14×10^{-24}	Aldehyde oxidase 2
RAD	Zm00001d046604	T/C	9	98488802	0.32	0.02	3.52×10^{-11}	(Z)-3-hexen-1-ol acetyltransferase
SRL	Zm00001d005892	A/G	2	191920029	0.48	-386.64	1.40×10^{-09}	Ethylene-responsive transcription factor ERF109
SRL	Zm00001d020747	T/C	7	131108804	0.34	-357.72	1.98×10^{-08}	Aquaporin TIP4-1
SRSA	Zm00001d052221	A/G	4	183616939	0.29	83.61	4.13×10^{-10}	Tetratricopeptide repeat (TPR)-like superfamily protein
	N stress							
RDM	Zm00001d013098	A/G	5	4668442	0.46	0.02	3.14×10^{-24}	Aldehyde oxidase2
RV	Zm00001d038300	A/T	6	153844954	0.32	-1.97	2.89×10^{-13}	Putative cytochrome P450 superfamily protein
RAD	Zm00001d005892	A/G	2	191920029	0.48	0.02	1.40×10^{-09}	Ethylene-responsive transcription factor ERF109
SRL	Zm00001d002930	A/G	2	27052534	0.21	487.55	3.24×10^{-11}	Hypothetical protein
SRSA	-	A/C	5	149998432	0.40	86.90	2.93×10^{-10}	There is no candidate gene in the region

[1] Chromosome

[2] Minor allele frequency

Table 3 List of candidate genes around of significant SNPs identified by heterozygous (dis)advantage GWAS model and their description from maizeGDB (www.maizegdb.org) and NCBI database for root dry mass (RDM), root volume (RV), root average diameter (RAD), specific root length (SRL), and specific root surface area (SRSA) evaluated in maize hybrids under N stress plus *Azospirillum brasilense* and N stress.

Trait	Candidate gene	SNP	Chr.[1]	Position	MAF[2]	APHo[3]	APHe[4]	*P*-value	Gene annotation
	N stress plus Azospirillum brasilense								
RDM	Zm00001d029115	T/C	1	58456902	0.09	1.34	1.51	$1.92x10^{-10}$	Protein strictosidine synthase-like
RDM	Zm00001d037182	C/G	6	114938556	0.10	1.40	1.26	$1.07x10^{-11}$	12-oxo-phytodienoic acid reductase3
RV	Zm00001d029115	T/C	1	58456902	0.09	17.75	20.31	$4.37x10^{-13}$	Protein strictosidine synthase-like
RV	Zm00001d032763	A/G	1	237658345	0.19	18.50	17.71	$1.57x10^{-08}$	Pre-mRNA-processing factor 19 homolog 2
RV	Zm00001d003312	T/G	2	39796017	0.19	18.70	17.37	$5.56x10^{-08}$	3-ketoacyl-CoA thiolase 2 peroxisomal
RV	Zm00001d037182	C/G	6	114938556	0.10	18.67	16.28	$3.58x10^{-13}$	12-oxo-phytodienoic acid reductase3
RAD	Zm00001d030590	A/G	1	146746338	0.17	0.66	0.69	$3.02x10^{-13}$	Hypothetical protein
RAD	-	T/G	1	251090900	0.22	0.67	0.66	$1.57x10^{-08}$	There is no candidate gene in the region
RAD	Zm00001d003312	T/G	2	39796017	0.19	0.68	0.65	$2.79x10^{-09}$	3-ketoacyl-CoA thiolase 2 peroxisomal
RAD	LOC103636767	T/C	8	14392135	0.18	0.66	9.68	$5.99x10^{-11}$	Formin-like protein 20
SRL	Zm00001d030590	A/G	1	146746338	0.17	4364.24	4079.051	$2.25x10^{-10}$	Hypothetical protein
SRL	Zm00001d002736	T/C	2	20783203	0.18	4179.55	4433.63	$2.52x10^{-09}$	Carotenoid cleavage dioxygenase7
SRL	Zm00001d008828	T/C	8	21875974	0.18	4146.37	4485.58	$1.02x10^{-11}$	Uncharacterized loci
SRSA	Zm00001d033957	A/T	1	27957495	0.20	656.80	680.96	$1.86x10^{-08}$	Helix-loop-helix DNA-binding domain containing protein
RSR	Zm00001d029115	T/C	1	58456902	0.09	0.20	0.26	$9.11x10^{-12}$	Protein strictosidine synthase-like
RSR	Zm00001d043812	A/G	3	210821486	0.20	0.21	0.20	$6.28x10^{-1}$	Isopentenyl transferase3B
RSR	Zm00001d020647	T/C	7	126412420	0.23	0.22	0.19	$7.50x10^{-08}$	Phospholipid:diacylglycerol acyltransferase 1
	N stress								
RDM	Zm00001d003331	T/C	2	40341681	0.22	1.41	1.32	$9.16x10^{-11}$	Putative WRKY transcription factor 34
RDM	Zm00001d006036	A/G	2	195919131	0.27	1.40	1.34	$3.55x10^{-08}$	Heat shock 70 kDa protein 9 mitochondrial
RDM	-	T/C	3	165642810	0.21	1.41	1.32	$5.96x10^{-08}$	There is no candidate gene in the region
RDM	Zm00001d044754	A/T	9	1340463	0.17	1.41	1.30	$4.52x10^{-11}$	Pyrophosphate--fructose 6-phosphate 1-phosphotransferase subunit beta 2
RV	LOC109941493	T/C	1	162580315	0.12	17.59	20.17	$7.31x10^{-16}$	Plasma membrane ATPase 2-like

(The table continues on the next page)

(Continuation of the previous table)

Trait	Candidate gene	SNP	Chr.[1]	Position	MAF[2]	APHo[3]	APHe[4]	*P*-value	Gene annotation
RV	Zm00001d036118	T/C	6	72999857	0.26	17.63	18.74	$1.09x10^{-09}$	Putative homeobox DNA-binding and leucine zipper domain family protein
RAD	Zm00001d006722	T/C	2	215259958	0.23	0.68	0.65	$3.50x10^{-08}$	Arabinosyltransferase RRA3
RAD	Zm00001d037514	T/C	6	127764798	0.21	0.68	0.65	$1.49x10^{-09}$	Putative uncharacterized mitochondrial protein
SRL	LOC100279630	T/C	1	4994455	0.15	4117.59	4646.48	$8.56x10^{-17}$	MADS-box transcription factor family protein
SRL	Zm00001d029134	T/C	1	59906568	0.25	4401.44	4138.52	$5.25x10^{-09}$	CW-type Zinc Finger
SRL	Zm00001d029247	T/C	1	63585160	0.12	4151.88	4632.43	$2.23x10^{-14}$	ARM repeat superfamily protein
SRL	Zm00001d029385	T/C	1	68562928	0.25	4429.56	4115.72	$1.74x10^{-07}$	AAA-type ATPase family protein
SRL	Zm00001d030287	T/C	1	119697532	0.25	4194.09	4343.34	$2.67x10^{-08}$	Protein CLT2 chloroplastic
SRL	Zm00001d013070	T/C	5	4219053	0.25	4300.51	4239.46	$7.64x10^{-09}$	Transcription factor MYB98
SRL	Zm00001d037596	A/T	6	130932567	0.20	4445.73	4013.68	1.78E-07	RING/U-box superfamily protein
SRSA	LOC100279630	T/C	1	4994455	0.15	636.82	739.57	$1.99x10^{-13}$	MADS-box transcription factor family protein
RSR	Zm00001d051886	C/G	4	173630271	0.15	0.18	0.22	$1.04x10^{-13}$	Putative MATE efflux family protein

[1] Chromosome

[2] Minor allele frequency

[3] Average phenotype of individuals with homozygous genotype.

[4] Average phenotype of individuals with heterozygous genotype.

FIGURES

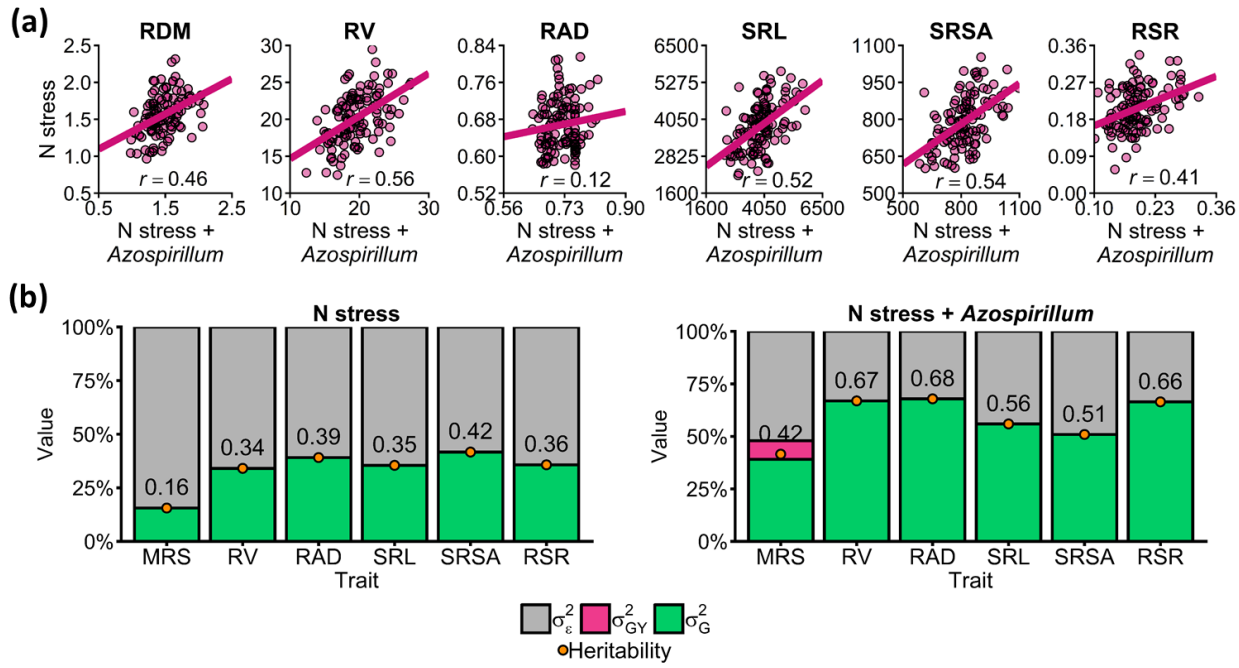

Fig. 1 (a) Pearson correlation between adjusted means of maize hybrids under N stress and N stress plus *A. brasilense*. **(b)** Estimates of variance components ($\hat{\sigma}^2_G$: genotypic variance; $\hat{\sigma}^2_{GY}$: genotype-by-year variance; $\hat{\sigma}^2_\epsilon$: error variance) and broad-sense heritabilities.

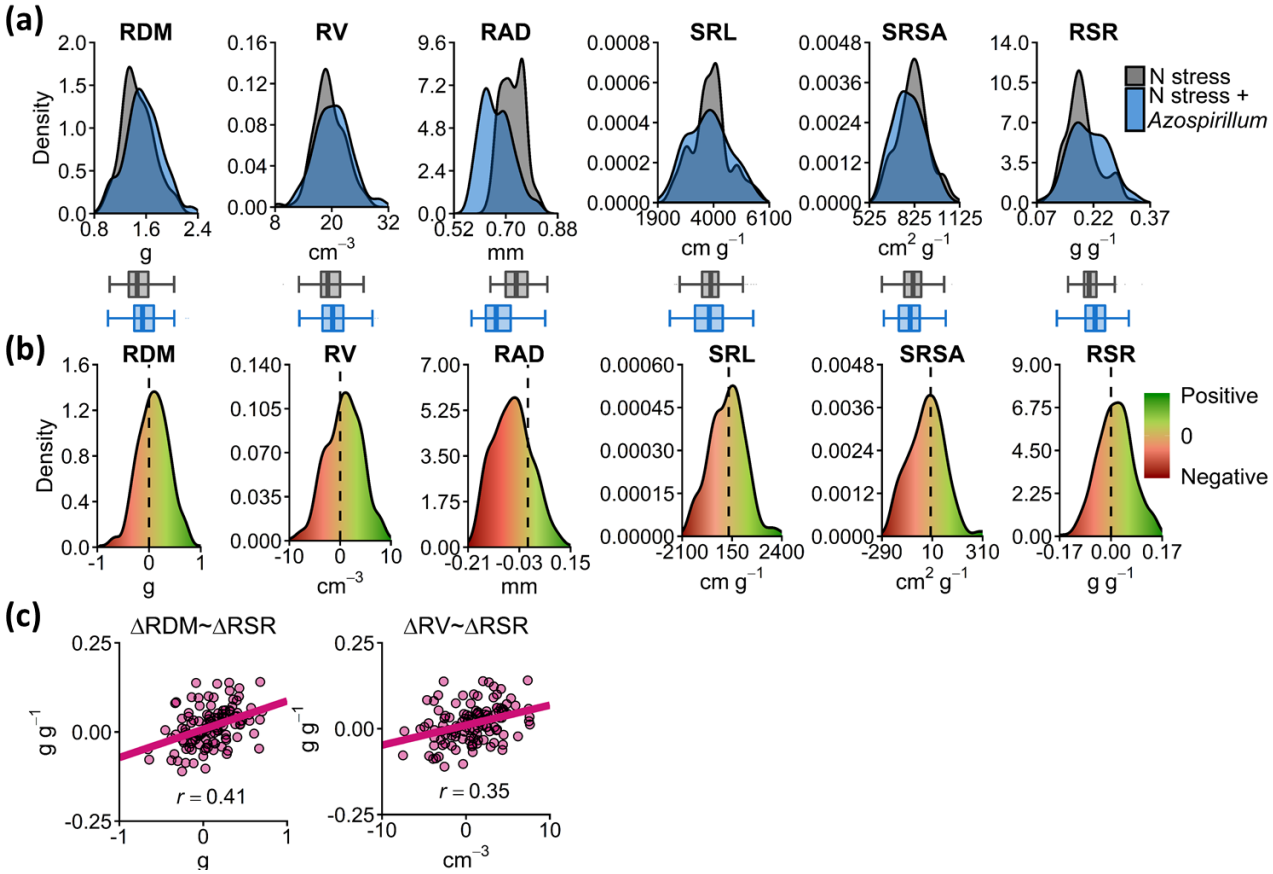

Fig. 2 (a) Density distribution and box-plot of the maize hybrids adjusted means under N stress and N stress plus *A. brasilense*. **(b)** Density distribution of the Δ (difference between adjusted means of inoculated and non-inoculated treatments). **(c)** Pearson correlation between adjusted means in both treatments.

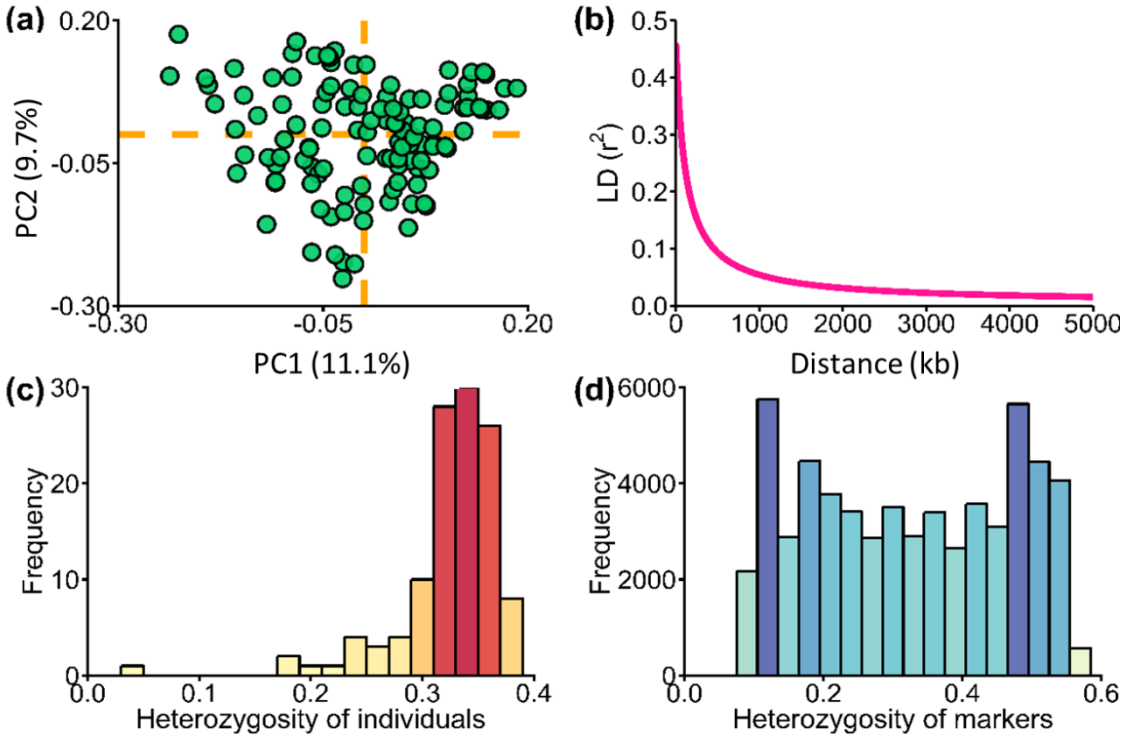

Fig. 3 **(a)** Population structure of the 118 maize hybrids revealed by the first two principal component of 59,215 SNP markers. **(b)** Linkage disequilibrium (LD) decay across the whole genome. **(c)** and **(d)** heterozygosity of individuals and markers, respectively.

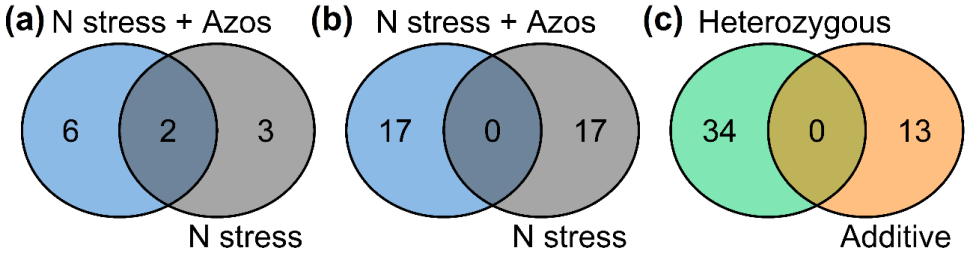

Fig. 4 Venn diagrams showing the unique and shared significant SNPs identified by **(a)** additive GWAS model, **(b)** heterozygous (dis)advantage model, and **(c)** both additive and heterozygous (dis)advantage models from a panel of 118 maize hybrids evaluated under N stress and N stress plus *Azospirillum brasiliense* treatments.

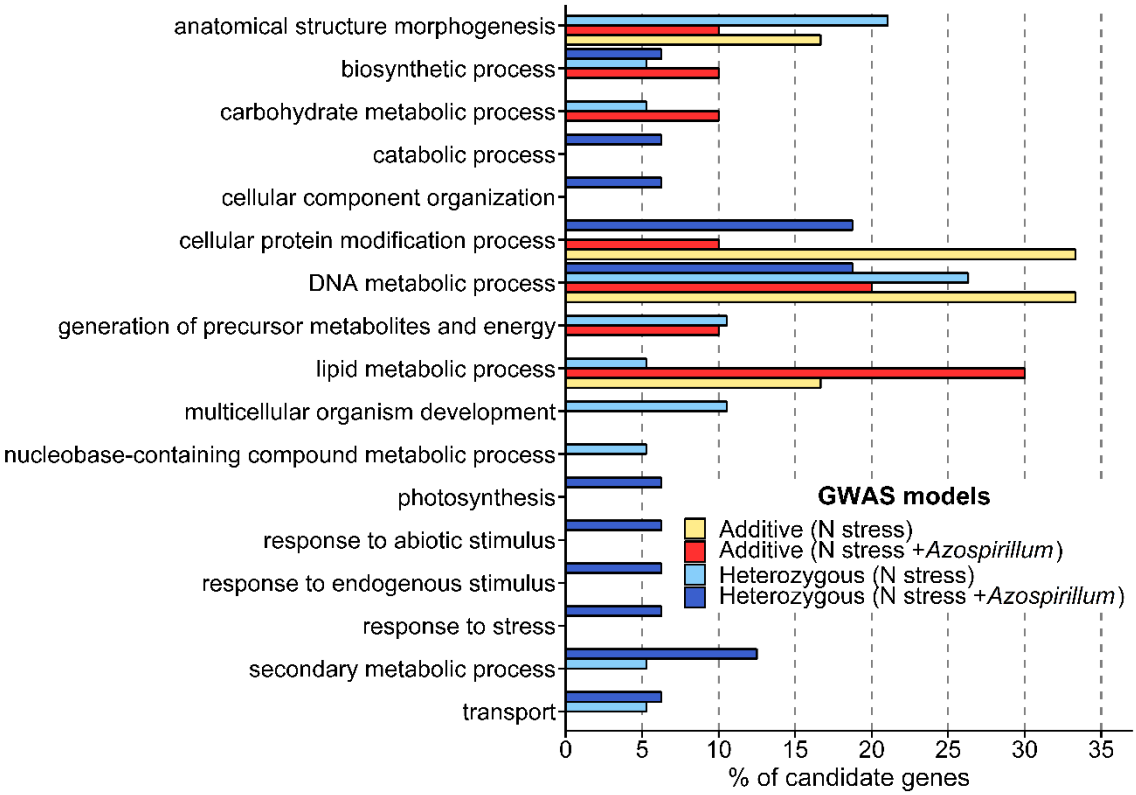

Fig. 5 Gene Ontology (GO) enrichment analysis of the candidates genes found by different GWAS models for traits evaluated in maize hybrids under N stress and N stress plus *Azospirillum brasilense*.

SUPPLEMENTARY FIGURES

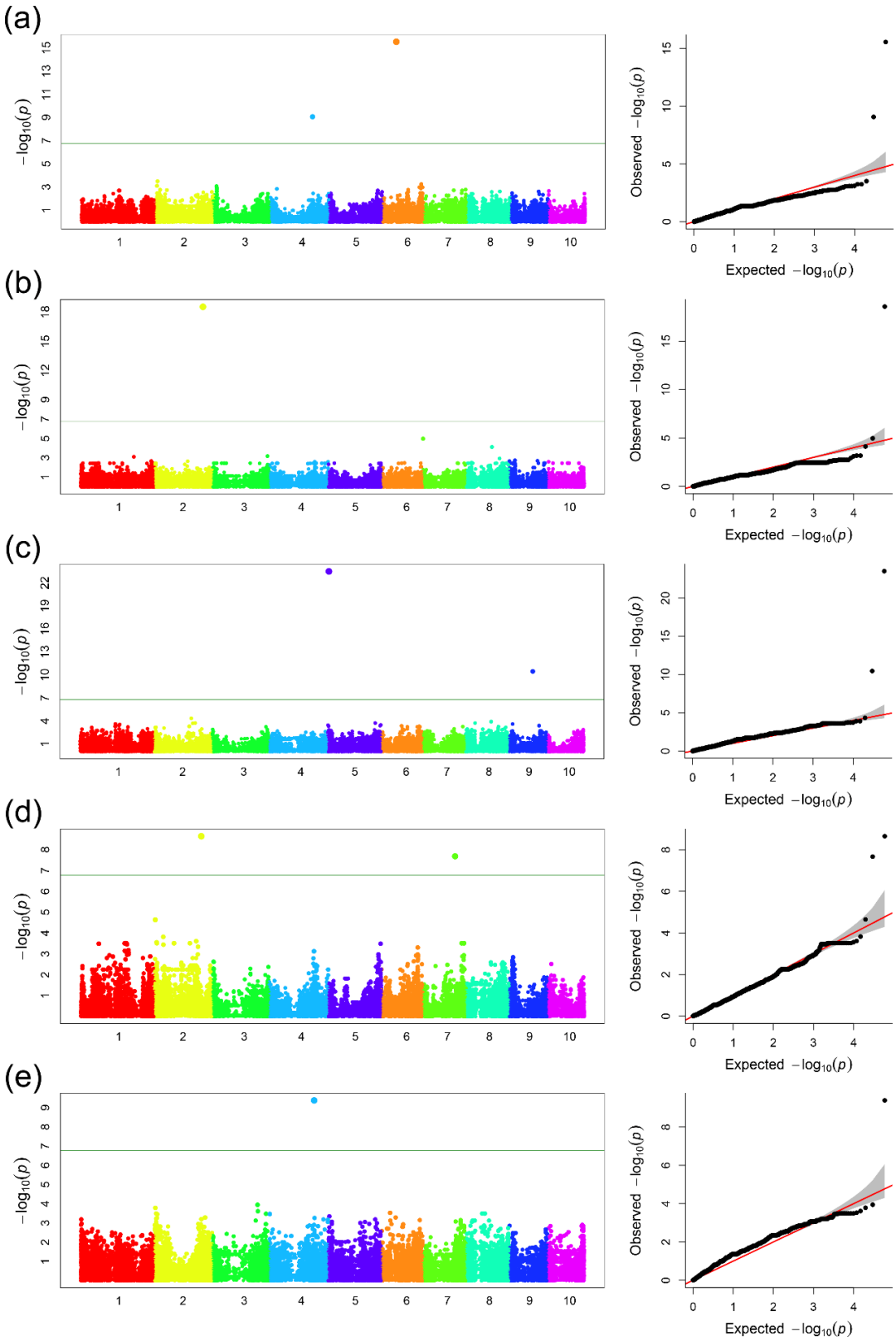

Fig. S1 Manhattan and Q-Q plots showing significant SNP markers identified by additive GWAS model for **(a)** root dry mass, **(b)** root volume, **(c)** root average diameter, **(d)** specific root length, and **(e)** specific root surface area from 118 maize hybrids evaluated under N stress plus *Azospirillum brasiliense*.

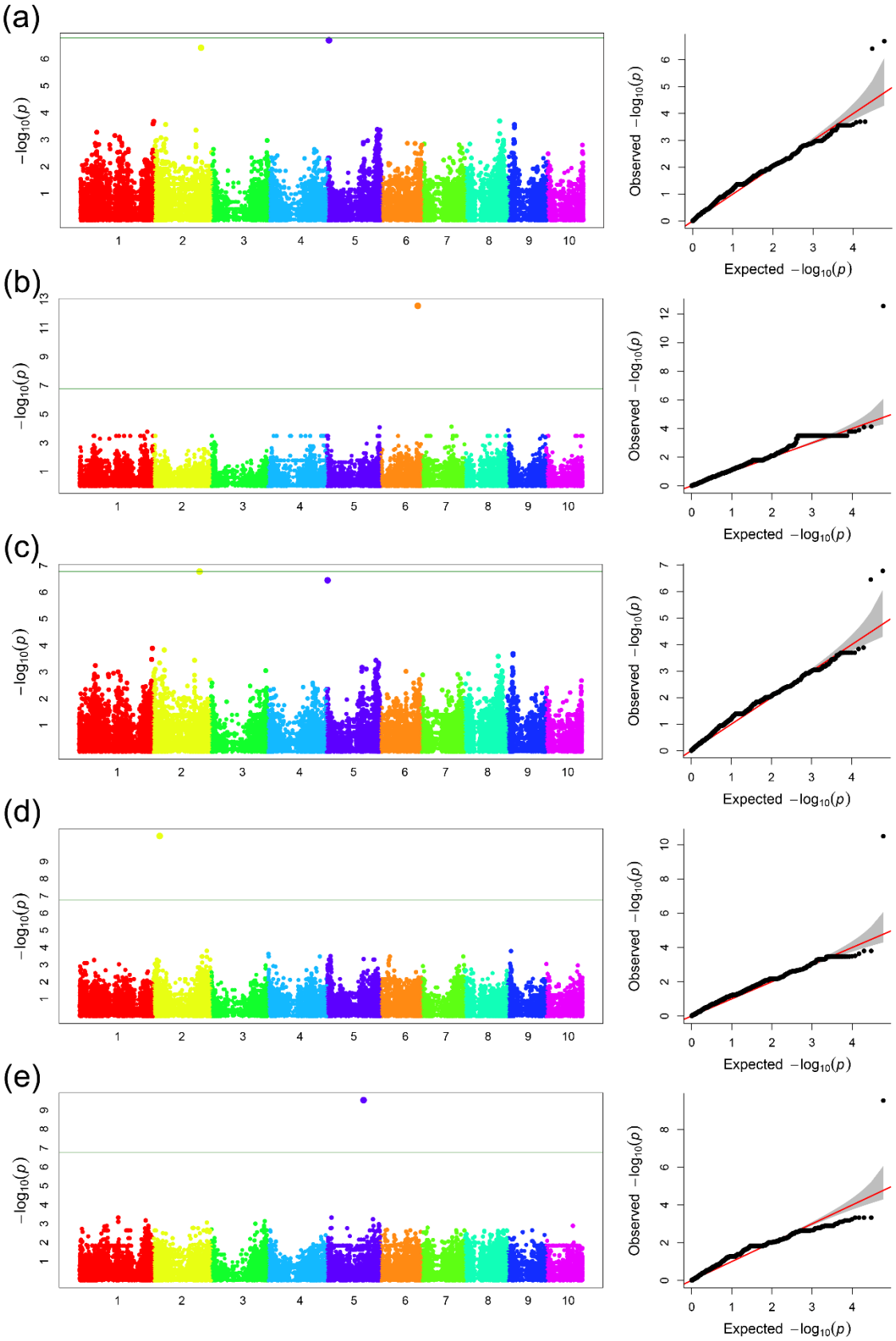

Fig. S2 Manhattan and Q-Q plots showing significant SNP markers identified by additive GWAS model for **(a)** root dry mass, **(b)** root volume, **(c)** root average diameter, **(d)** specific root length, and **(e)** specific root surface area from 118 maize hybrids evaluated under N stress.

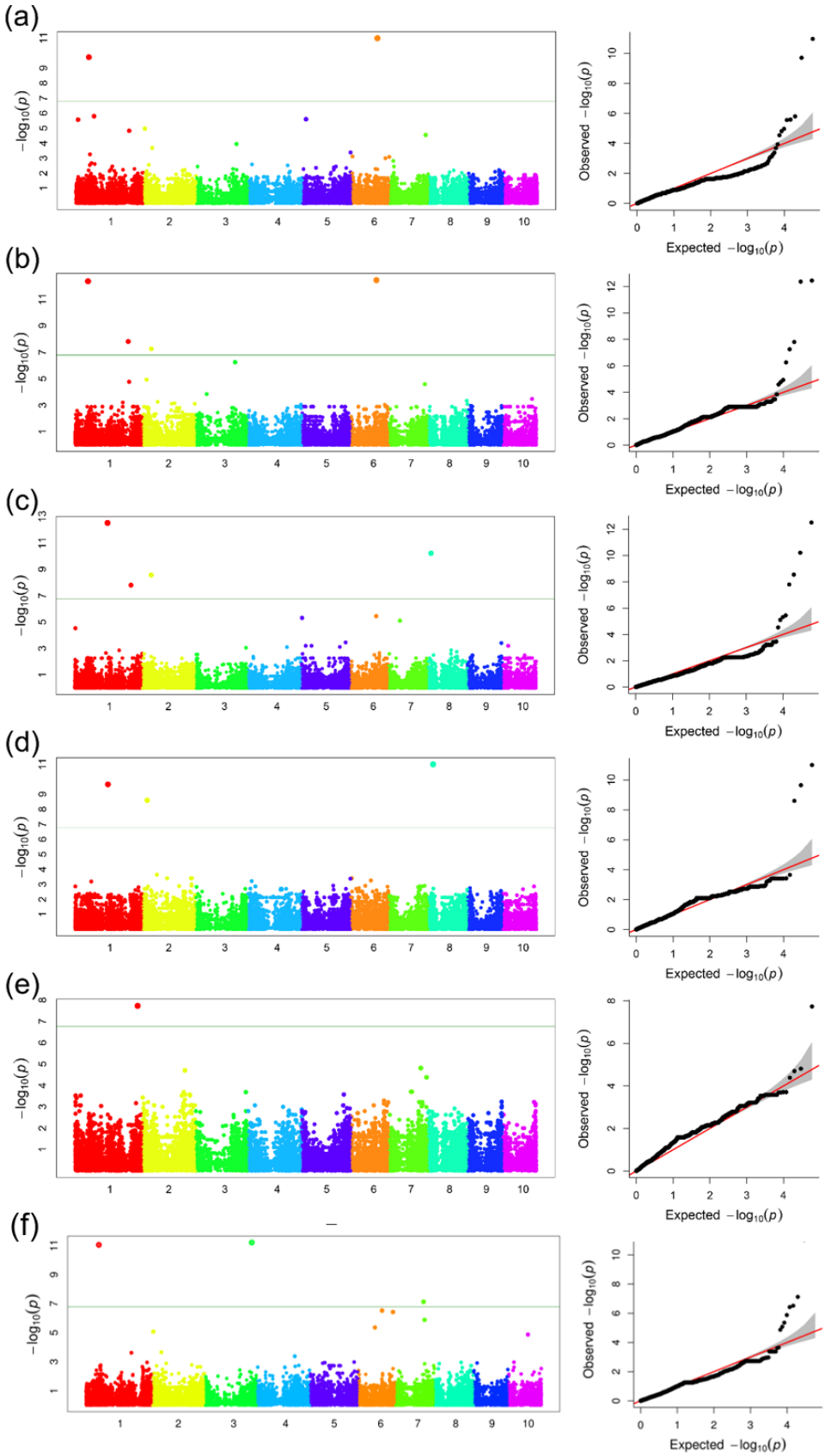

Fig. S3 Manhattan and Q-Q plots showing significant SNP markers identified by heterozygous (dis)advantage GWAS model for **(a)** root dry mass, **(b)** root volume, **(c)** root average diameter, **(d)** specific root length, **(e)** specific root surface area, and **(f)** root to shoot ratio from 118 maize hybrids evaluated under N stress plus *Azospirillum brasiliense*.

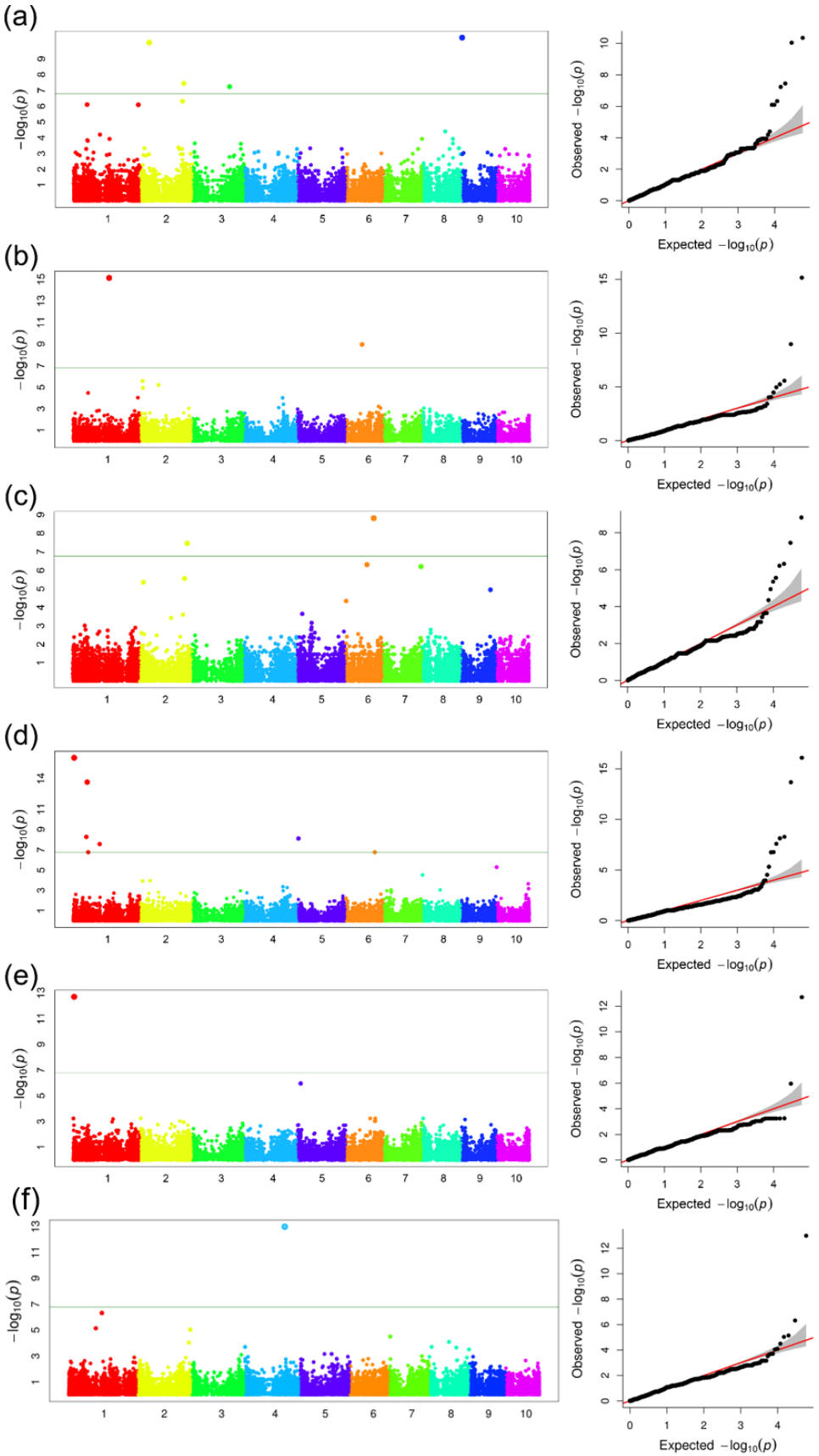

Fig. S4 Manhattan and Q-Q plots showing significant SNP markers identified by heterozygous (dis)advantage GWAS model for **(a)** root dry mass, **(b)** root volume, (c) root average diameter, **(d)** specific root length, **(e)** specific root surface area, and **(f)** root to shoot ratio from 118 maize hybrids evaluated under N stress.

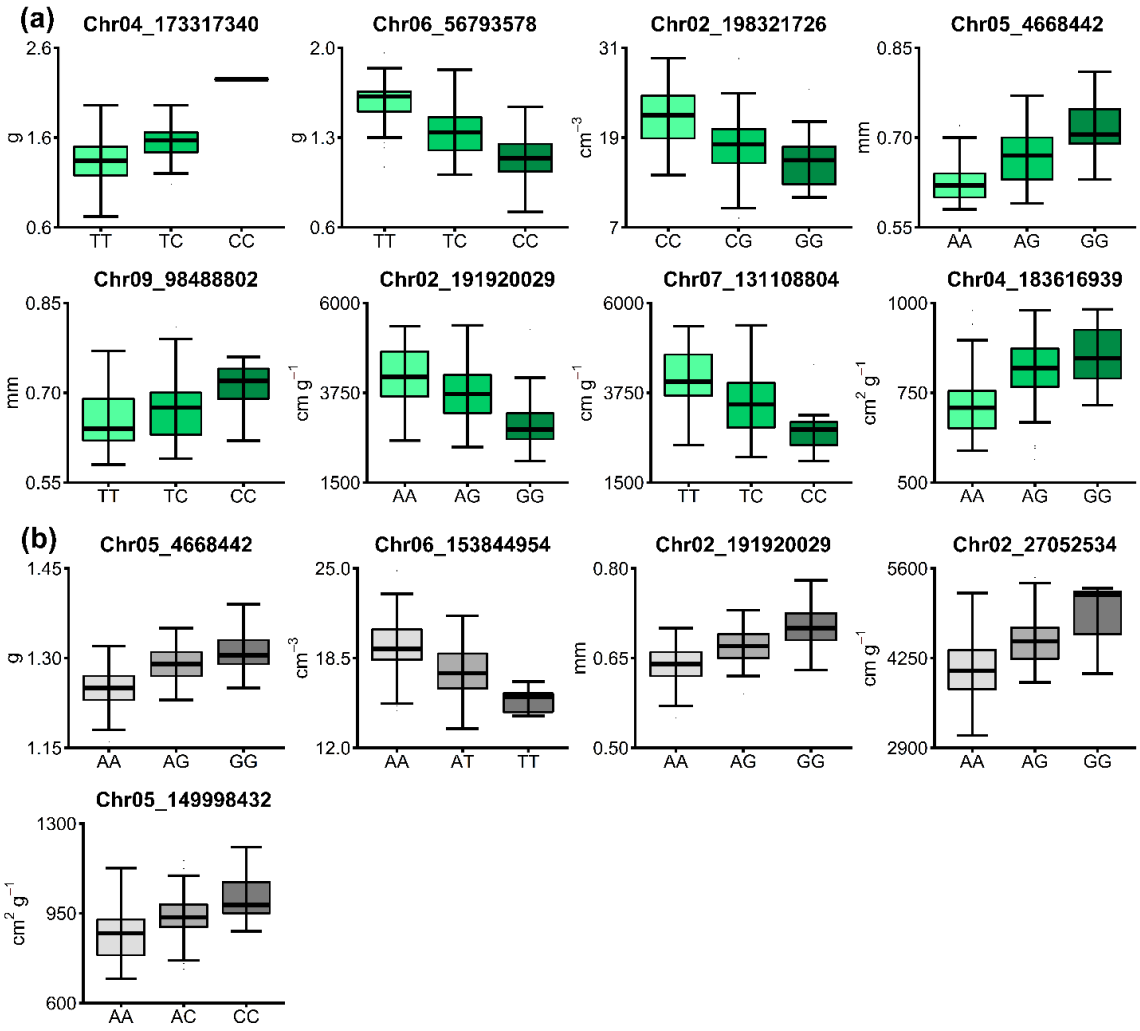

Fig. S5 Genetic impact of significant SNPs identified by additive GWAS model on five traits of 118 maize hybrids evaluated under **(a)** N stress plus *Azospirillum brasiliense*, and **(b)** N stress.

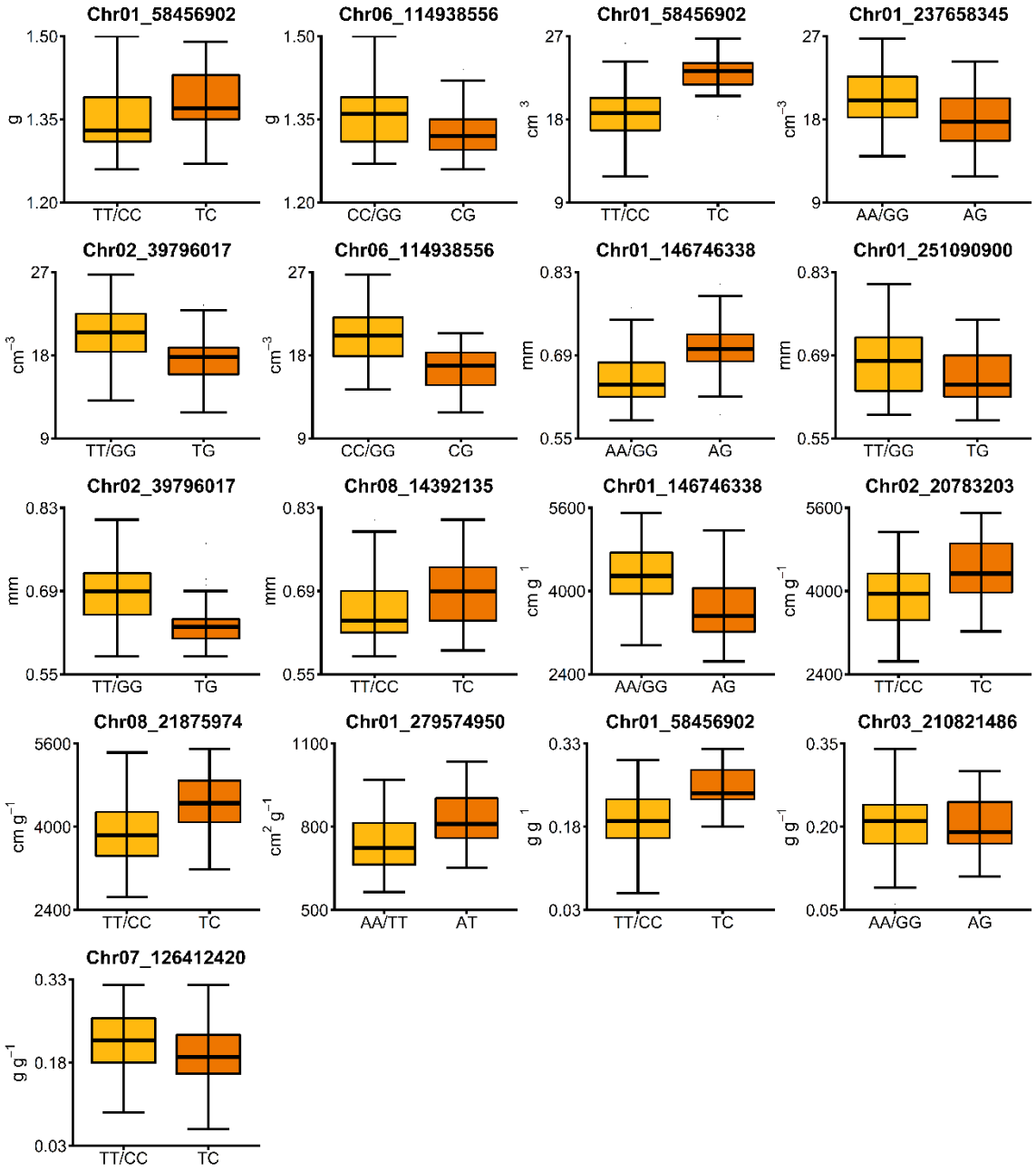

Fig. S6 Genetic impact of significant SNPs identified by heterozygous (dis)advantage GWAS model on six traits of 118 maize hybrids evaluated under N stress plus *Azospirillum brasiliense*.

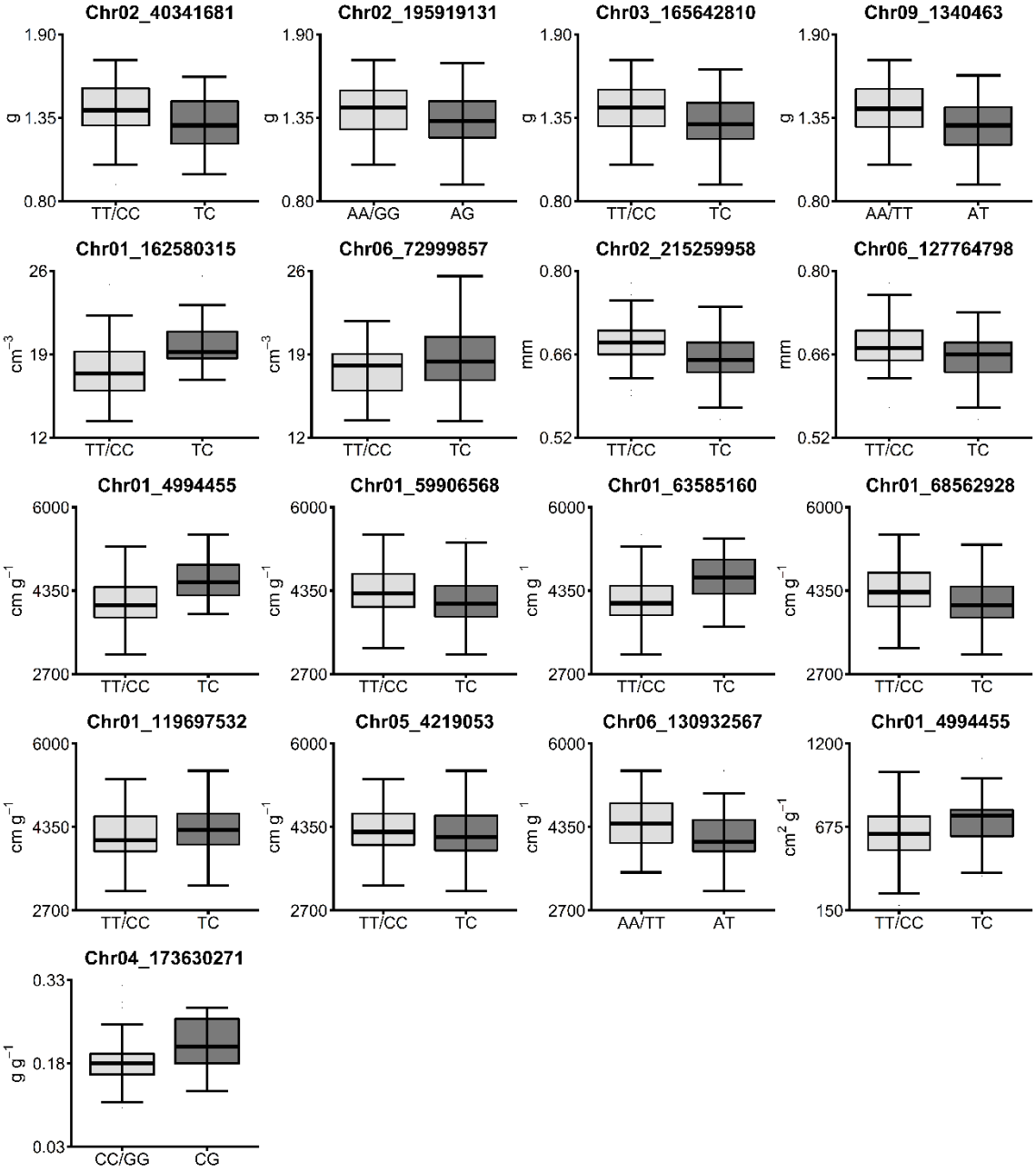

Fig. S7 Genetic impact of significant SNPs identified by heterozygous (dis)advantage GWAS model on six traits of 118 maize hybrids evaluated under N stress.